23236156

MICHIGAN STATE UNIVERSITY LIBRARIES

3 1293 00575 6881

LIBRARY
Michigan State
University

This is to certify that the

dissertation entitled

Adaptive control of continuous-flow
grain dryers

presented by

Rosana Galves Moreira

has been accepted towards fulfillment
of the requirements for

Doctoral degree in AE

Major professor

Date 1/26/89

MSU is an Affirmative Action/Equal Opportunity Institution

O-12771

PLACE IN RETURN BOX to remove this checkout from your record.
TO AVOID FINES return on or before date due.

DATE DUE	DATE DUE	DATE DUE
0 5 1 8 0 8 ~~MAR 1 7 2000~~ SEP 2 1 2001		
0 5 1 8 0 3		

MSU Is An Affirmative Action/Equal Opportunity Institution

ADAPTIVE CONTROL OF CONTINUOUS FLOW GRAIN DRYERS

By

Rosana Galves Moreira

A DISSERTATION

Submitted to
Michigan State University
in partial fulfillment of the requirements
for the degree of

DOCTOR OF PHILOSOPHY

IN

Agricultural Engineering

Department of Agricultural Engineering

1989

ABSTRACT

ADAPTIVE CONTROL OF CONTINUOUS FLOW GRAIN DRYERS

By

Rosana Galves Moreira

Adaptive control was evaluated as a tool for continuous-flow grain dryer control. The highly complex dynamics of the dryer provides an ideal test for adaptive control. An adaptive control technique based on a continuously updated linear controller was developed.

A control system was implemented and tested during two drying seasons on two commercial crossflow dryers. The system consists of a linear model, a control algorithm, an on-line moisture meter, a tachometer and a microcomputer. The outlet grain moisture content was controlled to within ±0.3% of the setpoint even for a large variation in the inlet moisture content.

An unsteady-state model of concurrentflow corn drying was developed consisting of four differential equations. The model was used to simulate the automatic control of a two-stage CCF dryer.

Five different empirical models were developed for describing the dynamics of the drying process. The best results were obtained with the Model II-b.

Two different adaptive controllers were used in both the experimental and theoretical parts of this study: (1) a generalized minimum variance controller (GMV) based on a time-series linear model and, (2) a pole placement controller (PP) based on an integrated moving average linear model.

The best control performance was obtained with the PP-controller, the worst with the MV-feedforward controller. The MV-feedback/feedforward controller also gave good results but it reacted too slowly for large variations in the inlet moisture content.

The PP-adaptive controller can be adopted to any dryer and grain type. It is stable, accurate, and has a quick response. It is recommended for any continuous-flow grain dryer automatic control.

Approved ______________________

Major Professor

Approved ______________________

Department Chairman

To my unforgettable Grandmother

Dolores Peres

(May/1898-June/1988)

ACKNOWLEDGMENTS

I am deeply indebted to Dr. Fred W. Bakker-Arkema for suggestion of the research topic and his continuous support, interest, and patient guidance throughout the course of this study.

Sincere appreciation is extended to the guidance comittee members: Dr. Roger C. Brook, Agricultural Engineering Department; Dr. Kris A. Berglund, Department of Agricultural Engineering and Chemical Engineering and Dr. Robert O. Barr, Department of Electrical Engineering and Systems Science.

Special thanks goes to Fernado A. Osorio and Dr. Abbas Y. Eltigani for their help and moral support. Special thanks is extended to Paul Maag and Sons, Inc. (Eagle, MI) and Anderson Grand River Grain Terminal (Webberville, MI) to allowing me to use their drying facilities.

To the entire Processing Group and the Graduate students of the Agricultural Engineering Department, Michigan State University, a special thanks for the encouragement and support.

Deepest appreciation goes to my mother Odette G. Moreira for her love, sacrifices and encouragement; to the Castell family, to my sister Walkiria, my brother Marcos, my aunt Rosaria M. Galves and my friend Ann for their moral support.

I specially wish to express my gratitude to my good friend Elena for her friendship, help, words of encouragement and continuous support which I will never forget.

Special thanks and appreciation is sincerely expressed to the Brazilian Government for financial support during part of this study.

"...Every acquisition, every step forward in knowledge, is the result of courage, of severity towards oneself, of cleanliness with respect to oneself..."

(F.Nietzsche, Ecce Homo)

TABLE OF CONTENTS

LIST OF TABLES

LIST OF FIGURES

LIST OF SYMBOLS

a	specific surface area, m^{-1}
c_a	air specific heat, kJ/kg-°C
c_p	product specific heat, kJ/kg-°C
c_v	vapor specific heat, kJ/kg-°C
c_w	water specific heat, kJ/kg-°C
D	diffusion coefficient, m^2/hr
G_a	air flow rate, kg/hr-m^2
G_p	grain flow rate, kg/hr-m^2
h'	convective heat transfer coefficient, kJ/hr-m^2-°C
h_{fg}	latent heat of vaporization , kJ/kg
M	moisture content, decimal d.b.
r	radius, m
T	air temperature, °C
t	time, minute or hour
V_a	air velocity, m/hr
V_p	product velocity, m/hr
W	absolute humidity of air, kg water/kg dry air
x	coordinate direction along the length of the dryer, m

Greek Symbols

θ	grain temperature, °C
ϵ	bed porosity
ρ_a	air density, kg/m^3
ρ_p	dry weight product density, kg/m^3

CHAPTER 1

INTRODUCTION

Grains are the major source of food for human and animals throughout the world. Grains include mainly: (1) cereal grains (wheat, corn, rice, barley, sorghum, millet), (2) the oil seeds (soybeans, canola seed, sunflower seed) and (3) legume grains (edible beans, peas).

Grains are grown in all parts of the world. Table 1.1 lists the annual world-wide production of the main cereal grains and of the most important oil seed (soybeans).

Table 1.1: Production of cereal crops and soybeans by region in 1986 (million tonnes).

Area	Wheat	Rice	Corn	Millet	Barley	Sorghum	Soybeans
Africa	11.6	9.8	30.8	11.8	6.3	14.3	0.4
North America	93.5	8.3	231.3	----	28.7	30.4	56.4
South America	16.8	15.3	38.2	0.1	0.8	6.2	21.3
Asia	189.6	434.1	99.7	15.3	18.7	17.4	15.4
Europe	115.8	2.2	68.0	0.03	70.3	0.4	1.6

Source: FAO (1987)

Wheat, rice and corn are the major crops, in terms of tonnage. Asia raises the most wheat and rice. The American Continent is the major producer of corn, sorghum and soybeans. Barley is most popular in Europe, while millet is in Asia and Africa.

In South America, Brazil is one of the most important grain producers. In Brazil, only 10% of the total land (851 million hectares) is used for agricultural production (FAO, 1987). About 80% of this total land is concentrated in the Southeast and South of Brazil where the agriculture system is almost completely mechanized.

The major grains grown in Brazil are corn, rice, wheat, soybeans and dry beans. Rice and dry beans are the staple foods in Brazil; Table 1.2 shows the 1979-1986 production of corn, rice, soybeans and wheat in Brazil and USA.

Table 1.2: Production of corn, rice, soybeans and wheat from 1979-1986 (million tonnes) in Brazil and USA.

Year	Country	Corn	Rice	Soybeans	Wheat
1979-81	Brazil	19.3	8.5	13.5	2.8
	USA	192.0	7.0	56.1	66.2
1984	Brazil	21.2	9.0	15.5	2.0
	USA	194.9	6.3	52.3	66.0
1985	Brazil	22.0	9.0	18.3	4.3
	USA	225.5	6.1	59.1	65.9
1986	Brazil	20.5	10.4	13.3	5.4
	USA	209.6	6.1	56.3	56.8

Source: FAO (1987)

From 1979-1985, the production of corn had an increase of 14% in Brazil and an increase of 17% in the United States; in 1986, the USA and Brazil had a reduction in corn production on order of 7% due to the bad weather conditions. The production of rice decreased in the USA and increased about 15% in Brazil during 1979-86. The soybeans production in Brazil has been rising since 1980; floods in the south of Brazil in

1986 caused the decrease of soybeans production. While in the United States the production of wheat has remained steady since 1980, in Brazil a rise of about 80% occurred during 1985 mainly due to the new production lands on the center west region of Brazil.

Even though the production of grains in Brazil has been rising steadily during the last 30 years (see Figure 1.1), Brazil still imports cereal grains (corn, wheat, rice). Soybeans is a major export grain of

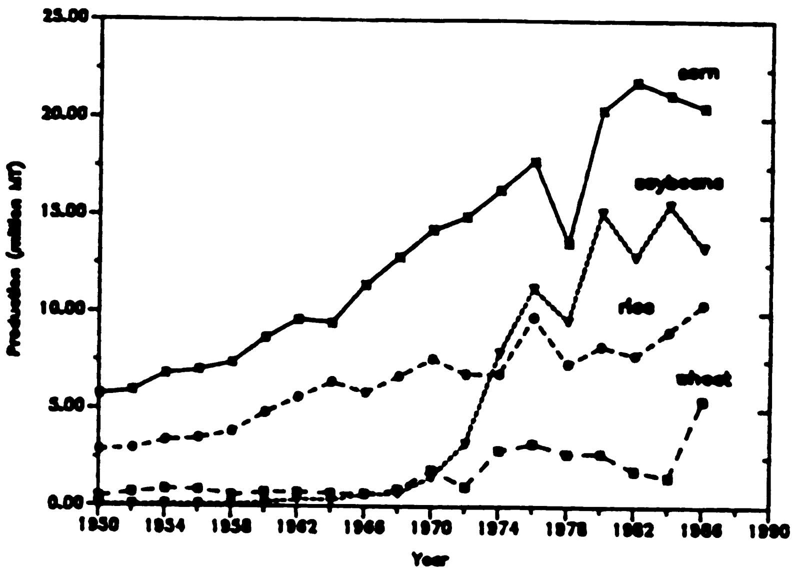

Figure 1.1: Main grains production in Brazil from 1950-1986 (Source: FAO, 1987).

Brazil. In 1986 Brazil exported 1.2 million tonnes of soybeans and imported 2.2 million tonnes of wheat (FAO, 1987). The major problems with Brazilian agriculture are the lack of government incentives, the lack of cultivated land and the low yield; the corn yield in Brazil is about 1,645 kg/ha compared with to 7,487 kg/ha in the USA (FAO, 1987).

Grain is often harvested at moisture contents that are too high to store without spoilage for the selected storage period. Table 1.3 lists the range in the average moisture content at which grains are usually harvested and stored. Different treatments are available to preserve grains at high moisture contents; drying of grain is the most widely used grain-preservation method (Brooker et al., 1981).

In the grain drying industry, the main objective is to obtain a uniform final product of high quality. A large variation in the inlet moisture content of the grain reaching the dryer usually results in

Table 1.3: Maximum and optimum moisture content (% w.b.) for grains at harvest and safe storage.

Cereal	Maximum Harvest Moisture	Optimum Harvest Moisture	6-12 mo. Storage	Over 1 yr. Storage
Barley	20	18	14	13
Edible Beans	20	17	16	14
Corn	30	23	14	13
Rice	28	22	14	13
Oats	20	18	14	13
Wheat	20	18	14	13
Soybeans	18	17	12	11
Sunflower	22	20	10	8

Source: Bakker-Arkema (1988)

underdrying and overdrying of part of the grain. Grain stored at a moisture content above the accepted standard is susceptible to spoilage. Overdrying of grain results in the loss of energy, quality and throughput.

The manual control of continuous-flow dryers is a difficult task. It is usually applied after observation of the inlet moisture content, the outlet moisture content and the outlet grain temperature by: (1) adjusting the throughput, (2) controlling the inlet air temperature, (3) changing the air-flow rate, or (4) combining (1) through (3).

In corn dryers, manual control usually consists of adjusting the throughput. In the rice industry, the operation of multi-stage concurrentflow dryers consists of adjusting the dryer inlet air temperatures according to the maximum allowable grain temperature in the tempering zones. The control performance depends basically on the qualification and experience of the operator. Large variations in the inlet grain moisture always result in some overdrying and underdrying. In general, the achieved manual control is only marginal.

The dryer operation can be improved by automatic control (Bakker-Arkema, 1984). The process is capable of saving 5-30% in energy compared to manual control systems and results in less underdrying/overdrying and loss of throughput.

Automatic control of the drying process has encountered considerable difficulties. The two main reasons are: (1) the complexity of the process, and (2) the lack of commercially reliable on-line moisture meters. The recent developments in digital computers, microelectronics, and control theory have contributed greatly to the implementation of control systems. Automatic moisture controllers already are available for single-stage grain dryers. However, the development of controllers for multi-stage dryers is still lacking.

The main objective of this study is to design a controller for multi-stages dryers which minimizes the variation in the outlet moisture content at arbitrary inlet moisture content oscillations. Different control strategies will be considered for two different dryer types (the crossflow dryer and the concurrentflow dryer).

CHAPTER 2

OBJECTIVES

The objectives of this dissertation are:

1. To develop different linear models for describing the dynamic of the drying process.

2. To develop several control systems for the control of continuous-flow grain dryers based on system identification and adaptive control.

3. To test the control systems on commercial crossflow grain dryers.

4. To develop the unsteady-state model of multi-stage concurrentflow grain drying.

5. To develop an automatic control system for multi-stage concurrentflow grain dryers.

CHAPTER 3

LITERATURE REVIEW

Continuous-flow grain drying is a complex process which requires expertise to obtain acceptable control performance. Large oscillations in the grain inlet moisture and BCFM content, in the ambient conditions, static pressure and drying characteristics often affect deleteriously the dryer operation.

The design of control systems for continuous-flow dryers requires creativity and ingenuity. A major difficulty in the design of a control-system is to reconcile the large-scale, complex, real problem with the simple, well defined problems that control theory considers.

It is difficult to study and compare control systems for grain dryers experimentally; a large amount of grain of varying moisture content and accurate instrumentation are required. Computer simulation provides a quicker method of assessing the performances. In this study, a model of a concurrentflow dryer is developed to predict the unsteady-state behavior of this dryer type resulting from varying inputs.

The chapter leads of with a review of grain dryer systems. The development of modeling different grain dryers is reviewed in the second part of the chapter. The design and implementation of grain dryer control systems are discussed in the third part.

3.1) GRAIN DRYER SYSTEMS

Grain dryers fall into two categories: (1) batch dryers, and (2) continuous-flow dryers. In batch dryers, the grain is dried either with heated air in shallow layers of less than 1 m thickness or with low-temperature air in beds of several meters in depth. The drying may take place in hours, days, weeks or even months. Batch dryers will not be considered further in this thesis.

Continuous-flow dryers are classified according to the relative direction of flow of the grain and the air. The four basic types are: (1) crossflow, (2) concurrentflow, (3) counterflow, and (4) mixed-flow. In the crossflow dryer, the drying air passes perpendicular to the direction of grain flow. In the concurrentflow dryer, the air and the grain flow in the same direction. In the counterflow dryer, the air and grain flow in opposite directions. Grain in mixed-flow dryers is dried by a combination of crossflow, concurrentflow and counterflow actions. Figure 3.1 illustrates a schematic of the four types of continuous-flow dryers. The crossflow and concurrentflow dryers are also available as multi-stage units.

3.1.1) Crossflow Dryers:

The main characteristics of the crossflow dryer can be seen in Figure 3.2.a:

a) Grain on the air inlet side dries first; by the time it leaves the dryer, some of this grain is overheated and overdried.
b) Grain on the air exhaust side is usually underheated and underdried.
c) The difference in moisture content between the air inlet and exhaust sides of the grain column makes mixing after drying essential.

Crossflow dryers are simple in construction. They generally have lower initial cost than other continuous-flow dryer types. Commercial crossflow dryers are usually non-mixing type dryers.

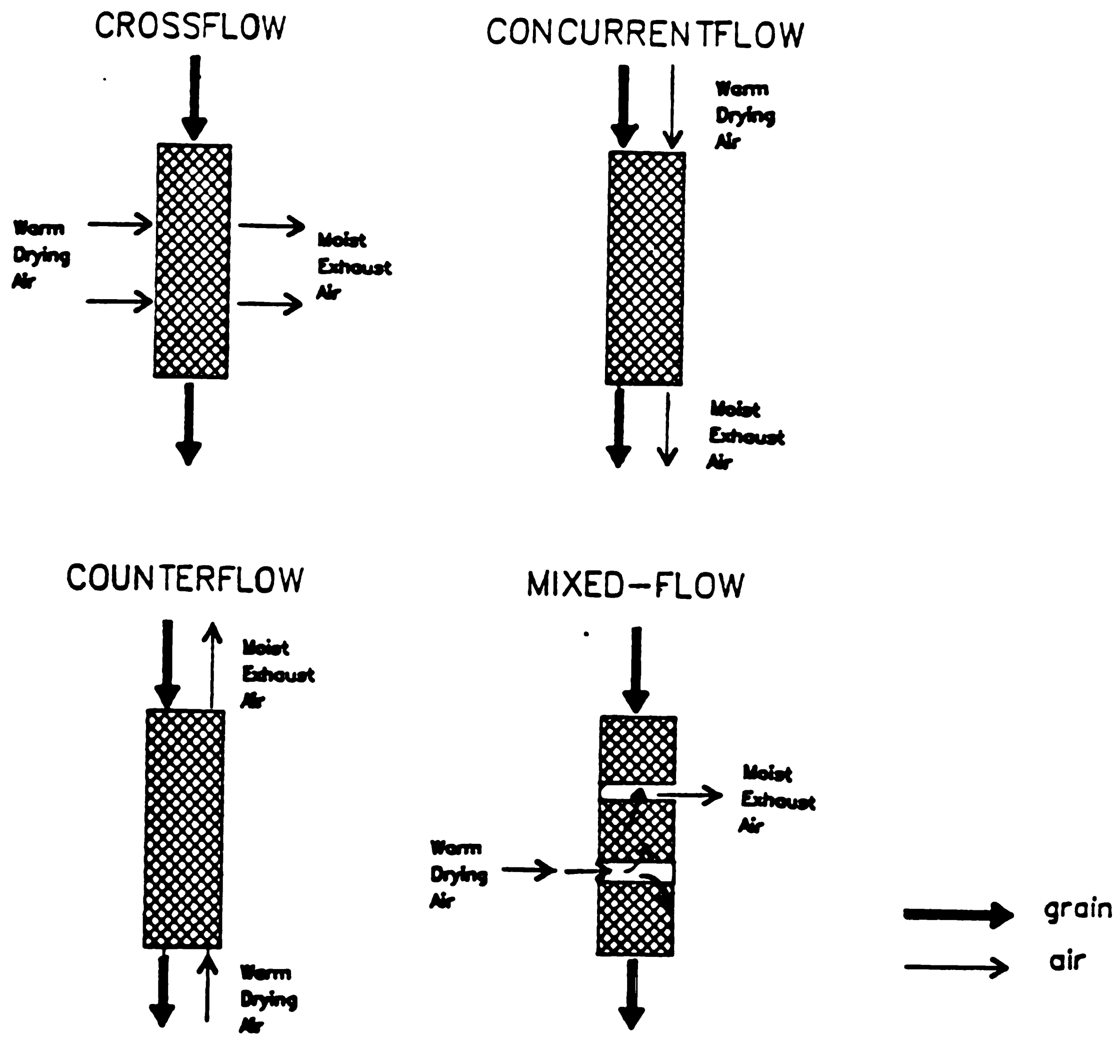

Figure 3.1: Schematic of the four basic types of continuous-flow grain dryers.

The crossflow dryer is at present the most widely used system in the USA. Figure 3.3 shows a schematic representation of the simple crossflow dryer with a crossflow cooler. This design leads to a energy consumption of 7,000-9,000 kJ/kg (Nellist, 1982).

An improvement in the energy efficiency is obtained by recycling the cooling air and part of the drying air (Lerew et al.,1972; Meiering and Hoefkes, 1977; Pierce and Thompson, 1982). Reversal of the airflow direction in crossflow dryers is a design used to reduce the moisture differential in the dried grain. Crossflow corn dryers without air-reversal (or a grain inverter) have gradients across the column as large as 20% in moisture content and 50% in grain breakage (Gustafson et al., 1981). An example of a crossflow dryer with air recirculation and air-reversal (the so-called Hart-Carter design) is illustrated in Figure 3.4.

The specification of a typical commercial-size crossflow dryer with air recirculation and air-reversal, and some specific test results of the drying of corn are shown in Table 3.1.

Three new features have recently been added to the basic crossflow design, differential grain-speed, grain mixing and tempering (Moreira, 1983). Tests have shown an improvement of this dryer type in the energy efficiency and grain quality compared to conventional crossflow drying (Bakker-Arkema et al., 1982). Figure 3.5 shows a schematic of the so-called differential grain-speed crossflow dryer.

Table 3.2 shows some specific test results of the drying of corn in a commercial-size crossflow dryer with differential grain speed.

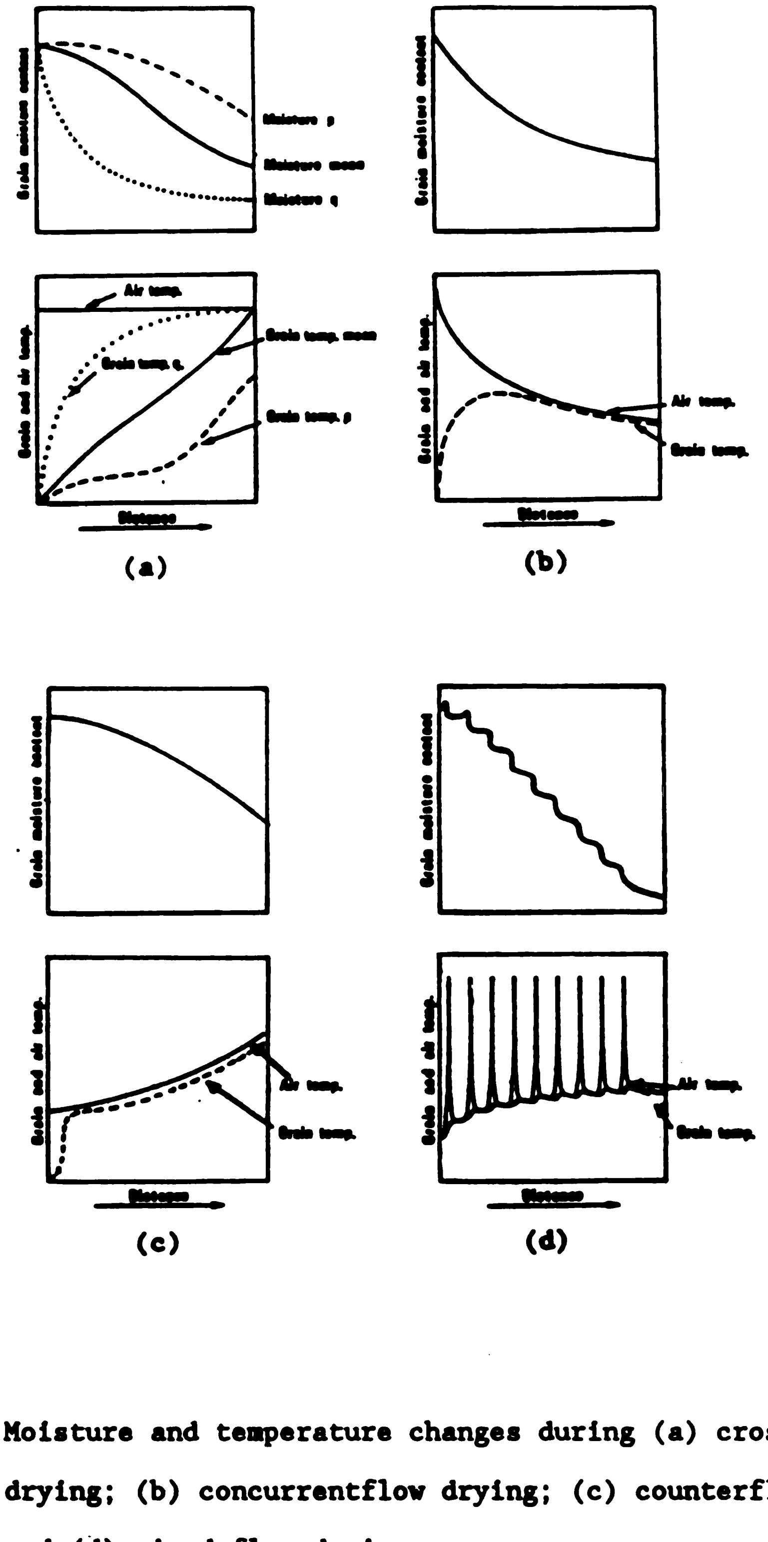

Figure 3.2: Moisture and temperature changes during (a) crossflow drying; (b) concurrentflow drying; (c) counterflow drying; and (d) mixed-flow drying.

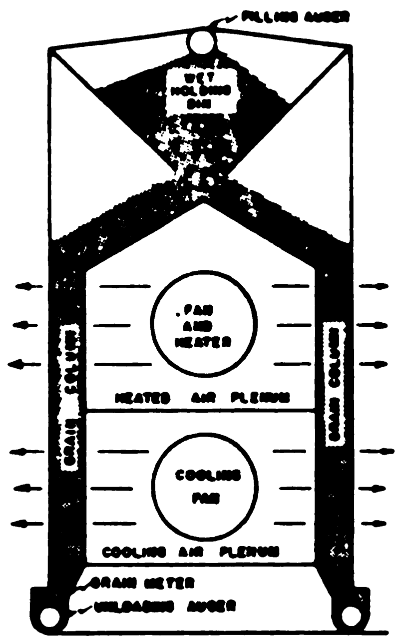

Figure 3.3: Crossflow dryer with forced-air drying and cooling (Brooker, 1981).

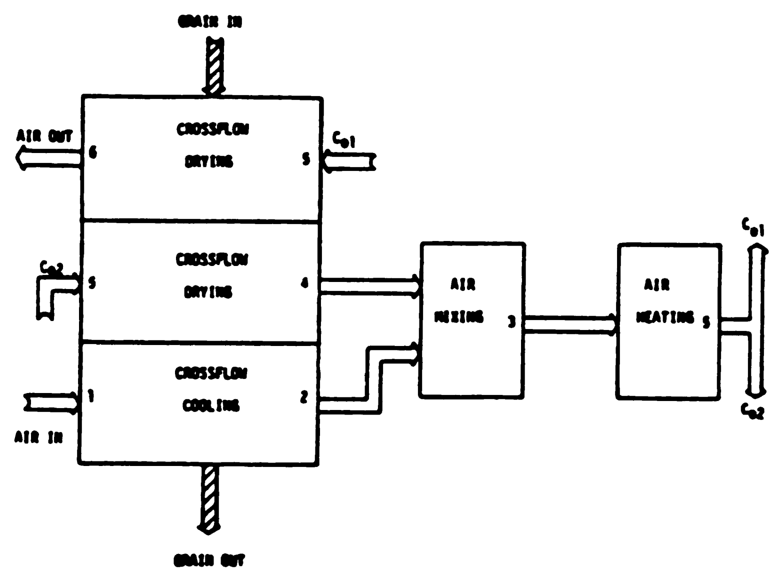

Figure 3.4: Schematic of 3-stage crossflow dryer with partial air recycling (Brooker, 1981).

Table 3.1: Experimental results of the drying of corn in a crossflow dryer with air recirculation and air-reversal.

PARAMETERS	VALUE
Grain flow rate [tons/hr-m^2]	7.8
Grain flow speed [m/hr]	8.0
Inlet moisture content [%w.b.]	29.0
Ambient temperature [°C]	1.0
Inlet corn temperature [°C]	8.0
Grain column length [m]	
first stage	7.6
second stage	5.2
cooling stage	5.5
Cross-section area [m^2]	3.2
Fan horsepower [HP]	200.0
Inlet air temperature [°C]	99.0
Air flow rate [m^3/min-m^2]	15.5
Static Pressure [Pa]	971.5
Outlet corn temperature [°C]	16.7
Outlet moisture content [%w.b.]	13.9
Percentage points removed [%w.b.]	15.1
Dryer efficiency [kJ/kg water]	4,536.0
Breakage suscept. increase [%]	17.5

Source: Rodriguez (1982)

Table 3.2: Experimental results of the drying of corn in a crossflow dryer with air recirculation, differential grain speeds and tempering.

PARAMETERS	VALUE
Grain flow rate [tons/hr-m^2]	
burner side	10.7
exhaust side	5.3
Inlet moisture content [%w.b.]	20.5
Ambient temperature [°C]	2.0
Inlet corn temperature [°C]	8.0
Grain column length [m]	
first stage	3.7
second stage	2.1
cooling stage	0.5
Cross-section area [m^2]	1.7
Fan horsepower [HP]	60.0
Inlet air temperature [°C]	94.0
Air flow rate [m^3/min-m^2]	9.9
Static Pressure [Pa]	672.6
Outlet corn temperature [°C]	---
Outlet moisture content [%w.b.]	15.4
Percentage points removed [%w.b.]	5.1
Dryer efficiency [kJ/kg water]	3,729.0
Breakage suscept. increase [%]	36.4

Source: Rodriguez (1982)

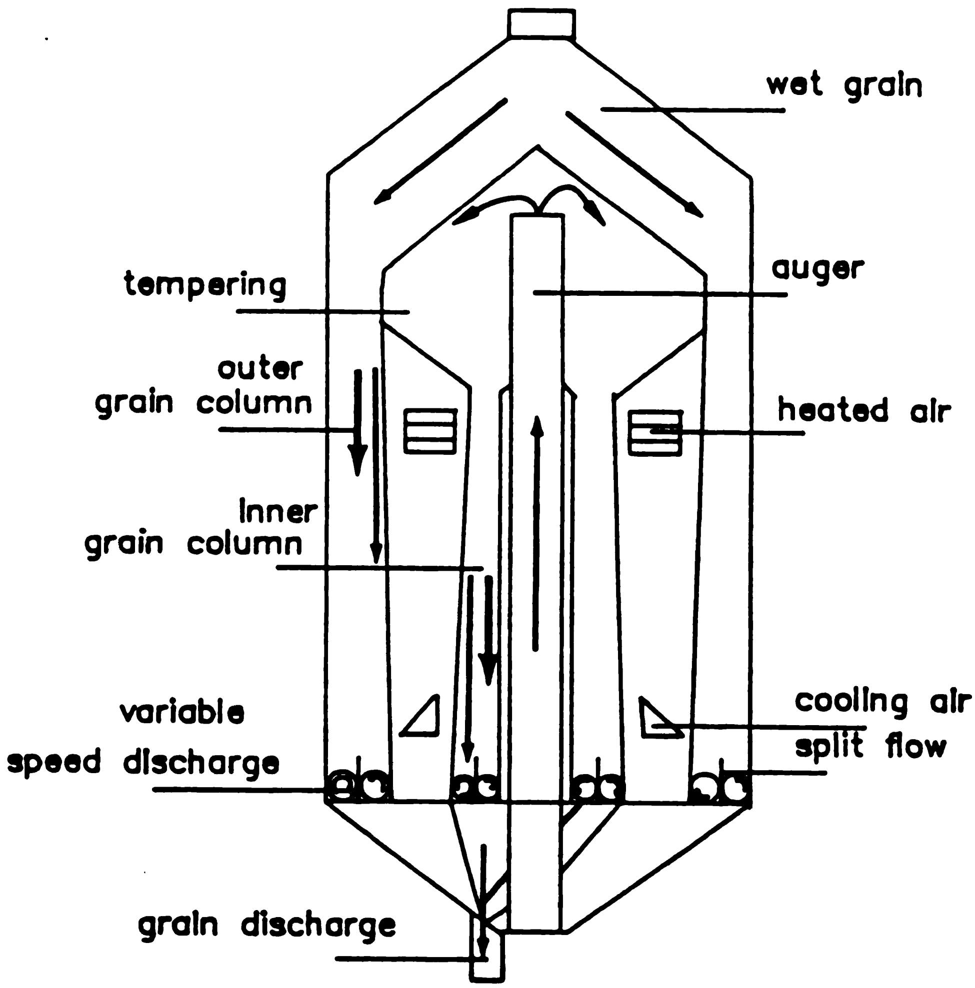

Figure 3.5: Schematic of a crossflow dryer with differential grain-speed and tempering.

3.1.2) Concurrentflow Dryers:

The main characteristics of the concurrentflow dryer (see Figure 3.2.b) are:

a) The grain and the drying air enter the drying section at the same point; thus the warmest drying air encounters the wettest, coldest grain.
b) There is a rapid conversion of sensible heat to latent heat of the water evaporated from the grain; this cools the air down.
c) The peak temperature reached by the grain is well below the temperature of the air at the inlet.
d) The grain is uniformly dried.

Compared with crossflow drying, concurrentflow drying is efficient because: 1) the use of high drying air temperature minimizes energy use and the quantity of drying air needed, 2) all the grain receives the same treatment, thus no energy is wasted in overdrying.

A concurrent/counterflow dryer consists of one or more concurrent flow drying stages coupled to a counterflow cooling bed; in the multi-stage units a tempering zone separates two adjoining drying beds (Brook and Bakker-Arkema, 1980).

The concurrent/counterflow dryer is a relatively new development and is at present only manufactured in the U.S.A. Figure 3.6 presents a schematic of a two-stage concurrent/counterflow dryer.

The maximum drying temperature in a concurrentflow dryer is not limited by the type or the moisture content of the product; grain velocity is the determining parameter (Bakker-Arkema, 1984). Air temperatures as high as 500°C have been used in drying corn without affecting product quality (Hall and Anderson, 1980). The energy efficiency of

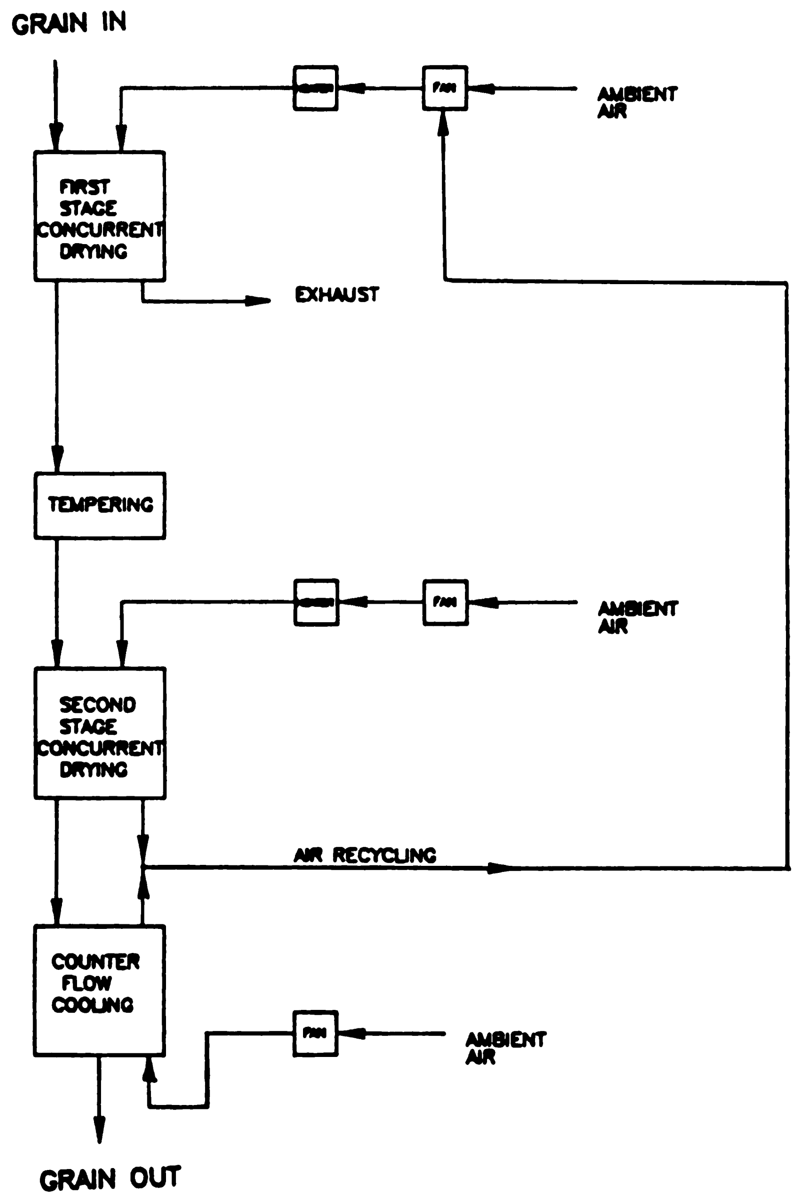

Figure 3.6: Schematic of a two-stage concurrentflow grain dryer with counterflow cooler and air recycling.

concurrentflow dryers with or without air recirculation ranges from 3,000 to 3,800 kJ/kg (Bakker-Arkema et al., 1982).

The specifications of a typical two-stage commercial-size concurrentflow dryer with counterflow cooler are given in Table 3.3. The operating conditions are for the drying of long-grain rice from 16.6 to 13% w.b. at a rice processing plant. The first drying stage exhibits a fuel efficiency of 5,389 kJ/kg of water removed compared to the second stage (3,177 kJ/kg water). The fuel efficiency of the second stage is affected by the tempering zone between the two drying stages. The moisture gradient in the rice is reduced from 5.2 to 0.2 percentage points after 76 minutes in the tempering zone (Fontana et al., 1982).

3.1.3) Counterflow Dryers:

The main characteristics of the counterflow dryer (see Figure 3.2.c) are:

a) The grain travels against the flow of the air.
b) When this process reaches a steady-state, the grain is exhausting at or near the ambient air temperature, and the air is exhausting at or near the temperature of the warm grain.

The process is efficient for cooling but its use for grain drying is limited because of the sensitivity of the grain to high temperatures.

3.1.4) Mixed-Flow Dryers:

The main characteristics of the mixed-flow dryer (see Figure 3.2.d) are:

a) The air temperature falls rapidly as it penetrates the grain bed.

Table 3.3: Experimental results of the drying of long-grain rice in a two-stage concurrentflow dryer.

PARAMETERS	VALUE
Grain flow rate [tons/hr-m^2]	2.4
Grain flow speed [m/hr]	4.1
Inlet moisture content [%w.b.]	16.6
Ambient temperature [°C]	24.0
Cross-section area [m^2]	5.0
Inlet corn temperature [°C]	21.0
FIRST STAGE	
Bed depth [m]	1.1
Tempering length [m]	5.2
Air flow rate [m^3/min-m^2]	36.6
Inlet air temperature [°C]	135.0
Outlet rice temperature [°C]	43.0
Outlet air temperature [°C]	43.0
Outlet moisture content [%w.b.]	15.0
Stage efficiency [kJ/kg water]	5,389.0
Static pressure [Pa]	2,000.0
SECOND STAGE	
Bed depth [m]	1.2
Tempering length [m]	0.0
Air flow rate [m^3/min-m^2]	39.2
Inlet air temperature [°C]	77.0
Outlet rice temperature [°C]	37.0
Outlet air temperature [°C]	38.0
Outlet moisture content [%w.b.]	13.5
Stage efficiency [kJ/kg water]	3,177.0
Static pressure [Pa]	2,240.0
COOLER	
Bed depth [m]	1.7
Air flow rate [m^3/min-m^2]	18.3
Inlet air temperature [°C]	24.0
Outlet moisture content [%w.b.]	13.0
Percentage points removed [%w.b.]	3.6
Dryer efficiency [kJ/kg water]	3,689.0
White rice inlet head yield [%]	60.0
White rice outlet head yield [%]	62.0

Source: Fontana et al. (1984)

b) The grain temperature only rises a few degrees per bed.

c) The grain receives a uniform drying treatment.

Mixed-flow or cascade dryers are popular in Western Europe and South America. Pollution control is constly in mixed-flow dryers which makes them unpopular in the United States (Hawk et al. 1978).

The inlet air temperature in a mixed-flow dryer can be higher than in crossflow models because the grain is not subjected to the high air temperature for as long a period of time; as a result, 40% less air and energy is needed compared to crossflow dryers (Nellist, 1982). Mixed-flow dryers have the advantage of a concurrentflow dryer without the mechanical complexity. Its disadvantage is that if a low flowrate is used, as when drying very wet grain in one pass, non-uniform moisture is obtained (Hawk et al., 1978). The energy efficiency of mixed-flow dryers with recirculation air has been reported to be 3,500-4,000 kJ/kg (CNEEMA, 1979).

Table 3.4 shows some test results of the drying of soybeans in a commercial-sized mixed-flow dryer.

Table 3.4: Experimental results of the drying of soybeans in a mixed-flow dryer.

PARAMETERS	VALUES
Dryer characteristic	
Effective drying bed length [m]	2.7
Effective cooling bed length [m]	0.9
Ambient air temperature [°C]	30.6
Ambient humidity ratio [kg/kg]	0.012
Inlet air temperature [°C]	100.0
Air flow rate [m^3/min]	378.0
Grain flow rate [tons/hr]	10.1
Inlet moisture content [%w.b.]	18.5
Final moisture content [%w.b.]	16.3

Source: Dalpasquale (1985)

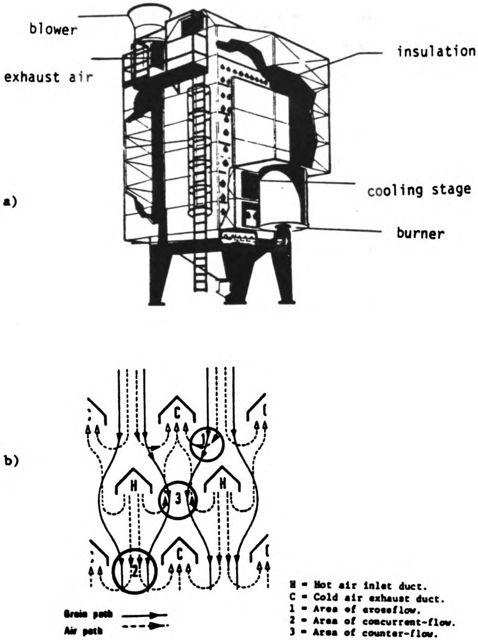

Figure 3.7: a) Schematic of a mixed-flow grain dryer; b) Distribution of air in the ducts of a mixed-flow dryer.

3.1.5) Other Dryer Types:

Different types of dryers other than those included in the preceding discussion have been used to dry cereal grains (Bakker-Arkema et al., 1978). The most important designs used in the grain industry are: (1) rotary dryers, (2) fluidized-bed dryers, and (3) spouted-bed dryers.

A rotary dryer consists of a slightly inclined long cylindrical shell which rotates slowly. In a concurrentflow rotary dryer, the moist grain kernels and the hot drying air are introduced at the same end of the dryer; the dried grain and moist air exit at the other end. Inside of the dryer, lifting flights lift the particle and shower it down in a moving curtain through the air. Figure 3.8 shows a concurrentflow rotary dryer (Keey, 1972). The drying air temperatures in rotary dryers can be as high as 510°C (Katic, 1974). Rotary dryers are utilized in many rice parboiling plants for removal of moisture from soaked and steamed rough rice (Bakker-Arkema et al., 1984). Rotary dryers are expensive to install and require considerable maintenance.

Table 3.5 shows typical experimental data for drying parboiled rice in three rotary dryers in series. Parboiled rice is dried in one pass from 35-14% w.b. at an air temperature of 288°C in the first dryer, 232°C in the second, and 149°C in the third unit. Eleven points of moisture are removed in the first dryer, six points in the second, and four in the last unit. The decrease in the fuel efficiency from dryer one to dryers two and three is significant.

Fluidized-bed dryers are used commercially for the drying of milk powder and other fine materials; they also have been tested for drying grains (Pawlowiski, 1975). Figure 3.9 illustrates the design of a

Table 3.5: Performance data of three-rotary dryer system in a rice parboiling plant.

PARAMETERS	VALUES
Dryer dimensions [m]	
length	9.8
diameter	2.6
Air temperature [°C]	
dryer 1	260.0
dryer 2	204.0
dryer 3	149.0
Rice flow rate [ton/hr]	9.4
RPM	10-12
Energy required [kW]	90.0
Inlet moisture content [%w.b]	
dryer 1	34.6
dryer 2	23.3
dryer 3	17.8
Outlet moisture content [%w.b.]	
dryer 1	23.3
dryer 2	17.8
dryer 3	14.1
Fuel efficiency [kJ/kg]	
dryer 1	4,105.0
dryer 2	7,408.0
dryer 3	8,729.0

Source: Bakker-Arkema et al.(1984)

typical fluidized-bed dryer. Heated air is blown through an orifice plate (grid) into a bed of particles at a flow rate to cause fluidization. As the particles dry, they lose weight and tend to float toward the product discharge. A proper combination of air velocity and particle velocity is critical for successful operation of a fluidized-bed dryer (Bakker-Arkema et al., 1978).

Advantages of a fluidized-bed drying system are (Pawlowiski, 1975): (1) the excellent contact and thus high heat transfer rate between the particles and the surrounding drying air, (2) the ability to closely control the particle temperature, (3) the uniformity of the drying of the particles, (4) the high thermal efficiency, and (5) the relatively low initial cost.

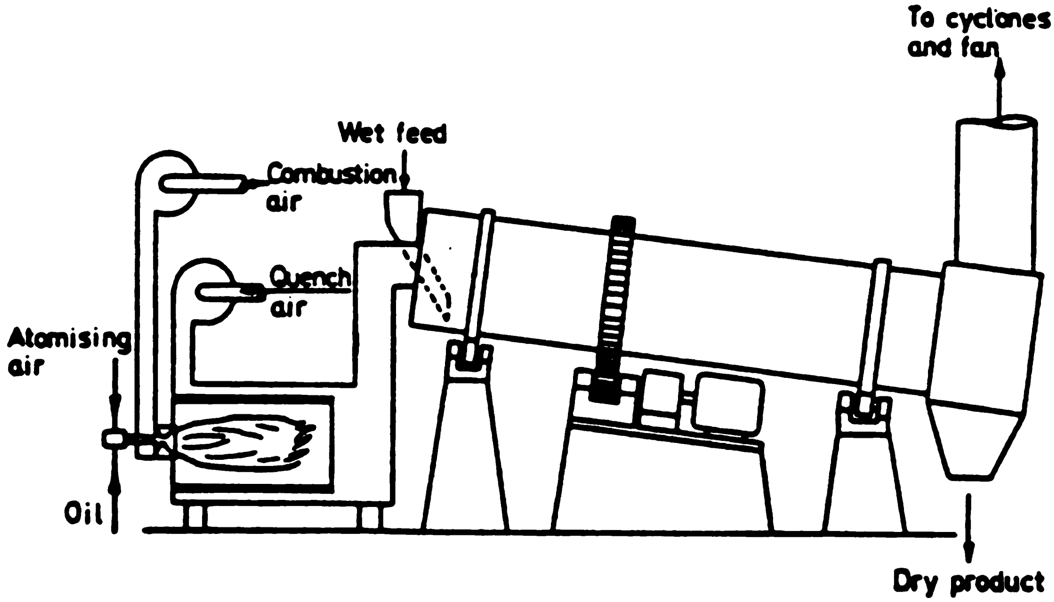

Figure 3.8: Concurrentflow rotary dryer (Source: Keey, 1972).

Disadvantages of fluidized bed dryers include: (1) the need for a very efficient dust arrestor system, (2) the requirement for a uniform particle size, (3) the high power demand, (4) the difference in fluidizing air velocities for different particles, and (5) the difficulty of switching from one crop to another.

Fluidized-bed dryers are not used commercially as grain dryers except for rice in China (Bakker-Arkema, 1988). They are best suited for products which lose moisture primarily during the constant-rate period (Nonhebel and Moss, 1971). Cereal grains, however, dry at the falling-rate period. The range of particles size is another important criterion. If the ratio of the largest to the smallest exceeds 8, the coarse particles tend to settle out while the smallest particles are immediately carried to the dust arrestor (Kearns, 1974).

The <u>spouted-bed</u> dryer, a modification of fluidized-bed, has been tested with different grains (Passos et al, 1987). A schematic of the spouted-bed dryer is shown in Figure 3.10. The inlet drying air is introduced into the cone-shaped bottom of the bed instead of uniformly over the cross section. The air flows upward through the center of the bed, causing a fountain of particles. The particles then fall into the annulus region near the wall, descending to the base before reentraiment into the central "spout".

Advantages of a spouted-bed dryer include (Passos et al., 1987): (1) it can handle particles with a diameter bigger than 1 mm, (2) the intensive particle circulation at low air flow rate, (3) the uniformity of the particle drying, (4) the use of high air temperature without particle damage, (5) the low investment cost, and (6) the reduced space for installation.

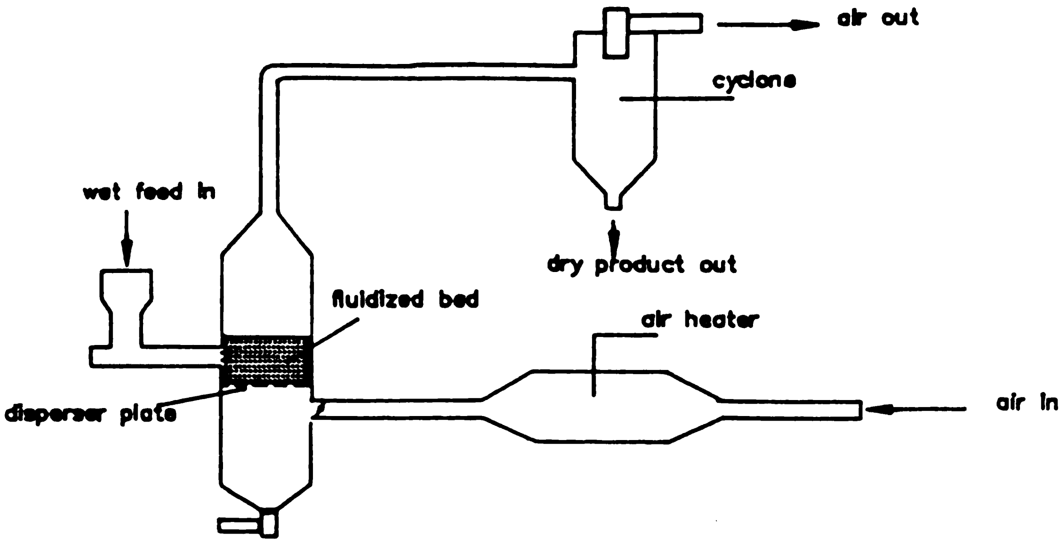

Figure 3.9: Fluidized-bed dryer.

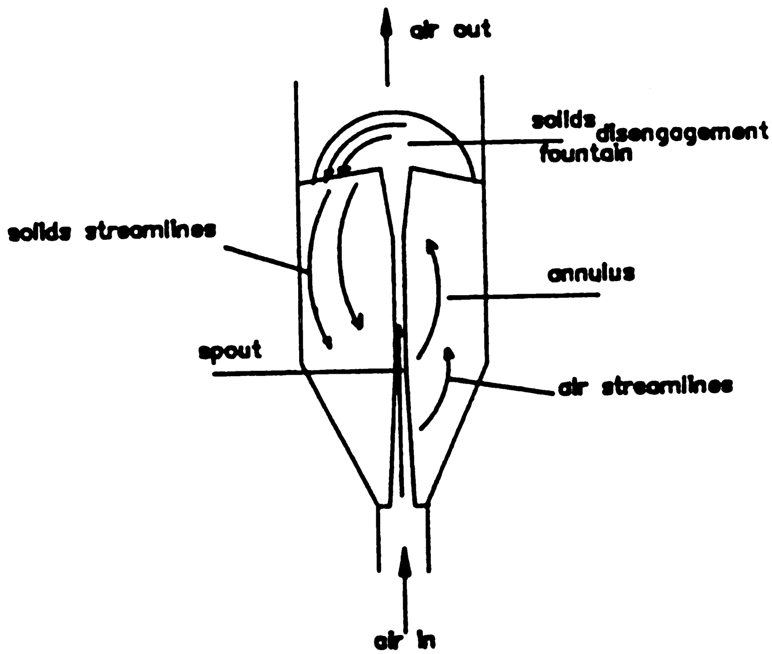

Figure 3.10: Spouted-bed dryer.

Disadvantages are: (1) the high pressure drop, (2) the limited capacity per unit space, (3) fluid mechanics controls the air flow rather than heat and mass transfer, and (4) the difficulty to scale up.

Spouted-bed dryers are not used widely in the drying industry; most applications are associated with high value, low volume materials.

Table 3.6 lists results of a sample design calculation for drying wheat in a spouted-bed dryer (Passos et al., 1987). The capacity

Table 3.6: Performance data of the drying of wheat in a spouted-bed dryer with a crossflow cooler.

PARAMETERS	VALUES
Ambient temperature [°C]	18.0
Initial moisture content [%w.b.]	19.0
Wheat flow rate [kg/hr]	840.0
Inlet grain temperature [°C]	21.0
Bed diameter [m]	0.6
Inlet air nozzle diameter [m]	0.1
Cone angle [°]	90.0
Dryer height [m]	1.2
Fan power [kW]	3.7
Airflow rate [kg/hr]	907.2
Mean residence time [minutes]	17.0
Inlet air temperature [°C]	230.0
Outlet moisture content [%w.b.]	14.0
Outlet wheat temperature [°C]	23.0
Percentage points removed [% w.b.]	5.0
Dryer efficiency [kJ/kg water]	4,300.0

Source: Passos et al. (1987)

of this spouted-bed dryer is small, about 1.00 tonne per hour at 5 points removal; the energy efficiency in removing 5 points of moisture from 19.0 to 14.0% moisture content is 4,300 kJ/kg.

3.2) MATHEMATICAL MODELING OF CONTINUOUS-FLOW GRAIN DRYING

3.2.1) Thin-Layer Drying Equations

In thin-layer drying experiments, air at constant humidity, temperature and mass flow rate is passed through a thin-layer of moist material. It was observed in early experiments (Sherwood, 1936) that drying takes place at two distinct rates:

(1) at constant-rate during which the evaporation is limited by external moisture transfer; and

(2) at falling-rate period during which the evaporation is limited by internal moisture diffusion.

For cereal grains, the drying usually takes place in the falling-rate period. This implies that the drying rate of the individual kernels decreases continuously during the course of drying.

Prediction of the drying rate of biological products is more complicated during the falling-rate period than during the constant-rate period. External transfer mechanisms (convection and convective mass transfer) and internal transfer mechanisms (conduction and diffusion) have to be considered in the analysis. Many theories have been proposed for predicting the drying behavior of cereal grains in the falling-rate period. They can basically be divided into diffusion and empirical type of relationships (Brooker et al., 1981).

Luikov (1966) described the phenomenon of drying capillary porous products in terms of the following physical mechanisms:

(1) liquid transport due to capillary forces (molar transport) and moisture concentration gradients (diffusion);

(2) vapor and liquid transport due to moisture and temperature gradients;

(3) liquid vapor transport due to total pressure differences.

By considering the various fluxes involved in a four-component mixture (four-phase system) of air, vapor, liquid and solid, and using the basic laws of mass and energy transfer, Luikov derived a model of the following form:

$$\frac{\partial \boldsymbol{\chi}}{\partial t} = \mathbf{K}\nabla^2\boldsymbol{\chi} \qquad \text{........(3.1)}$$

where $\chi = (x,t) = (M,T,p)$

M = moisture content within the particle

T = temperature content within the particle

p = total pressure within the particle

$\mathbf{K} = \{K_{ij}\}$ = elements which depend on the physical properties of the particle; K_{ii} are phenomenological coefficients and K_{ij}, $i \neq j$, represent coupling between various transport mechanisms.

Although Eqns.(3.1) are widely applicable, they have not been used to describe single kernel grain drying since insufficient data is available for the estimation of the coupling coefficients in the matrix $\mathbf{K}$. However, under various simplifying assumptions, modified versions of Eqns.(3.1) have been adapted for the description of grain drying.

In the drying of cereal grains, the temperature attained by the grain is sufficiently low to regard the effect of the total pressure gradient term as negligible (Luikov, 1966). Eqns.(3.1) are then reduced to a two-equation system involving only the grain moisture content (M) and the temperature (T). It was concluded that for engineering accuracy, consideration of the coupling effects of temperature and moisture in the analysis of grain drying is not required (Brooker et al., 1981). Therefore, Eqns.(3.1) reduce to the system:

$$\frac{\partial M}{\partial t} = D_m \nabla^2 M \qquad \text{......(3.2.1)}$$

$$\frac{\partial T}{\partial t} = D_t \nabla^2 T \qquad \text{......(3.2.2)}$$

where D_m and D_t represent the moisture and thermal diffusivities, respectively.

Since Eqn.(3.2.2) is seldom significant in drying grains (Brooker et al., 1981), grain drying can be represented by Eqn.(3.2.1):

$$\frac{\partial M}{\partial t} = D\left[\frac{\partial^2 M}{\partial r^2} + \frac{c}{r}\frac{\partial M}{\partial r}\right] \qquad \text{........(3.3)}$$

where D is assumed to be constant. The constant c is zero for a slab, 1 for a cylindrical body, and 2 for a sphere. The following initial and boundary conditions are frequently assumed in solving Eqn.(3.3) (Brooker et al., 1981):

$$M(r,0) = Min \qquad \text{......(3.4.1)}$$

$$M(r_0,t) = Me \qquad \text{......(3.4.2)}$$

where Min is the initial moisture content and Me is the equilibrium moisture content of the grain kernel.

The equilibrium moisture content is defined as the moisture content of the material after it has been exposed to a particular environment for an infinitely long period of time. The Me is dependent upon the humidity and temperature conditions of the environment as well as on the species, variety and hystory of the grain (Brooker et al. 1981).

A number of theoretical and empirical models have been proposed for calculating the moisture equilibria of grains. The theoretical equilibrium moisture content models are based on: (1) capillary condensation [Kelvin model], (2) kinetic adsorption [Langmuir, BET, GAB models], and the field-strength potential [Harkins-Jura model] (Brooker et al. 1981). The theoretical models are not applicable to grains over the entire range of relative humidity and temperature values. Therefore, it is preferable to use purely empirical equations until a better understanding of the physical process involved in moisture equilibria is obtained.

A well-known relationship for predicting the Me of grains is the semi-empirical model proposed by Henderson (1952):

$$1-[P_v/P_{vs}] = \exp\ [-h*T_{abs}M^i] \qquad \ldots\ldots(3.4.3)$$

where P_v is the water vapor pressure of the grain, P_{vs} is the saturated water vapor pressure at the equilibrium temperature of the system, M is the moisture equilibrium content (%d.b.) and h and i are product constants.

Henderson's original Eqn.(3.4.3) has proven to be inadequate for grains (Bakker-Arkema et. al, 1981). Thompson (1967) modified the Eqn.(3.4.3) and proposed the following empirical model of the Me of grains:

$$1-[P_v/P_{vs}] = \exp\ [-K(T+C)(100*M)^N] \qquad \text{......(3.4.4)}$$

where T is the temperature (°C) and the M the moisture content (decimal d.b.); K, N and C are product constants.

The empirical Chung equation (Chung and Pfost, 1967) also predicts well the Me values of grain well. The Chung equation has the form:

$$M = E-F\ \ln[-(T+C)\ \ln(P_v/P_{vs})] \qquad \text{......(3.4.5)}$$

where M is the moisture equilibrium content (decimal d.b.) and T is the temperature (°C); E and F are product constants.

At the present time, the modified Henderson and Chung Me equations are recommended for use in grain-drying calculations.

The analytical solution of Eqn.(3.3) for the average moisture content of various regulary shaped bodies can be found in Crank (1957).

Pabis and Henderson (1961) made use of the analytical solution of Eqn.(3.3) to describe the drying of shelled corn. They assumed an Arhenius type relation for the moisture diffusivity, D:

$$D = D_0\exp(-E_0/R_0T) \qquad \text{........(3.5)}$$

Chu and Hustrulid (1968) solved Eqn.(3.3) numerically for corn, using an explicit finite-difference method, and assumed the diffusion coefficient to be of the form:

$$D = a_0\exp(b_0M) \qquad \text{........(3.6)}$$

Bakker-Arkema and Hall (1965), Young and Whitaker (1971), Rowe and Gunkey (1972), Steffe and Singh (1982), also used the diffusion Eqn.(3.3) to analyze the drying of grains.

Lewis (1921) suggested an empirical model to describe the drying rate, analogous to Newton's law of cooling:

$$\frac{dM}{dt} = -k_0(M-Me) \qquad ....(3.7)$$

where k_0 is a constant. After integrating, Eqn.(3.7) becomes:

$$MR = \exp(-k_0 t) \qquad ....(3.8)$$

where: MR = moisture ratio = $\frac{M(t)-Me}{Min-Me}$

Eqn.(3.8) is often referred to as the exponential (or logarithmic) model. It has been widely used as a basis for modeling the drying rate of grains (Parry, 1985).

Page (1949) presented a modification of Eqn.(3.8) for describing the drying of shelled corn. The model has the following form:

$$MR = \exp(-k' t^n) \qquad ....(3.9)$$

where k' and n are drying constants. A number of investigators have used Eqn.(3.9) to describe the thin-layer drying of grains (White et al., 1973; Misra and Brooker, 1980; Syarief et al., 1980; and, Huizhen and Morey, 1984).

Thompson (1967) proposed the following empirical equation for the drying of shelled corn:

$$t = A_0 \ln(MR) + B_0 \ln(MR)^2 \qquad ....(3.10)$$

where t is the drying time in hours, MR is the moisture ratio, and A_0 and B_0 are empirical coefficients which are functions of temperature.

The two-term exponential model of the form:

$$MR = A_0 \exp(-k_1 t) + B_0 \exp(-k_2 t) \qquad ....(3.11)$$

has been used by several researchers (Nellist et al, 1971; Rowe and Gunkel, 1972; Henderson, 1974; Nellist, 1976) to fit the experimental drying data for different grains. Sharaf-Eldem et al. (1980) found that the two-term exponential model adequately describes thin-layer drying of shelled corn, rough rice and soybeans.

3.2.1.1) Discussion of Drying Equations

Neither the theoretical nor the empirical drying equations discussed in the previous section represent the drying process of cereal grains accurately over the full moisture range.

The reasons why the drying equations based on diffusion theory do not predict the drying behavior of grains accurately are: (1) the improper choice of boundary conditions, and (2) the incorrect assumption that D and k are independent of moisture content (Brooker et al., 1981).

The boundary conditions in Eqn.(3.4.2) imply that the grain surface moisture content reaches the equilibrium moisture content instantaneously. This assumption is a simplification. It is more realistic to solve the diffusion equation with a convective type boundary condition:

$$D \frac{\partial M}{\partial r} \Big|_{r=r_0} = h'_d[M(surf)-Me] \qquad \text{.......(3.12)}$$

Since the h'_d (convective mass-transfer coefficient) is finite, the grain surface moisture does not come to equilibrium instantaneously at the start of the drying process, but comes to equilibrium exponentially. Solutions of Eqn.(3.3) with boundary conditions of the type of Eqn.(3.12) can be found in standard heat-transfer books (Holman, 1984).

In the development of the drying equations it has been assumed that the diffusion coefficient (D) or the drying constants (k_0, k_1, k_2, and k') are constant, i.e., they are not dependent on the grain moisture contents. If the drying takes place over a significant moisture content range, this assumption leads to serious errors in the calculated moisture contents (Brooker et al.,1981). Another important factor is the effect of the grain-hybrid and grain-damage on the drying rate of a grain kernel; significant differences in drying rate between different corn hybrids, and between low-level and high-level damaged corn of the same hybrid have been observed (Bakker-Arkema, 1988).

Different models for calculating the drying rates of cereal grains have been presented. Eqns.(3.3), (3.8), and (3.9) give satisfactory results if D or k-values are known, and the drying takes place over a limited moisture content range. If greater accuracy is required in the predicted drying rates, as in simulation of deep-bed drying, the convective boundary condition of Eqn.(3.12) and a variable

-diffusion coefficient equation may have to be employed in conjunction with the diffusion equation. Finally, the empirical equations such as Eqn.(3.10) and (3.11) give excellent results within the temperature and moisture range for the particular grain for which they were developed.

3.2.2) Deep-Bed Drying Models

A thin-layer model does not describe the heat, mass and momentum transfer processes in deep-beds of grain; it only provides the necessary equation for the drying rate of the particular grain which is dried in the deep bed.

Deep-bed models are generally divided in two types: (1) empirical or semi-theoretical, and (2) theoretical. The first type leads to algebraic-type equations; the second to more complex partial differential equations (p.d.e.). The empirical models have contributed significantly to the understanding of the process involved in deep-bed grain drying. However, due to the various assumptions inherent in their derivation, they are less accurate than the theoretical p.d.e. models (Parry, 1985).

Thompson et al. (1968) presented semi-theoretical models for the continuous-flow drying of grain. The models are based on heat and mass balances taken over a thin-layer of grain in which it is assumed that conditions are constant over a given increment in time. Steady-state crossflow, concurrentflow and counterflow drying were developed. Boyce (1966), and Henderson and Henderson (1968) used a similar approach to simulate the drying of a stationary deep-bed of grain.

Bakker-Arkema et al. (1974) presented a more fundamental approach. Based on the laws of simultaneous heat and mass transfer, they developed the steady-state fixed-bed, crossflow, concurrentflow and counterflow models. Sets of three differential equations (p.d.e.), plus an appropriate thin-layer rate equations are employed to describe the drying in various stationary and continuous-flow drying systems. The p.d.e. models for crossflow, concurrentflow, counterflow and fixed-bed are similar in form; however, they are solved using different numerical methods. Laws and Parry (1983) presented the Michigan State University (MSU) p.d.e. models in a general form.

O'Callaghan (1971) presented a discretization of the p.d.e. models to simulate continuous-flow grain dryers. Nellist (1974) used the same approach to simulate the drying of a fixed-bed of grains. The drying bed is considered to consist of several thin-layers of grains. Heat and mass transfer equations are solved to calculate the changes in grain and air conditions for every layer for every time step until steady state is reached (Parry, 1985). The model has been successfully used in a number of simulations, including those of concurrentflow, counterflow, and mixed-flow type dryers (Bruce, 1984), and of crossflow dryer (Nellist, 1987).

3.2.2.1) Continuous-flow Grain Dryer Models

The MSU steady-state crossflow model with the appropriate boundary conditions has the following form (Brooker et al., 1981):

$$\frac{\partial T}{\partial x} = \frac{-h'a}{G_a c_a + G_a c_v W} (T-\theta) \qquad .....(3.13.1)$$

$$\frac{\partial \theta}{\partial y} = \frac{h'a}{G_p c_p + G_p c_w M} (T-\theta) - \frac{h_{fg} + c_v(T-\theta)}{G_p c_p + G_p c_w M} G_a \frac{\partial W}{\partial x} \qquad .....(3.13.2)$$

$$\frac{\partial W}{\partial x} = \frac{G_p}{G_a}\frac{\partial M}{\partial y} \quad .....(3.13.3)$$

$$\frac{\partial M}{\partial t} = \text{a single-kernel drying equation} \quad .....(3.13.4)$$

$T(0,y) = T(\text{inlet})$

$\theta(x,0) = \theta(\text{initial})$

$W(0,y) = W(\text{inlet})$

$M(x,0) = M(\text{initial})$

The MSU steady-state concurrentflow model with the appropriate boundary conditions has the following form (Brooker et al., 1981):

$$\frac{dT}{dx} = \frac{-h'a}{G_a c_a + G_a c_v W}(T-\theta) \quad .....(3.14.1)$$

$$\frac{d\theta}{dx} = \frac{h'a}{G_p c_p + G_p c_w M}(T-\theta) - \frac{h_{fg} + c_v(T-\theta)}{G_p c_p + G_p c_w M} G_a \frac{dW}{dx} \quad .....(3.14.2)$$

$$\frac{dW}{dx} = \frac{G_p}{G_a}\frac{dM}{dx} \quad .....(3.14.3)$$

$$\frac{\partial M}{\partial t} = \frac{1}{r^2}\frac{\partial}{\partial r}\left(Dr^2\frac{\partial M}{\partial r}\right) \quad .....(3.14.4)$$

$$\bar{M} = \frac{1}{r}\int_0^r M\,dr \quad .....(3.14.5)$$

$T(0) = T(\text{inlet})$

$\theta(0) = \theta(\text{initial})$

$W(0) = W(\text{inlet})$

$M(0) = M(\text{initial})$

Equations 3.14.4 and 3.14.5 allow calculation of the single-particle drying rate and the moisture content distribution within the particles. The simulation of a tempering in a multi-stage concurrentflow dryer is accomplished by solving Eqn.(3.14.4) for isothermal and isomoisture conditions over a period of time equal to the traverse-time of the grains through the tempering zone (Bakker-Arkema, 1987).

Brook (1977) applied the MSU concurrentflow model to multi-stage concurrentflow corn drying. A diffusion type thin-layer equation was used to describe moisture content distribution inside the kernel in order to model the tempering process. Bakker-Arkema et al. (1982) used the thin-layer diffusion model developed by Steffe (1979) to evaluate tempering time required in a multi-stage concurrentflow rice dryer.

The MSU steady-state <u>counterflow model</u> with the appropriate boundary conditions has the following form (Brooker et al., 1981):

$$\frac{dT}{dx} = \frac{h'a}{G_a c_a + G_a c_v W} (T-\theta) \qquad .....(3.15.1)$$

$$\frac{d\theta}{dx} = \frac{h'a}{G_p c_p + G_p c_w M} (T-\theta) + \frac{h_{fg} + c_v(T-\theta)}{G_p c_p + G_p c_w M} G_a \frac{dW}{dx} \qquad .....(3.15.2)$$

$$\frac{dW}{dx} = \frac{G_p}{G_a} \frac{dM}{dx} \qquad .....(3.15.3)$$

$$\frac{\partial M}{\partial t} = \text{a single-kernel drying equation} \qquad .....(3.15.4)$$

$T(L) = T(\text{inlet})$

$\theta(0) = \theta(\text{initial})$

$W(L) = W(\text{inlet})$

$M(0) = M(\text{initial})$

In addition to a set of differential equations, an expression for the equilibrium moisture isotherm for the particular grain being dried along with a model for the psychrometric chart are combined to form the simulation model of one of the drying systems.

Each system of equations describing crossflow, concurrentflow and counterflow grain dryers is solved simultaneously by numerical integration, using finite difference substitution in the derivatives. The crossflow model is solved by standard finite-difference methods. The counterflow model equations, which constitute a two-point boundary system, require application of optimization techniques. The concurrent-flow model can be solved by directly applying standard Runga-Kutta techniques.

The basic deep-bed grain-drying models presented in this section are capable of predicting the steay-state performance of crossflow, concurrentflow and counterflow grain dryers to within 10% of the experimental drying rates and temperatures (O'Callaghan et al., 1971).

Mixed-flow dryers, unlike concurrentflow, crossflow and counterflow dryers, are not described by a specific mathematical model. This dryer type can be simulated by alternately using counterflow and concurrentflow models, instead. This approach has been successfully used by O'Callaghan et al. (1971) and Bruce (1984).

3.2.2.2) Other Dryer Type Models

Modeling of rotary dryers requires simultaneous solution of a series of equations expressing (1) the heat and mass transfer of the individual particles, and (2) the movement of the particles in the rotary dryer.

Sharples et al. (1964) developed a steady-state rotary dryer model which is very similar to the concurrentflow dryer [see Eqns.(3.14.1 - 3.14.5)]. The major difference in the two simulation models is found in the term G_p, the particle transport rate through the dryers. In the case of the concurrentflow dryer, G_p is a direct function of the positive displacement of the unload augers; for the rotary dryer, the particle transport is a complicated function of the cascading, bouncing, rolling and airflow encountered by the particles in the dryer (Bakker-Arkema et al. 1987).

The term G_p in the rotary dryer is equal to the product of the product density (ρ_p) and the velocity of the particles (V_p) along the dryer axis. In turn, V_p is the ratio of the dryer length (L) and the average particle residence-time (T_r) at the dryer.

In general, the equation for the residence-time in a rotary dryer is of the following form (Sharples et al., 1964):

$$T_r = \frac{L}{C_1 D\ N\ (\tan\alpha + C_2 V_a)} \qquad \text{.....(3.16.1)}$$

where L is the dryer length, D the effective inside dryer diameter, N the rotational dryer speed, α the drum slope, V_a the air velocity, and C_1 and C_2 are constants depending on the flight design and the material to be dried.

In <u>fluidized-bed</u> dryers, as well as in <u>spouted-bed</u> dryers, the mass of particles is expanded by the air flow and is vigorously mixed. The particles do not remain in layers as in the packed-bed dryers, but they are considered to move at random. Thus, modeling of fluidized-bed and spouted-bed dryers requires simultaneous solution of the single-particle heat and mass transfer equations, and the residence-time distribution of the particles in the dryer.

The term V_p, the particle velocity, in a fluidized-bed or spouted-bed is the ratio of the weight of the particles in the bed (w) and the mean residence time (T_r).

The residence-time distribution, E(t), in a fluidized-bed dryer or spouted-bed dryer can be expressed as (Vanecek et al., 1966):

$$E(t) = (1/T_r)*e^{-t/T_r} \qquad .....(3.16.2)$$

where t is the time (sec) and T_r is the mean residence time of the particles in the bed.

Attempts to model fluidized-bed dryers have been made by O'Callaghan et al. (1971), Pabis (1971), Pabis (1974), and Thorpe Stokes (1987); to simulate spouted-bed dryers by Becker and Sallans (1960), Zuritz and Singh (1982), and Claflin and Fane (1984).

3.3) CONTROL SYSTEMS

The literature on the automatic control of grain dryers can be divided into two categories:

1) control of in-bin grain dryers; and
2) control of continuous-flow grain dryers.

The basic objective is similar for both types, namely to maximize dryer throughput at optimum energy efficiency and minimum grain-quality deterioration.

The control of in-bin dryers consists of controlling the drying fan or/and the dryer heater. In continuous-flow dryers, the rpm of the dryers discharge auger or/and the dryer heater are controlled.

Continuous-flow grain dryers are frequently manually controlled. This procedure often leads to overdrying and stress-craking of part of the grain; it is also labor-intensive because of the half-hourly data-taking requirement (Brooker et al., 1981).

Overdrying of grain is costly because the grain price is usually based on a specific moisture content. Therefore, overdrying leads to the loss in weight of the grain to be sold due to excessive moisture evaporation. Table 3.7 lists the cost of overdrying corn in different years for a 25,416 tonnes (1 million bu) drying facility. One percent overdrying in 1987 resulted in a shrink loss of US$ 15,205.

In addition to the loss in weight, overdrying is costly because

Table 3.7: Shrinkage in bushel and cost resulting from various levels of overdrying of 25,401.6 tonnes of 15.5% w.b. corn.

OVERDRYING	SHRINKAGE	YEAR 1987	1985	1983
		COST PER BU (US$)		
(%)	(bu)	1.30	2.35	3.20
		$/10^6 bu (25,401.6 ton)		
0.25	2,950	3,834	6,932	9,440
0.50	5,882	7,647	13,824	18,824
1.00	11,696	15,205	27,485	37,427
1.50	17,442	22,674	40,988	55,814
2.00	23,121	30,058	54,335	73,988

Source: Bakker-Arkema et al. (1987)

of the extra energy required to dry the grain beyond the moisture content at which it is priced by the market (i.e. 15.5% for corn). The extra energy needed in the drying process, an extra energy cost, is listed in Table 3.8 for different percentages of overdrying. The data show that at 1.0% overdrying requires 2,114 BTU additional per bu, and costs US$ 10,570 per 25,401.6 tonnes assuming the 1987 average U.S. energy cost was US$ 5.00 per 10^6 BTU. In other years the losses might have been higher or lower depending on the corn price and energy costs during those years.

Table 3.8: Energy required per bushel and cost resulting from various levels of overdrying of 25,401.6 tonnes of 15.5% w.b. corn.

OVERDRYING	ENERGY REQUIRED	ENERGY COST PER MCF (US$)		
		3.00	5.00	7.00
(%)	(BTU/bu)	$\$/10^6$ bu (25,401.6 ton)		
0.25	531	1,593	2,655	3,717
0.50	1,061	3,183	5,305	7,427
1.00	2,114	6,342	10,570	14,798
1.50	3,184	9,552	15,920	22,288
2.00	4,346	13,038	21,730	30,422

Source: Bakker-Arkema et al. (1987)

Underdrying of grain is more serious, since wet spots and spoilage may result. If considerable mixing takes place soon after drying, some underdrying is not serious, as moisture equalization will occur.

For many years, the automatic control of continuous-flow dryers was limited to temperature/feedback controllers which measure the exhaust air temperature at several locations along the drying column. As the grain inlet moisture increases, the exhaust air temperature decreases; this change in temperature acts as the input signal to the controller for adjusting the speed of the discharge auger, and thus the grain flow rate. Control of the outlet moisture content based on a change in the air-exhaust temperature has in practice proven to be inaccurate and inconsistent (Palmer, 1984). The main reason for the inaccuracy is the uncertainty of the functional relationship between the air-exhaust temperature and the dryer-outlet moisture content.

Now follows a review on the most significant studies on the automatic control of continuous-flow grain dryers.

One of the first papers on automatic control of continuous-flow grain dryers was presented by Zachariah and Isaacs (1966). They used the Hukill dying model (1954) to simulate an automatic control system for a crossflow corn dryer. Four control systems were investigated: (1) a proportional-integral-derivative (PID) control, (2) a PID controller with a proportional feedforward from the inlet grain moisture content, (3) an on-off feedback controller and, (4) a combination of on-off and PID controllers. Optimization methods were used to determine the controller parameters by minimizing the quadratic error of the dryer-outlet moisture content in response to a step change in the inlet moisture content. The system was not implemented on a commercial dryer due to the lack of on-line computing and moisture sensors at that time.

The Zachariah-Isaacs controller is dependent on the working conditions. Simulation results showed that the control system would be very unstable under drying conditions different from the one under which it was optimized.

Holtman and Zachariah (1969b) designed the first optimal controller for continuous-flow grain dryers. They first investigated the accuracy of a logarithmic and a simple linear models in control of a simulated crossflow grain dryer (1969a). Because of its simplicity, the linear model was preferred and it was used in the follow-up study. The linear model, as described in Holtman and Zachariah (1969a) has the following form:

$$MO(k) = b*t(k) + MI(k) \qquad ....(3.17)$$

where MO is the outlet moisture content (decimal d.b.), t is the dryer residence time (hours), MI is the initial moisture content (decimal d.b.) and b the drying constant. In designing the optimal control system, Holtman and Zachariah (1969b) used the minimum integral square error as the performance criterion:

$$I = \sum_{i=1}^{N} [M(i)-\bar{W}]^2 \qquad ....(3.18)$$

where $\bar{W}$ is the setpoint and N is the number of layers in the dryer column. Linear quadratic programming was used to solve the control problem. The control system could not be implemented due to the excessive on-line calculation requirements.

The Holtman-Zachariah optimal control is an adaptive controller where the value of the drying constant b is updated at each sample interval. Unlike the Zachariah-Isaacs controller, the Holtman-Zachariah control system has the advantage of adjusting its behavior to the change characteristics of the controlled process and its signals.

A feedforward control strategy was investigated by Clifford (1978) for a concurrentflow dryer. He developed an unsteady-state dryer model to study different control alternatives. The inlet air temperature was used as the control input instead of the grain flow rate. The

Clifford feedforward control system works in this manner: in response to a step change in the inlet grain moisture content, the control parameter (inlet air temperature) is altered according to a predetermined pattern. This method is ideal for moving from one steady-state to another. However, it can not cope with continually varying inputs.

Olesen (1978) presented an automatic controller for a mixed-flow dryer based on a "weighted-sum" feedforward method. The dryer output rate is adjusted according to a pseudo-moisture content defined as the weighted average of the inlet moisture content values of the grain currently within the dryer. Shift registers are used to memorize the value and position of each initial moisture content as it moves trough the dryer. The Olesen's control requires a feedback loop in the system to check for the output error. The controller has been used on the Cimbria dryers in Denmark, but no published test results are available.

Fábián et al. (1980) designed and implemented an on-off feedback control system on a mixed-flow corn dryer. A capacitance-type moisture meter, located at the lower part of the drying zone, was used to continuously measure the outlet grain moisture content. The accuracy of the automatic controller is reported to be three times better than the manual control. One of the advantages of an on-off control method is that it can prevent any of the grain leaving the dryer underdried. This method can be considered more a control aid than an automatic control system (Agness and Isaacs, 1967).

Modén and Nybrant (1980) designed an adaptive control system for rotary drum dryers. The control system is a combination of the recursive least square identification with the generalized minimum variance controller (Isermann, 1981). Temperature was used instead of moisture content as the control output due to the lack of reliable moisture meters at that time. The drying process was described by a linear stochastic difference model of the following:

$$A(z^{-1})*Y(k) = B(z^{-\tau})*U(k)+D(z^{-\tau'})*\bar{V}(k)+C(z^{-1})*\xi(k)+f \quad ....(3.19)$$

where Y is the control output, U the control input, $\bar{V}$ is the known disturbance to the process, f describes the working level, ξ is the white noise, and A, B, C and D are polynomials of this form:

$$A = 1+a_1z^{-1}+...+a_mz^{-m} \quad .....(3.20.1)$$
$$B = b_0+b_1z^{-1}+...+b_mz^{-m} \quad .....(3.20.2)$$
$$C = 1+c_1z^{-1}+...+c_mz^{-m} \quad .....(3.20.3)$$
$$D = d_0+ d_1z^{-1}+...+d_mz^{-m} \quad .....(3.20.4)$$

where z^{-1} is the backward shift-operator, $z^{-1}Y(k)=Y(k-1)$; τ is the control input time delay, τ' is the feedforward delay, and $a_1...a_m$, $b_0...b_m$, $c_1...c_m$, and $d_0...d_m$ are the model parameters.

The control system was designed based on the minimization of the variance of the quadratic of the control error:

$$I = E\{[Y(k+1)-\hat{W}]^2+ \rho[U(k)-U_r(k)]^2\} \quad ....(3.21)$$

where ρ is a penalty factor on the control input and U_r is the input reference. Also, an integral method was included in the control system to avoid offset. The control system was implemented on a commercial rotary drum dryer. A small output variance without offset was experienced with the adaptive controller.

A multi-input multi-output feedback control system was developed by Jaaksoo et al. (1982) for the control of a crossflow grain dryer. Two single input-output linear state variable models were used to describe the drying process: one relating grain flow rate (U_1) and grain outlet moisture content (Y_1) and, other relating inlet air temperature (U_2) and outlet grain temperature. The process model in state-space representation has the following form:

$$\mathbf{X}(k+1) = \mathbf{F}\mathbf{X}(k) + \mathbf{G}\mathbf{U}(k) + \mathbf{d}(k)$$
$$Y(k) = \mathbf{h}'\mathbf{X}(k) \qquad \text{.......(3.22)}$$

where the state $\mathbf{X}$ is an n-vector which is formed from measured temperatures along the dryer column, the vector $\mathbf{d}$ represents uncertainty in the model parameters ($\mathbf{F},\mathbf{G}$) and unmeasurable disturbances. An incremental control law of the following form was used:

$$\Delta U(k) = L_1\Delta X_1(k)+\ldots+L_n\Delta X_n(k)+L_e e(k) \qquad \text{.......(3.23)}$$

where $\Delta U(k)=U(k)-U(k-1)$, $\Delta\mathbf{X}(k)=\mathbf{X}(k)-\mathbf{X}(k-1)$, $e(k)=Y-\tilde{W}$ (the control error), and $L_1\ldots L_e$, are the control parameters. The controller parameters were determined by minimizing the quadratic criterion [Eqn.(3.20)] with the help of a computer aid design. The control system was implemented with a microprocessor 8085 based controller. It was reported that the accuracy of the control system is between ±0.5% of the setpoint.

Unlike the adaptive control system developed by Modén and Nybrant (1980), the Jaaksoo control system is of a fixed-type, i.e., the control parameters are determined only once and the control system is designed. To cope with different working conditions (high or low inlet air temperature), two different models had to be developed to describe the dryer operating at low and high temperature. This procedure increases the computation and storage requirements for the controller calculations.

A microcomputer-based dryer control system (Borsum et al., 1982) was developed and tested on a pilot-scale, single stage concurrentflow dryer. The controller is of the feedback type using information regarding outlet grain temperature. The Ziegler-Nichols open-loop tuning method was used to determine the PI controller parameters. Borsum observed that the drying process dynamics are dependent on the discharge rate and then used a sampling interval that is proportional to the grain transportation time in the dryer. Borsum concluded that the calculated controller parameters are dependent on the dryer and grain type. Based on the experimental results, the authors suggested that a feedforward be developed in conjunction with a moisture meter. It was also recommended that for multi-stage CCF dryers different control variables such as, inlet air temperature should be used in each dryer stage.

Mann (1982) designed a multi-cascade control system for a rotary sugar dryer. The controller is a combination of feedback and feedforward control. A linear difference equation was used to describe the dynamics of the drying process. In addition to a cascade controller, the state-space control design was also investigated. Because of its simplicity, the multi-cascade controller was preferred. Computer aid design was used to determine the control parameters. Experimental tests with a commercial rotary dryer showed improved perfomance as compared to manual control.

Forbes et al. (1984) developed a model-based adaptive control strategy for commercial corn crossflow dryers. A microcomputer based control system was designed to automatically control the outlet moisture content. Based on the internal model control technique (Garcia et al., 1982), the controller was implemented with a PC-type computer. An exponential decay type model was used to describe the process dynamics. The model is of the form:

$$MO(k) = MI(k)*e^{-b't} \qquad ....(3.24)$$

where MO is the moisture content (%d.b.), MI is the initial moisture content (%d.b.), t is the dryer residence time (sec) and β grain drying characteristics (sec^{-1}). The controller input is based on a pseudo-inlet moisture value similar to that proposed by Olesen (1978). Field test results demonstrate that the average outlet moisture content can be kept to within ± 1.0% of the setpoint.

Forbes' control can be described as a feedforward adaptive control system. It was the first controller to combine the "weighted-sum" feedforward method with the adaptive approach. The result is a very simple control system. Its accuracy depends on the accuracy of the empirical function which determines the pseudo-moisture content value.

An adaptive controller for crossflow wheat dryers has been developed by Nybrant et al. (1985). The feedback controller is based on the self-tuning regulator method developed by Åstrom et al. (1973); it combines a recursive identification method with the minimum variance control method. A linearization method was employed to determine a linear process model. The microprocessor-based controller is based on the exhaust air temperature, and was tested on a pilot-scale crossflow dryer. It was suggested that a controller based on direct moisture measurements might lead to an improvement of the adaptive dryer control.

Nybrant (1986), in a follow-up study, investigated different adaptive controllers for concurrentflow and crossflow grain dryers. Basically, two linear equations were considered in order to model the dynamics of the dryers: a linear stochastic difference model [Eqn.(3.19)] and a linear model [Eqn.(3.17)]. Experiments, based on temperature measurements were carried out with laboratory dryers. Simulation studies with direct control of the moisture content are also described. It was found that a feedback/feedforward controller significantly improves the control quality compared to a feedback controller.

Whitfield (1986) developed an unsteady-state simulation model to study the control of a single-stage concurrent/counterflow grain dryer. The control system is a proportional and integral feedback type. A step-function in the inlet moisture content was used to determine the controller parameters. Simulation results show that the control system is very dependent on the working conditions. It was concluded that a different control system working over a wider range of conditions would be preferred for continuous-flow grain dryers.

A microprocessor-based automatic controller was developed and tested on several commercial crossflow dryers (Eltigani et al., 1986;

and Eltigani, 1987). A semi-continuous moisture meter was used to measure the inlet and outlet grain moisture contents. The control system uses a model-based feedforward control algorithm with a feedback loop. Two simple drying process models were used in the control system: an exponential model [Eqn.(3.24)] and a linear model of the form:

$$MO(k) = MI(k)[B_1+B_2*t] \qquad ....(3.25)$$

where MO is the outlet moisture content (decimal w.b.), MI is the initial moisture content (decimal w.b.), t is the dryer residence time (hours), and B_1 and B_2 are constants. The constants in Eqn.(3.25) were recursively estimated using the least square method. A pseudo inlet-moisture content value is the input and aids in determining the desired grain flow rate. The pseudo-moisture value is calculated from the following empirical relationship:

$$M_{ps} = \kappa_1 MI(1)+...+\kappa_n MI(n) \qquad ....(3.26)$$

where $\kappa_1+...+\kappa_n=1.0$, and n is the number of samples used in the calculation of M_{ps}. The value of $\kappa_1 ... \kappa_n$ were determined by trial-and-error and are kept constant through the course of drying. Since the working conditions are different from test to test, a method for estimating the κ's values should be incorporated in the software. Tests with commercial crossflow grain dryers resulted in ± 0.6% outlet moisture content variation of the setpoint at a variation of the inlet moisture content of 16% to 34% (w.b.).

In conclusion, it is clear that automatic control of continuous-flow grain dryers requires microcomputer process-control in conjunction with on-line moisture meters. Because of the large variations in ambient conditions, inlet moisture content and drying characteristics, adaptive controllers have advantages for continuous-flow grain dryers over proportional, PI and PID classical controllers. A simple, but accurate model is required for the adaptive control system design. Also, a feedback/feedforward controller gives significant improvement in the control quality.

CHAPTER 4

THEORY

The theoretical part of this investigation is divided into two sections. In the first section, the design of the control system for continuous-flow grain dryers is discussed. In the second section, the modeling of the concurrentflow dryer during steady and unsteady state operation is considered.

4.1) CONTINUOUS-FLOW GRAIN DRYER CONTROL DESIGN

The progress in the development of digital computers and microelectronics has enabled the implementation of complex control algorithms in the grain drying industry. Also, progress in the field of process identification and of control theory has greatly contributed to the development of adaptive controllers. Therefore, interest in adaptive control has increased considerable in the last decade (Isermann, 1981).

In this section, adaptive control is evaluated as a tool for continuous-flow grain dryer control. The highly complex dynamics of the dryer provides an ideal test for adaptive control. An adaptive control technique based on a continuously updated linear controller is developed.

To design and implement an adaptive control system, three elements are needed: (1) the process model, (2) the control algorithm, and (3) the compensation for offsets. The three elements are investigated below with reference to the control of continuous-flow grain dryers.

For detailed information on adaptive control, the reader is referred to Åstrom and Wittenmark (1984) and Isermann (1981).

4.1.1) Drying Process Models

There are different ways to decrease the grain moisture content in a continuous-flow grain dryer:

- by adjusting the throughput
- by controlling the air temperature
- by changing the air flow rate.

Control of corn dryers (concurrentflow and crossflow) is made by adjusting the throughput. No change is usually made to the air flow rate on either corn or rice dryers. For concurrentflow rice dryers, the adjustment is made to the inlet air temperature.

In this study, corn dryers are studied. It is assumed that no adjustment is made in the air-temperature or air flow rate during the drying operation.

The main physical input to the process of corn drying is the grain flow rate (GFR). The main output is the outlet moisture content. The main disturbance is the change in the grain inlet moisture content (known disturbance).

The objective of the modeling of the drying process is to find the dynamic relationships between the described input, output and disturbance variables.

The partial differential equation grain-drying models are steady-state in nature, and need main-frame capability for on-line calculation (see Chapter 3). Thus, a simple drying non steady-state process model, sufficiently accurate for control purposes, needs to be developed.

The adaptive control theory often applies the linear model described by Eqn.(3.19). Therefore, it is assumed that a continuous-flow drying process can be described by a linear difference model of the following form:

$$A(z^{-1})*Y(k) = B(z^{-1})*U(k) + \nu(k) \qquad .....(4.1.1)$$

where: Y = the controlled variable (outlet moisture content)

U = the manipulated variable (grain flow rate)

ν = the disturbance signal

k = t/T_o = the discrete time

T_o = the sample time

$A(z^{-1})$ and $B(z^{-1})$ are polynomials of the form:

$$A(z^{-1}) = 1+a_1*z^{-1}+...+a_m*z^{-m} \qquad ......(4.1.2)$$

$$B(z^{-1}) = b_1*z^{-1}+...+b_m*z^{-m} \qquad ......(4.1.3)$$

where m is the model order, z^{-1} is the backward shift (or delay) operator: $z^{-1}Y(k)=Y(k-1)$, and $a_1...a_m$ and $b_1...b_m$ are parameters.

The disturbance signal $\nu(k)$ can be considered to be one or a combination of the following:

(a) a zero-mean unmeasurable disturbance of the form $C(z^{-1})*\xi(k)$ where C is a polynomial in z^{-1}, and $\xi(k)$ is an uncorrelated random sequence or white noise;

(b) a measurable disturbance $\tilde{V}(k)$ which can be suitable for feedforward control;

(c) a stepwise load-disturbance occurring at a random time:

$$\nu(k) = \nu(k-1)+\xi(k) \qquad ....(4.1.3)$$

(d) a constant offset of the process output, due to a nonlinearity of the process, the actuator, or the sensor.

In this study, three forms of combining $\nu(k)$ and Eqn.(4.1) are considered.

4.1.1.1) <u>Time-Series Model I</u>

By considering that the disturbance signal [$\nu(k)$] is described by a white noise signal [see category (a) described above], the drying process model [Eqn.(4.1.1)] becomes:

$$A(z^{-1})*Y(k) = B(z^{-1})*U(k) + C(z^{-1})*\xi(k) \qquad ....(4.2)$$

where:

$C(z^{-1}) = 1 + c_1 z^{-1}+...+c_m z^{-1}$

$\xi(k)$ = white noise with zero mean and covariance σ^2.

Eqn.(4.2) is known as the ARMAX (autoregressive moving average) model (Isermann, 1981) because the model is a combination of an autoregressive (AR) part [$A(z^{-1})*Y(k)$], a moving average (MA) part [$C(z^{-1})*\xi(k)$], and a control part [$B(z^{-1})*U(k)$].

The parameter terms in Eqn.(4.2) can be considered to represent the drying characteristics for a particular dryer and grain. Variation in the values directly affects the magnitude of the change in the residence time, and thus the control.

The variations in inlet moisture content, the ambient conditions and other disturbances are accounted for in this drying model by the noise polynomial $[C(z^{-1})*\xi(k)]$.

4.1.1.2) <u>Time-Series Model II-a</u>

By considering that the disturbance signal $[\nu(k)]$ is described by a measurable signal [see category (b) described above], the drying process model [Eqn.(4.1.1)] becomes:

$$A(z^{-1})*Y(k) = B(z^{-1})*U(k) + D(z^{-1})*\bar{V}(k-\tau') \qquad \text{........(4.3)}$$

where: $\bar{V}$ = measurable disturbance (inlet moisture content)

τ' = is the feedforward time delay

$D(z^{-1}) = d_1*z^{-1}+...+d_m*z^{-m}$

Eqn.(4.3) is similar to Eqn.(4.2) with the exception that the disturbance signal $\nu(k)$ is considered to be known which allows for feedforward control.

4.1.1.3) <u>Time-series Model II-b</u>

By considering that the disturbance signal $[\nu(k)]$ is described by a combination of the four disturbances [see categories (a), (b), (c) and (d) described above], the drying process model [Eqn.(4.1.1)] becomes:

$$A(z^{-1})*Y(k) = B(z^{-1})*U(k) + D(z^{-1})*\bar{V}(k-\tau') + C(z^{-1})\xi(k)/\Delta \quad ....(4.4)$$

where: Δ = differencing operator $(1-z^{-1})$

Eqn.(4.4) is described in Clarke et al. (1985) and is known as the CARIMA (controlled autoregressive integrated moving average) model.

4.1.1.4) <u>Linear Model</u>

It is assumed that the drying section of a continuous-flow dryer is divided into n layers (see Figure 4.1). Grain travels as a series of batches, with the batch-speed determined by the discharge rate (GFR). The time [$t_r(i)$] required for a batch of grain, moving as a plug, to pass through a distance equal to the layer depth is defined by:

$$t_r(i) = \frac{\ell}{GFR(i)} \quad ......(4.5.1)$$

and, the dryer residence time (T_r) is equal to:

$$T_r = \sum_{i=1}^{n} t_r(i) \quad ......(4.5.2)$$

where ℓ is a constant which depends on the dryer characteristics, GFR(i) is the discharge rate, and n is the number of layers in the dryer.

The linear dryer model is developed by discretizing the drying section and calculating the residence time for the batches at different levels.

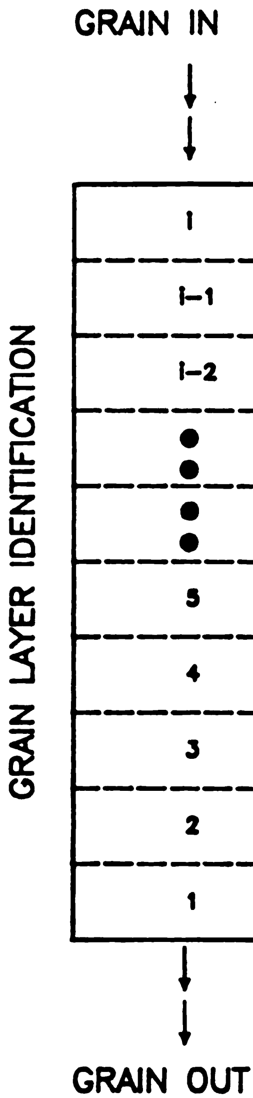

Figure 4.1: Identification of dryer segments and grain layers considered in the linear model of the continuous-flow grain drying process.

Therefore, by defining the measured output (MO) as a linear combination of the residence time, and incorporating the inlet moisture content as a known disturbance, the drying model can be written as:

$$MO(k) = b*T_r(k-1) + f*MI(k-\tau') \qquad ....(4.6)$$

where: MO = outlet moisture content correspondenting to the inlet moisture content (% w.b.)

T_r = residence-time of the grain exiting the dryer (hours)

MI = inlet moisture content (% w.b.)

b,f = parameters

4.1.1.5) Exponential model

This model was proposed for the design of control systems for grain drying by Marchant (1985):

$$MO(k) = MI(k-\tau')*e^{[-b'*T_r(k)]} \qquad ....(4.7)$$

where b' is the model parameter.

The models described in section 4.1.1 were selected because they are simple and have been used to design control systems for continuous-flow grain dryers. Eqn.(4.2) has successfully described the dynamics of complex processes, such as grain dryers. The main drawback of Eqn.(4.2) is the great number of terms (more than four) needed to adequately represent the process (Nybrant, 1986). A larger model order requires additional computer time and storage for the control parameters calculations.

Eqn.(4.3) and Eqn.(4.4) are a better representation of the drying process than Eqn.(4.2) since the models include the measurable disturbance (inlet moisture content). Eqn.(4.4) is still more complete than Eqn.(4.3) because it contains elements of each type of disturbances. These disturbances may represent: grain inhomogenities, non-linearities in the moisture meter and/or discharge auger, shrinkage and mixing of the grain under drying, etc. Therefore, Eqn.(4.4) is the most realistic representation of the true nature of a grain dryer.

Eqn.(4.6) and Eqn.(4.7), although simple, accurately model continuous-flow grain dryers. Their advantage is the small number of terms needed to be estimated for calculating the control parameters. The disadvantage of using the non-linear Eqn.(4.7) to design a control system is that control theory is based on linear systems; thus, the control problem is limited to only one solution. Another limitation of Eqn.(4.7) is that it is specific only for grain moisture content-grain flow rate signals.

Other workers have suggested the use of Eqn.(4.2)-Eqn.(4.7) for the modeling of the dynamics of continuous-flow grain dryers (see section 3.3). However, they have not investigated the general application of such models for both crossflow and concurrentflow grain dryers. This study discusses how these equations can be used to provide accurate control for continuous-flow grain dryers.

4.1.2) Parameter Estimation

For on-line identification of the unknown process model parameters, recursive estimation (or sequential estimation) methods are suitable.

To estimate the parameters in Eqn.(4.2) a FORTRAN subroutine was developed. It performs the recursive prediction error (RPE) method described in Ljung and Sodertrom (1986). The RPE is based on a stochastic Gauss-Newton algorithm and can be expressed as follows:

The prediction error (e) is equal to:

$$e(k)=Y(t)-\hat{Y}(t) \qquad \text{........(4.8)}$$

$$S(k)=\phi'(k)P(k-1)\phi(k)+\lambda(k) \qquad \text{........(4.9)}$$

The gain vector (γ) is equal to:

$$\gamma(k)=P(k-1)\phi(k)S^{-1}(k) \qquad \text{.......(4.10)}$$

$$\theta(k)=[a_1...a_m|b_1...b_m|c_1...c_m] \qquad \text{.......(4.11)}$$

$$\hat{\theta}(k)=\hat{\theta}(k-1)+\gamma(k)e(k) \qquad \text{.......(4.12)}$$

$$P(k)=[P(k-1)-\gamma(k)S(k)\gamma'(k)]/\lambda(k) \qquad \text{.......(4.13)}$$

The residual ($\bar{e}$) is equal to:

$$\bar{e}(k)=Y(k)-\hat{c}_1(k)\bar{e}(k-1)-....-\hat{c}_m(k)\bar{e}(k-m_c) \qquad \text{.......(4.14)}$$

$$\phi'(k+1)=[-Y(k)\ ...\ -Y(k-m_a+1)|U(k)\ ...\ U(k-m_b+1)|\bar{e}(k)\ ...\ \bar{e}(k-m_c+1)] \qquad \text{.......(4.15)}$$

$$\hat{Y}(k+1)=\hat{\theta}'(k)\phi(k+1) \qquad \text{.......(4.16)}$$

The filtered signals ($\tilde{Y}$, $\tilde{U}$, $\tilde{e}$) are equal to:

$$\tilde{Y}(k)=Y(k)-\hat{c}_1(k)\tilde{Y}(k-1)-....-\hat{c}_m(k)\tilde{Y}(k-m_c) \qquad \text{.......(4.17)}$$

$$\tilde{U}(k)=U(k)-\hat{c}_1(k)\tilde{U}(k-1)-\ldots-\hat{c}_m(k)\tilde{U}(k-m_c) \qquad \ldots\ldots.(4.18)$$

$$\tilde{e}(k)=\bar{e}(k)-\hat{c}_1(k)\tilde{e}(k-1)-\ldots-\hat{c}_m(k)\tilde{e}(k-m_c) \qquad \ldots\ldots.(4.19)$$

$$\psi'(k+1)=[-\tilde{Y}(k)\ \ldots\ -\tilde{Y}(k-m_a+1)|\tilde{U}(k)\ \ldots\ \tilde{U}(k-m_b+1)|\tilde{e}(k)\ \ldots\ \tilde{e}(k-m_c+1)] \qquad \ldots\ldots.(4.20)$$

Note: The symbols (') and (^) in Eqns.(4.6)-(4.20) mean transpose and estimate, respectively.

The RPE method is based on the minimization of the loss function due the unknown parameter vector $\hat{\Theta}$ (the estimation of the model parameters):

$$LF(k) = \sum_{s=1}^{k} \frac{e^2(s)}{\lambda(k) + \psi'(s)P(s-1)\psi(s)} \qquad \ldots\ldots.(4.21)$$

where LF(k) is the loss function and e is the error. The loss function is defined as the sum of the squared prediction errors which here was modified to include uncertainties in the transient phase (Ljung and Sodertrom, 1986), i.e., the use of Eqn.(4.21) allows the estimator to track the time-varying dynamics of the process.

In the RPE algorithm used, the matrix P is update using the U-D algorithm given by Thornton and Bierman (1980).

The subroutine contains the following steps:

(1) Set the initial conditions:

at k=0

$P(I,I)=1; \quad P(I,J)=0$

$\hat{\Theta}(0)=0; \quad \lambda(k)=\lambda=0.98$

(2) Compute the prediction error: Eqn.(4.19)

(3) Update the parameter estimates: Eqn.(4.12)

In order to ensure that C(z) contains only zeros inside the unit circle, a stability test is performed in a separate subroutine NSTABL. This routine is based on the Schur-Cohn algorithm [Kucera, (1980)].

(4) Compute the residuals: Eqn.(4.14)

(5) Compute the filtered signals: Eqns.(4.17-19)

(6) Update the vectors $\phi(k)$ and $\psi(k)$: Eqns.(4.15) and (4.20)

(7) Compute the gain vector $\gamma(k)$, and update P(k) and V: Eqn.(4.10), (4.13), and (4.21), respectively.

An extension of the RPE algorithm to Eqn.(4.4) is straighforward. The vectors ϕ, ψ and Θ become:

$$\Theta(k)=[a_1,\ldots,a_m|b_1,\ldots,b_m|d_1,\ldots,d_m|c_1\ldots c_m] \qquad ....(4.22)$$

$$\phi'(k+1)=[-Y(k)\ldots-Y(k-m_a+1)|U(k)\ldots U(k-m_b+1)|\bar{V}(k)\ldots\bar{V}(k-m_d+1)|\bar{e}(k)\ldots \bar{e}(k-m_c+1)] \qquad ....(4.23)$$

$$\psi'(k+1)=[-\tilde{Y}(k)\ldots-\tilde{Y}(k-m_a+1)|\tilde{U}(k)\ldots\tilde{U}(k-m_b+1)|\tilde{V}(k)\ldots\tilde{V}(k-m_d+1)|\tilde{e}(k)\ldots \tilde{e}(k-m_c+1)] \qquad ....(4.24)$$

To solve Eqn.(4.3), the vectors ϕ, ψ and Θ in the RPE algorithm reduce to:

$$\Theta(k)=[a_1,\ldots,a_m|b_1,\ldots,b_m|d_1,\ldots,d_m] \qquad ....(4.25)$$

$$\psi'(k+1)=[-Y(k)\ldots-Y(k-m_a+1)|U(k)\ldots U(k-m_b+1)|\bar{V}(k)\ldots\bar{V}(k-m_d+1)] \qquad ....(4.26)$$

$$\phi'(k+1)=\psi'(k+1) \qquad ....(4.27)$$

To solve Eqn.(4.6), the vectors ϕ, ψ and Θ in the RPE algorithm reduce to:

$$\Theta(k)=[b,f] \qquad ....(4.28)$$

$$\psi'(k+1)=[T_r(k),MI(k)] \qquad ....(4.29)$$

$$\phi'(k+1)=\psi'(k+1) \qquad ....(4.30)$$

The parameter b′ in Eqn.(4.7) is determined directly from the equation and therefore, no parameter estimation is needed.

4.1.3) <u>Sampling Strategy</u>

The dryer is discretized in n layers as is illustrated in Figure 4.1.

The sampling strategy chosen in this study is based on <u>fixed-distance</u> intervals instead of on <u>fixed-time</u> intervals. By fixed-time is meant that the time interval between samples is fixed and the number of layers in the dryer varies as a function of the discharge rate. By using the fixed-distance sample strategy, the number of layers are kept fixed and the time interval is variable.

The advantage of the fixed-distance strategy is that it allows the determination of a batch of grains at the exact position in the dryer; for instance, the grain outlet moisture content can be exactly matched with the corresponding inlet moisture content.

By fixing the time interval between samples, the outlet moisture content around the bottom of the dryer flutuate with the magnitude of the error varying with the size of the time increment and the drying rate (Zachariah and Isaacs, 1966).

The consequence of the fixed-distance sample strategy is that, at the end of each sample instant k, the following sample interval is calculated:

$$t_r(k) = \frac{\ell}{GFR(k)} \qquad ......(4.5.3)$$

4.1.4) Control Algorithms

A control algorithm for adaptive control should have the following properties:

- small computation and storage requirement for the parameter calculations;
- applicability to several processes types and signals.

In the case of grain dryers, a controller should fit different dryers, and must be able to adapt to any variation in the drying process, such as the inlet moisture content, grain characteristics, ambient conditions, etc.

Three algorithms are developed for the control of continuous-flow grain dryers in the following sub-sections.

4.1.4.1) Generalized Minimum Variance Controller-(GMV)

The generalized minimum variance control is based on a self-tuner presented by Åstrom and Wittenmark (1973). It combines a control law based on linear quadratic criteria with recursive least square identification.

The control law is based on the minimization of the linear quadratic criterion:

$$I(k+1) = E[Y^2(k+1) + \rho U^2(k)] \qquad \text{.......(4.31)}$$

where I is the quadratic criterion, ρ is a penalty on the control input variance, E is the variance, Y is the control output and U the control input.

4.1.4.1.1) Minimum Variance Feedback Controller

Assuming that the drying process is described by Eqn.(4.3), the feedback control which minimizes the quadratic criterion [Eqn.(4.31)] is (Appendix A presents the derivation of the MV controller):

$$G_{mv}(z) = \frac{U(z)}{Y(z)} = -\frac{Q(z^{-1})}{R(z^{-1})} \qquad \text{.......(4.32)}$$

where:

$G_{mv}(z)$ = generalized minimum variance feedback control

$Q(z) = [C(z^{-1}) - A(z^{-1})]*z$

$R(z) = z*B(z^{-1}) + (\rho/b_1)*C(z^{-1})$

By substituing Eqn.(4.32) into Eqn.(4.3) the closed-loop system is:

$$Y(z) = \frac{zB(z^{-1}) + \mu C(z^{-1})}{\mu A(z^{-1}) + zB(z^{-1})}\ \xi(z) \qquad \text{.......(4.33)}$$

where Y(z) = outlet moisture content and $\mu = \rho/b_1$. The value of μ can be interpreted as a penalty on the input variance [see Eqn.(4.3)], or as a root locus parameter for the characteristic equation of the closed-loop system:

$$\mu A(z) + zB(z) = 0 \qquad ....(4.34)$$

A small value of μ results in high input and low output, and a large μ in low input and high output.

4.1.4.1.2) Minimum Variance Feedforward Controller

The minimum variance feedforward controller is derived in the same way as the minimum variance feedback controller (see Appendix A). The only difference is that $\nu(k)$ (the inlet moisture content) is measurable for the feedforward control; as a result instead of a control [U(k)/Y(k)], a feedforward control $[U(k)/\tilde{V}(k)]$ is of primary interest.

By considering that the drying process is described by Eqn.(4.3), the feedforward control which minimizes Eqn.(4.31) is:

$$G_{mvf}(z) = \frac{U(z)}{\tilde{V}(z)} = - \frac{Q''(z^{-1})}{R''(z^{-1})} \qquad ....(4.35)$$

where:

$G_{mvf}(z)$ = generalized minimum variance feedforward control

$Q''(z) = [D(z^{-1}) - A(z^{-1})]*z\lambda$

$R''(z) = z*B(z^{-1}) + (\rho/b_1)*A(z^{-1})$

$\tilde{V}(z)$ = inlet moisture content

Immediately after a change in the disturbance $\tilde{V}$ the process input U is manipulated by a feedforward control (G_{mvf}) which does not wait, as with feedback control, until the disturbance has effected the control variable Y.

4.1.4.1.3) Minimum Variance Feedback/Feedforward Controller

The difference between the minimum variance feedback/feedforward controller and the feedback controller described in section 4.1.4.1.1 is that a known disturbance [$\bar{V}(k)$] is included in the former. The derivation of the minimum feedback/feedforward controller is the same as for the minimum variance feedback controller described above.

It is assumed that the drying process is described by Eqn.(4.4). The controller which minimizes Eqn.(4.31) becomes:

$$U(z) = - \frac{Q(z)}{R(z)} Y(z) - \frac{D(z)}{R(z)} z \bar{V}(z) \qquad ....(4.36)$$

By substituing Eqn.(4.36) into Eqn.(4.4), the closed-loop system gives:

$$Y(z) = \frac{[zB(z^{-1}) + \mu C(z^{-1}) - z]D(z^{-1})\bar{V}(k) + [zB(z^{-1}) + \mu C(z^{-1})]C(z^{-1})\xi(k)}{C[\mu A(z^{-1}) + zB(z^{-1})]}$$

$$.......(4.37)$$

Note: The term Δ is omitted for simplicity.

4.1.4.1.4) Offset Compensations for Minimum Variance Controllers

The minimum variance controllers described in 4.1.4.1.1 and 4.1.4.1.2 can be applied without additional methods for removing output offset from the reference values (Isermann, 1981). However, if the assumed disturbance has a non-zero mean, the compensation for the offset must be considered. The simplest way to reduce the offset is by adding a pole at z=1 to the controller transfer function, i.e.:

$$G_{mv}(z) = \frac{U'(z)}{Y(z)} \qquad \text{.......(4.38)}$$

where: $\frac{U(z)}{U'(z)} = \frac{1}{1 - z^{-1}}$ (the integral acting term).

In addition to reducing a large change in the output, the first order differences in the parameter estimation are considered (Åstrom, 1970):

$$\begin{aligned} \Delta y &= e_w(k) = \hat{W}(k)-Y(k) \\ \Delta u &= U(k)-U(k-1) \qquad \text{.......(4.39)} \\ \Delta\bar{v} &= \bar{V}(k)-\bar{V}(k-1) \end{aligned}$$

where $\hat{W}(k)$ is the reference value (setpoint).

Therefore, an offset-free output can be achieved by first adding the pole z=1 to the process and then replacing the model variables Y(k), U(k) and/or $\bar{V}$ by Δy, Δu and $\Delta\bar{v}$ [Eqns.(4.37)], respectively.

Note that in Eqn.(4.4), the term $(1-z^{-1})$ is already included in the model, therefore there is no need for off-set compensations.

4.1.4.2) Pole Placement Controller-(PP)

The minimum variance controllers presented in section 4.1.4.1, frequently lead to an offset between the measured and the desired value when regulating a process. The insertation of an integrator [see Eqn.(4.38)] solves the problem. Here, a controller is presented where the integration is realized in an alternative way.

Compared with the minimum variance controller, the pole placement controller is based on the desired characteristic equation of the closed-loop system, and not on the criterion minimization.

The pole placement controller was developed by Tuffs and Clarke (1985a) and later modified by Nybrant (1986) to include a feedforward controller. It was derived by assuming that the dryer process is described by Eqn.(4.4). Since the pole placement design is based on polynomial manipulations, solving the control problem using Eqn.(4.4) is complex. An alternative was to use a simpler model, i.e., the linear model [Eqn.(4.6)] which was modified to include the term ξ/Δ:

$$MO(k) = b*T_r(k-1) + f*MI(k-\tau') + \xi(k)/\Delta \qquad ....(4.40)$$

Note: Eqn.(4.40) is a simplified version of Eqn.(4.4), the controlled autoregressive integrated moving average model.

From Eqn.(4.5.2) :

$$T_r = t_r(1) +...+ t_r(i) \qquad ......(4.41.1)$$

or

$$T_r(k) = t_r(k) +...+ t_r(k-n) \qquad ......(4.41.2)$$

where t_r is the residence time of each layer in the dryer (see Figure 4.1). Using the shift operator z^{-1}, Eqn.(4.41.2) becomes:

$$T_r(k) = Z = (1 + z^{-1} + ... + z^{-j+n})*U(k) \qquad ....(4.42)$$

where n is the number of layers and U is the control input (t_r).

By substituing Eqn.(4.42) into Eqn.(4.40) there results:

$$\Delta MO(k) = z^{-1}(bZ)*\Delta U(k) + z^{-\tau'} f*\Delta MI(k) + \xi(k) \qquad ....(4.43)$$

By assuming that the drying process is described by Eqn.(4.43), and a general integrating control law is defined by:

$$J(z^{-1})\Delta u(k) + F(z^{-1})MO(k) - H(z^{-1})\bar{W}(k) + E(z^{-1})\Delta MI(k) = 0 \qquad ....(4.44)$$

where J, F and H are polynomials, E is a transfer function and $\bar{W}(k)$ is the setpoint (Note: the term z^{-1} is omitted for simplicity). The closed-loop can be obtained by substituing Eqn.(4.44) into Eqn.(4.43):

$$[\Delta J+z^{-1}(bZ)F]MO(k)=z^{-1}\{(bZ)H\bar{W}(k)+[z^{-\tau'}fJ-z^{-1}(bZ)]E\}\Delta MI(k)+J\xi(k) \qquad ....(4.45)$$

Let the desired characteristic equation of the closed-loop be given by the polynomial:

$$L = \Delta J + z^{-1}(bZ)F \qquad ....(4.46)$$

where degree J = degree Z and degree F = 0.

Since a unit static gain of the closed-loop is desired, it follows from Eqn.(4.45) and Eqn.(4.46) that:

$$L(1) = bZ(1)H(1) \qquad ....(4.47)$$

A simple choice of H is:

$$H(z^{-1}) = \frac{L(1)}{bZ(1)} \qquad ....(4.48)$$

Ideal feedforward is obtained by letting:

$$z^{-\tau'} fJ = z^{-1}(bZ)E \qquad ....(4.49)$$

which gives:

$$E = z^{\tau'+1} \frac{fJ}{bZ} \qquad ....(4.50)$$

From Eqn.(4.46) it follows that:

$$L(1) = bZ(1)F(1) \qquad ....(4.51)$$

since degree F = 0, Eqn.(4.51) substituted into Eqn.(4.46) gives:

$$J = \frac{1}{\Delta} [L - z^{-1} \frac{L(1)Z}{Z(1)}] \qquad ....(4.52)$$

The closed-loop system then becomes:

$$MO(k) = z^{-1}\frac{L(1)Z}{Z(1)L} \tilde{W}(k-\tau') + \frac{J}{L}\xi(k) \qquad ....(4.53)$$

where the characteristic equation of the closed-loop system L is assumed to be equal to:

$$L = Z + \beta \qquad ....(4.54)$$

where β is a design variable that determines how close the stable poles are to the process zero at the unit circle. The effect of β is the following:

- small β: will give poles that almost cancel the zeros of Z and a fast closed-loop system with large inputs;
- large β: will give poles that are closer to the open-loop poles in z=0. The zeros of Z will not be cancelled and the system response will be slower with small inputs.

Therefore, the pole placement controller is given by:

$$J*\Delta U(k) = H*\tilde{W}(k) - F*MO(k) - E*\Delta MI(k-\tau') \qquad ....(4.55)$$

In summary, the pole placement controller can be viewed in the following way: given the polynomial Z for a particular dryer, specify the desired closed-loop properties by defining L. With the given L and Z polynomials, the parameters b and f can be estimated and the control law can be calculated.

4.1.4.3) Model-Based Controller-(MB)

The model-based control is described in Eltigani (1987), and consists of a feedforward model-based type with feedback correction and dynamic compensation.

By considering that the drying process can be described by Eqn.(4.7), the controller parameter is calculated using the following equation:

$$b' = \{\ln[MI(k-\tau')/MO(k)]\}/T_r \qquad ....(4.56)$$

The residence time T_r is calculated from the following equation:

$$T_r = \{\ln[M_{ps}(k)/\bar{W}]\}/b' \qquad ....(4.57)$$

where M_{ps}, the pseudo-inlet moisture content is defined by Eqn.(3.26). The values of $\kappa_1 \ldots \kappa_i$ in Eqn.(3.26) are defined as in Eltigani (1987):

$$\kappa_i = 1/[1 + (\sum_{i=2}^{n} 2/i)] \qquad ....(4.58)$$

$$\kappa_{i-1} = (2/i)/[1 + (\sum_{i=2}^{n} 2/i)] \qquad ....(4.59)$$

where the subscript i represents the inlet moisture content, and the subscript 1 the outlet moisture content.

The sample strategy employed in the control system described in Eltigani (1987) differs from the one that has been discussed in this study; i.e., in Eltigani's control system, the sample is made at fixed time intervals. In this study, the fixed-distance sample strategy is used with Eqn.(4.57).

4.1.5) Filtering of the Parameter Estimation

Under noisy conditions, the controller parameters vary considerably, and sudden disturbances such as jumps, peaks or outliers may change the controller parameters without being desired (Isermann et al., 1982). To avoid unexpected disturbances, filtering of the parameters estimates, before they are used in the controller parameter calculations, is thus used. It results in a smoothing of the parameter estimates. The filter algorithm is:

$$\theta_{fi}(k) = \alpha*\theta_{fi}(k-1) + (1-\alpha)*\theta_i(k) \qquad ....(4.60)$$

with $0<\alpha<1$

4.1.6) Control Algorithm Flow Diagram

The parameter-adaptive controller is programmed in a modular way by separating the parameter estimation and the controller algorithms. The calculation scheme for the control algorithm is:

(1) set the initial conditions (setpoint, rpm, moisture contents);

(2) measure the inlet moisture content, outlet moisture content and auger rpm;

(3) differentiate the variables in (2) by using Eqn.(4.39);

(4) perform the parameter estimation - [Eqns.(4.8-20)];

(5) filter the calculated parameters using Eqn.(4.60);

(6) make the parameter calculation values of $Q(z^{-1})$, $R(z^{-1})$, $Q"(z^{-1})$ and $R"(z^{-1})$ for the MV-controller, the L, S, E, J and H values for the PP-controller, and b' for the MB-controller.

(7) add Eqn.(4.39) for the MV-controller ;

(8) calculate the new manipulated variable [Eqns.(4.34), (4.35), (4.36), (4.55), or (4.57)];

(9) go back to step (2).

Figure 4.2 shows the flow diagram of the control algorithm for continuous-flow grain dryers.

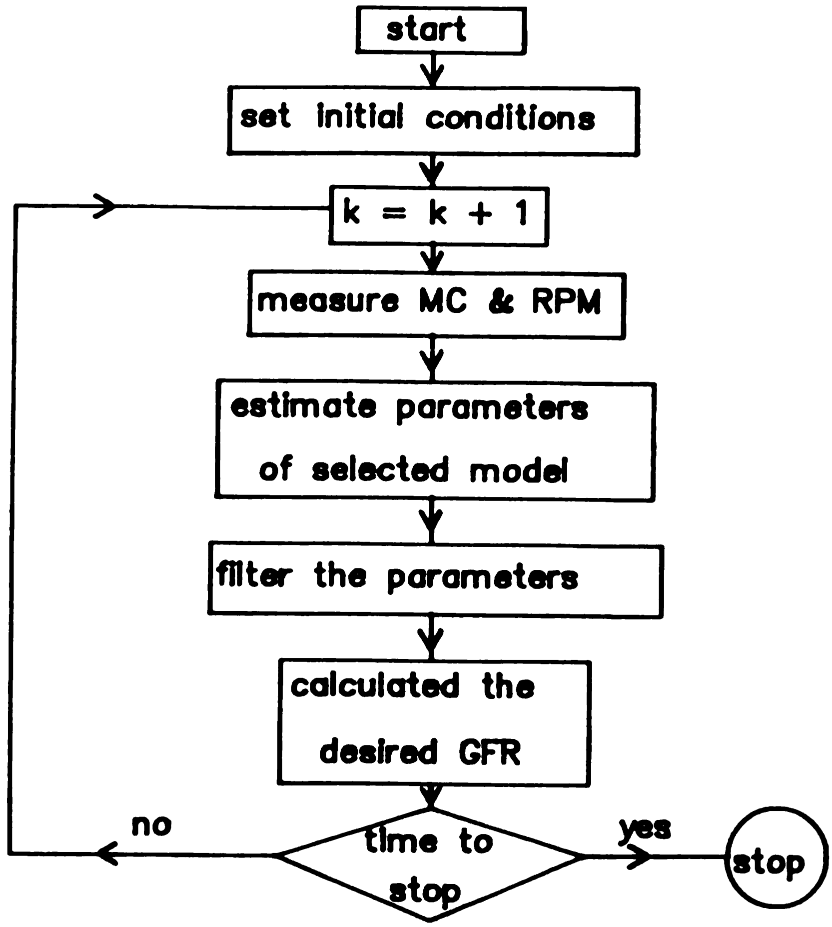

Figure 4.2: Control algorithm for continuous-flow grain dryers.

4.2) UNSTEADY-STATE CONCURRENTFLOW DRYING

It is difficult to study and compare grain dryer control systems experimentally because large amounts of grain of varying moisture content are needed, and accurate recording of the dryer inputs/outputs (i.e. grain moisture content, ambient conditions, etc.) is necessary to be able to assess the results.

Computer simulation provides a quicker method of comparing the performance of grain dryers. In the simulation, the inputs to the dryer, such as the grain moisture content, the ambient air humidity, etc. can be set to the exact desired values, and these can be repeated for other dryers.

The simulation of dryers in steady state (i.e. prediction of the conditions in the dryer when all the inputs remain constant) is well established (Brooker et al., 1981). In this study, an unsteady state model is developed for concurrentflow drying to allow control systems to be analyzed.

4.2.1) Development of the Unsteady-State Model

Heat and mass balances are made to develop mathematical models to describe the drying process. The drying of grains depends on the contact between the hot air and a bed of grain kernels. The heat transfers from the hot air to the cold grain, while the moisture is transferred from the grain to the air.

The steady-state simulation model for concurrenflow grain drying is represented by Eqns.(3.14.1-14.5). The model is used extensively in analyzing and designing multi-stage concurrent-flow grain dryers (Brooker et al., 1981). In order to simulate the concurrentflow grain drying when the inputs to the dryer are changing, an unsteady-state model is required. It is presented in the following section.

Unsteady-state energy and mass balances for grain and air are written on a differential volume located at an arbitrary position in the grain bed of a concurrentflow dryer. Figure 4.3 shows the control volume bed.

The following assumptions are made in the development of the unsteady-state concurrentflow grain drying model:

1. the volume shrinkage is negligible during the drying process;
2. no temperature gradients exist within the grain particles;
3. the particle to particle heat conduction is negligible;
4. the air and grain flow rates are plug type;
5. the dryer walls are adiabatic, with negligible heat capacity;
6. the heat capacities of moist air and grain are constant;
7. the grain flow rate V_p is constant during a dt time step.

The first of these assumptions is the most suspect since shrinkage occurs during drying. However, the decrease of the bed height is not substantial, especially not in the case of continuous-flow dryers (Brooker et al., 1981).

The other assumptions have shown to be valid for continuous-flow dryers (Bakker-Arkema et al., 1974).

There are four unknowns in this problem: M, the grain moisture content; W, the humidity ratio of the air; T, the air temperature; and θ, the grain temperature. Four balances are made, resulting in four equations:

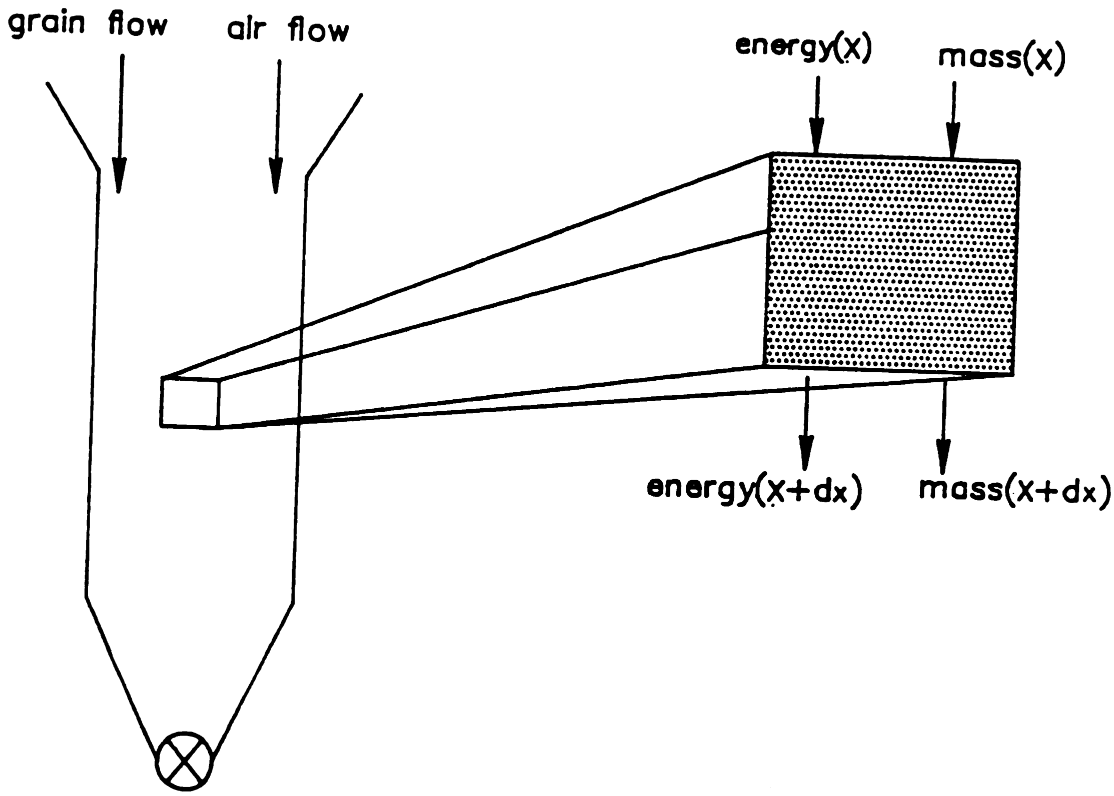

Figure 4.3: Energy and mass balances on a control volume within a concurrentflow grain dryer.

a) Energy Balance of the Air

energy in in dt - energy transferred in dt - energy accumulated in dt = energy out in dt

$$(\rho_a V_a c_{am} T)Sdt - h'a(T-\theta)Sdxdt - \left[\rho_a c_{am}\,\epsilon\,\frac{\partial T}{\partial t}\right]Sdxdt =$$

$$\rho_a V_a c_{am}\left(T + \frac{\partial T}{\partial x}dx\right)Sdt$$

or,

$$\epsilon \rho_a c_{am}\frac{\partial T}{\partial t} = -\rho_a V_a c_{ma}\frac{\partial T}{\partial x} - h'a(T-\theta)$$

and,

$$\frac{\partial T}{\partial t} = -\frac{V_a}{\epsilon}\frac{\partial T}{\partial x} - \frac{h'a\,(T-\theta)}{\rho_a\, c_{am}\,\epsilon} \qquad \text{.......(4.61)}$$

where:

$$c_{am} = c_a + c_v W$$

b) Energy Balance of the Product

energy in in dt + energy transferred in dt = energy out in dt + energy to evaporate water in dt + change in sensible heat of grain w.r.t. time + change in sensible heat of water vapor in dt

$$(\rho_p V_p c_{pm}\theta)Sdt + h'a(T-\theta)Sdxdt = \rho_p\, V_p\, c_{pm}\left(\theta + \frac{\partial \theta}{\partial x}dx\right)Sdt +$$

$$h_{fg}\left(-\rho_p\frac{\partial M}{\partial t}\right)Sdxdt + \left(\rho_p c_{pm}\frac{\partial \theta}{\partial t}\right)Sdxdt +$$

$$c_v(T-\theta)\left(-\rho_p\frac{\partial M}{\partial t}\right)Sdxdt$$

or,

$$h'a(T-\theta) - \left[c_v(T-\theta) + h_{fg}\right]\frac{\partial M}{\partial t} - \rho_p\, c_{pm}\, V_p\frac{\partial \theta}{\partial x} = \rho_p\, c_{pm}\frac{\partial \theta}{\partial t}$$

and,

$$\frac{\partial \theta}{\partial t} = \frac{h'a}{\rho_p\, c_{pm}}(T-\theta) + \left[\frac{c_v(T-\theta)}{c_{pm}} + \frac{h_{fg}}{c_{pm}}\right]\frac{\partial M}{\partial t} - V_p\,\frac{\partial \theta}{\partial x} \qquad \text{.......(4.62)}$$

where:

$$c_{pm} = c_p + c_w M$$

c) Mass Balance of the Air

water vapor in in dt + change of water in the air within the control volume in dt = water vapor out in dt + rate of water vapor evaporated from the grain in dt

$$(\rho_a V_a W)Sdt + \left(\epsilon\rho_a\,\frac{\partial W}{\partial t}\right)Sdxdt = \rho_a V_a\left(W + \frac{\partial W}{\partial x}\,dx\right)Sdt + \left(\rho_p\frac{\partial M}{\partial t}\right)Sdxdt$$

and,

$$\frac{\partial W}{\partial t} = \frac{V_a}{\epsilon}\,\frac{\partial W}{\partial x} + \frac{\rho_p}{\rho_a\,\epsilon}\,\frac{\partial M}{\partial t} \qquad \text{.......(4.63)}$$

d) Mass Balance of the Product

water in solids in dt = water in solids out in dt + change of moisture of solids in the control volume w.r.t. time

$$(\rho_p\, V_p M)Sdt = \rho_p V_p\left(M + \frac{\partial M}{\partial x}\,dx\right)Sdt + \rho_p(Sdxdt)\frac{\partial M}{\partial t}$$

and,

$$\frac{\partial M}{\partial t} = -\,V_p\,\frac{\partial M}{\partial x} \qquad \text{.......(4.64)}$$

Thus, the four equations for the model are:

$$\frac{\partial W}{\partial t} - \frac{V_a}{\epsilon}\,\frac{\partial W}{\partial x} = \frac{\rho_p}{\rho_a\,\epsilon}\,\frac{\partial M}{\partial t} \qquad \text{.....(4.65.1)}$$

$$\frac{\partial M}{\partial t} + V_p\,\frac{\partial M}{\partial x} = 0 \qquad \text{.....(4.65.2)}$$

$$\frac{\partial T}{\partial t} + \frac{V_a}{\epsilon}\left(\frac{\partial T}{\partial x}\right) = - \frac{h'a\,(T-\theta)}{\rho_a\, c_{am}\, \epsilon} \qquad .....(4.65.3)$$

$$\frac{\partial \theta}{\partial t} + V_p\,\frac{\partial \theta}{\partial x} = \frac{h'a}{\rho_p\, c_{pm}}\,(T-\theta) + \left[\frac{c_v(T-\theta)}{c_{pm}} + \frac{h_{fg}}{c_{pm}}\right]\frac{\partial M}{\partial t} \qquad .....(4.65.4)$$

Eqns.(4.65.1-65.4) constitute the unsteady-state concurrentflow grain drying model. It is similar to the system of unsteady-state equations developed by Eltigani (1987) for crossflow drying. The four equations are of the same form as those obtained from the general continuous-flow grain drying model presented by Laws and Perry (1983).

4.2.2) Numerical Solution

The finite difference technique is used to solve the system of Eqns.(4.65) along with the empirical thin-layer and equilibrium moisture content equations for corn developed by Thompson (1968), and the SYCHART package for moist air properties given by Bakker-Arkema et al. (1974). The grain flow rate is assumed to be constant during each time step but can vary between time steps.

The following finite difference terms are substituted for the corresponding partial differential terms:

$$\frac{\partial T}{\partial x} = \frac{T_{x+dx,t+dt} - T_{x,t+dt}}{dx} \qquad ....(4.66)$$

$$\frac{\partial T}{\partial t} = \frac{T_{x+dx,t+dt} - T_{x+dx,t}}{dt} \qquad ....(4.67)$$

$$\frac{\partial \theta}{\partial x} = \frac{\theta_{x+\frac{1}{2}dx,t} - \theta_{x,t}}{dx} \qquad ....(4.68)$$

$$\frac{\partial\theta}{\partial t} = \frac{\theta_{x+\frac{1}{2}dx,t+dt} - \theta_{x+\frac{1}{2}dx,t}}{dt} \qquad \text{.......(4.69)}$$

$$\frac{\partial M}{\partial x} = \frac{M_{x+\frac{1}{2}dx,t} - M_{x,t}}{dx} \qquad \text{.......(4.70)}$$

$$\frac{\partial M}{\partial t} = \frac{M_{x+\frac{1}{2}dx,t+dt} - M_{x+\frac{1}{2}dx,t}}{dt} \qquad \text{.......(4.71)}$$

$$\frac{\partial W}{\partial x} = \frac{W_{x+dx,t+dt} - W_{x,t+dt}}{dx} \qquad \text{.......(4.72)}$$

$$\frac{\partial T}{\partial x} = \frac{T_{x+dy,t} - T_{x+dx,t+dt}}{dt} \qquad \text{.......(4.73)}$$

Substituting Eqns.(4.66-73) into Eqns.(4.65) results in the following equations:

$$\theta(i,j+1) = (1-CON_1)*\theta(i,j) + (CON_2*THT)/CON_3 - [CON_4*(c_v*THT+h_{fg})*(W(i+1,j) - W(i,j)]/CON_3 + CON_1*TPP \qquad \text{.......(4.74)}$$

$$T(i+1,j+1) = [T(i,j) + CON_5*TTT + CON_6*\theta(i,j+1)]/CON_7 \qquad \text{.......(4.75)}$$

$$W(i+1,j+1) = \{WW - CON_8*W(i,j+1) - CON_9*[M(i,j+1) -M(i,j)]\}/CON_{10} \qquad \text{.......(4.76)}$$

M(i,j+1) is calculated using the thin-layer equation evaluated at:

$$\text{Temperature} = [\theta(i,j) + T(i,j+1)]/2$$

$$\text{Specific Humidity} = \{[W(i,j) + W(i+1,j)]/2 + W(i,j+1)\}/2$$

$$\text{Relative Humidity} = RH(\text{Temperature, Specific Humidity})$$

where:

$$CON_1 = G_p*dt/(\rho_p*dx)$$

$$CON_2 = (h'*a/\rho_p)*dt$$

$$CON_3 = c_p+c_w*M(i,j)$$

$$CON_4 = G_a*dt/(\rho_p*dx)$$

$$CON_5 = G_a*dt/(\rho_a*\epsilon*dx)$$

$$CON_6 = [h'*a*dt/(\rho_a*\epsilon)]/\{c_a+c_v*[W(i,j+1)+W(i+1,j+1)]/2\}$$

$$CON_7 = 1+CON_5+CON_6$$

$$CON_8 = G_a*dt/(\rho_a*\epsilon*dx)$$

$$CON_9 = \rho_p/(\epsilon*\rho_a)$$

$$CON_{10} = 1-CON_8$$

$$THT = [T(i,j) + T(i+1,j)]/2 - \theta(i,j)$$

$$TPP = [\theta(i,j) + \theta(i+1,j)]/2$$

$$TTT = [T(i,j) + T(i+1,j+1)]/2$$

$$WW = [W(i,j) + W(i+1,j+1)]/2$$

The solution of the system of Eqns.(4.65) is obtained with the help of a computer. A program is written in FORTRAN and contains the following steps:

(1) read the initial conditions:

at time=0

M(0,0)=Min; θ(0,0)=θin

T(0,0)=Tin; W(0,0)=Win

(2) read the inlet moisture content

(3) increment the time and depth (Δt and Δx)

(4) calculate T, θ, W, and M

(5) read the new inlet moisture content

(6) is the depth increment completed?

<u>yes</u>: continue; <u>no</u>: go to (3)

(7) set the depth=0

(8) is the input data completed?

<u>yes</u>: stop; <u>no</u>: go to (2)

The program simulates the unsteady-state drying of a single-stage concurrenflow dryer. To simulate a two-stage CCF dryer, it is assumed that the tempering stage is sufficiently long for moisture and temperature equalization to occur within each grain kernel. It is assumed that the corn does not change in average moisture content or temperature as it passes through a tempering zone (Bakker-Arkema et al., 1982).

The values of the physical properties for air and corn used in the simulation program are given in Table 4.1. At Δx = 0.168 cm (0.0055 ft) the program is stable for all grain flow rates used during the simulation (i.e. 2.12 to10.83m/hr). The stability of the simulation program is not affected by a change in Δt (0.57 to 2.91 sec) due to changes in the grain flow rate.

The computer program is implemented on a VAX/VMS minicomputer system. The computer uses considerable CPU time. To simulate 8 hours of drying time an average of 14 hours of CPU time is required (for 5 points moisture removal). The CPU time is a function of the amount of moisture to be removed, i.e., the CPU time increases with an increase in the moisture to be extracted.

The heat transfer coefficient is considered to vary with the airflow rate according to the equation given in Table 4.1. Since the airflow rate is constant, the heat transfer coefficient is also constant. This may introduce a slight error due to the lack of information how the heat transfer coefficient varies with grain flow rate.

The surface area of corn per unit volume bed is assumed to be constant. As discussed earlier, shrinkage does occur but is considered to be of minor influence.

The remaining properties (density, specific heat, etc.) for air and grain are assumed to be independent of the temperature. They may vary with temperature but the changes are assumed small and result in negligible errors in the simulation results.

The theoretical developments and contributions of this study can be summarized as follows:

(1) Several empirical models are developed for the description of the dynamics of continuous-flow grain dryers and control design.

(2) Several adaptive control algorithms are employed for the investigation of on-line continuous-flow grain drying process. No application to multi-stage dryers has been attempted before.

(3) The recursive predicted error method (RPE) is used for the estimation of the model parameters of Eqn.(4.2) and Eqn.(4.4). The

Table 4.1: Physical properties of air and corn used in the unsteady-state simulation model.

PARAMETERS	VALUE* SI units	ENGLISH units
a	784.1 m^{-1}	239 ft^{-1}
c_a	1.013 kJ/kg°C	0.242 Btu/lb°F
c_v	1.884 kJ/kg°C	0.450 Btu/lb°F
c_w	4.187 kJ/kg°C	1.000 Btu/lb°F
c_p	1.122 kJ/kg°C	0.268 Btu/lb°F
ρ_a	1.200 kg/m^3	0.075 lb/ft^3
ρ_p	620.1 kg/m^3	38.700 lb/ft^3
ϵ	0.45	0.45
Δx	0.168 cm	0.0055 ft
Δt	0.57-2.91 sec	0.57-2.91 sec

$$h_{fg}^{*} = \begin{cases} & \text{for } M\geq 0.17 \qquad\qquad \text{for } M<0.17 \\ \text{SI units} & 2326 \text{ kj/kg} \qquad (2502-2.309\theta)\left[1+4.35e^{(-28.25M)}\right] \\ \text{English units} & 1000 \text{ BTU/lb} \qquad (109,457\theta)\left[1+4.35e^{-(28.25M)}\right] \end{cases}$$

$$h'^{*} = \begin{cases} \text{SI units} & \begin{cases} 6.483*a*G_a^{0.49}; & G_a<2443 \text{ kg/hr-m}^2 \\ 2.919*a*G_a^{0.59}; & G_a\geq 2443 \text{ kg/hr-m}^2 \end{cases} \\ \text{English units} & \begin{cases} 0.690*G_a^{0.49}; & G_a<500 \text{ Btu/hr-ft}^2 \\ 0.363*G_a^{0.59}; & G_a\geq 500 \text{ Btu/hr-ft}^2 \end{cases} \end{cases}$$

* From Bakker-Arkema et al. (1974)

least-square method is employed for the estimation of the parameters of Eqns.(4.3) and (4.6).

(4) An unsteady-state concurrentflow drying model is developed to allow control systems to be analyzed.

(5) The applicability of the control systems to continuous-flow grain dryers is analyzed. Advantages and disadvantages of each control system are determined.

CHAPTER 5

EXPERIMENTAL INVESTIGATION

This chapter is divided in three main sections. The first section describes the equipment and the control system used for the implementation of the adaptive control system. In the second section, the procedure used to simulate the automatic control of a two-stage CCF grain dryer is discussed. And finally, a statistical test to evaluate the model order for the system identification experiment is described.

5.1) CONTROL OF CROSSFLOW GRAIN DRYERS

During the 1986 and 1987 harvest seasons, the adaptive control system was implemented on two commercial-scale crossflow dryers manufactured by Meyer-Morton Company, Morton, IL; and, Zimmerman Equipment Company, Litchfield, IL.

In 1986, grain drying tests were conducted with the Meyer-Morton dryer using the GMV-control algorithm. In 1987, the PP-controller was tested on the Zimmerman dryer.

Due to field test problems, such as dryer malfunction, bad weather conditions and lack of grain, the drying tests had to be suspended often. The number of control tests were limited, and only the MV-feedback, the MV-feedback/feedforward and the PP controllers could be implemented. The simulation model for the CCF dryer fortunately provides a means for testing all the control algorithms.

5.1.1) Equipment

The Meyer-Morton 850 dryer is schematically shown in Figure 5.1. In Table 5.1 a list of the dryer specifications is presented (Anderson, 1985). The dryer is 14.86 meters in height. The lengths of the drying and cooling sections are 8.39 meters and 3.50 meters, respectively. The grain column thickness is 25.40cm at the upper and 30.48cm in the lower part of the dryer. The heating and cooling sections have individual fans. The drying air fan for the heating section is driven by a 60 HP motor. Air for this fan is a combination of ambient air and recycled air (cooling plus part of drying air) from the heat recovery enclosure. The cooling fan (ambient air) is driven by a 25 HP motor. The air flow in the heating and cooling section is in the same direction (no air-reversal). The rated capacity is 35.6 tonnes of wet corn per hour at 5 points moisture removal at 110°C drying air temperature.

A schematic of the Zimmerman ATP 5000 dryer along with its specifications is shown in Figure 5.2 and Table 5.2, respectively (Anderson, 1985). The heating section is 29.36 meters in length, the cooling section is 5.64 meters. The column thickness is 30.48cm over the entire dryer length. At the mid-point in the heating section the grain passes through a grain exchanger; the grain column is split so that the inside and outside halves of the grain column are interchanged. The air flow direction is reversed in the cooling section; air from the cooling section is blended with ambient air. The air system consists of three 100 HP motors and three centrifugal fans. The rated capacity is 127 tonnes of wet corn per hour at 5 points moisture removal at 82.2°C drying air temperature.

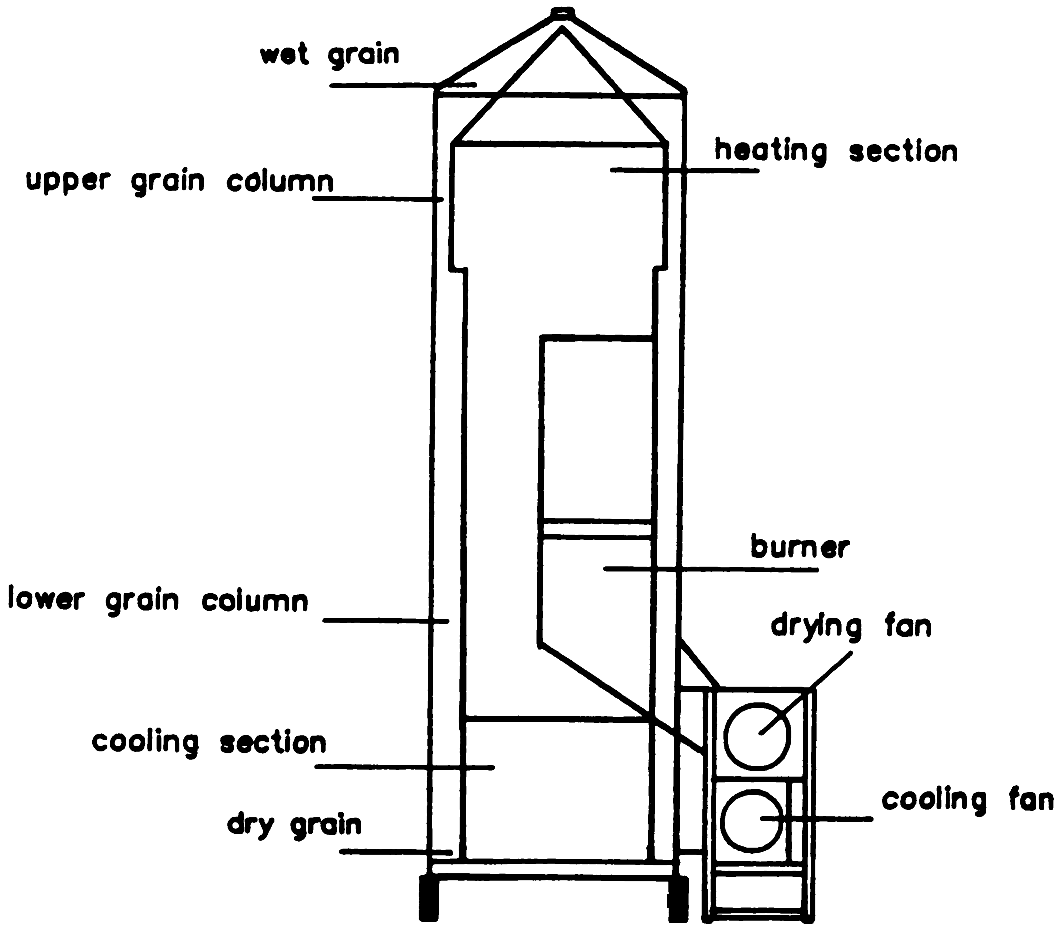

Figure 5.1: Schematic of the Meyer-Morton 850 crossflow dryer.

Table 5.1: Meyer-Morton 850 crossflow dryer specifications.

PARAMETER		VALUE
Airflow rate, [m/min]	heat section	31.1
	cooling section	38.4
Static Pressure, [Pa]	heat section	747.3
	cooling section	747.3
Grain flow rate, [m/hr]	at 5 points moisture removal	20.0
Drying Temperature, [°C]	recommended	110.0
Dryer Dimensions [m]		
	length of drying section	8.4
	length of cooling section	3.5
	columns widths	0.25 & 0.3
	outside dryer diameter	3.5
Column Cross Sectional Area, [m^2]		3.1
Rated Capacity, [tonne/hr]	20%-15% MC	35.6
Retention Time, [hr]		0.6
Burner Capacity, [W]x10^6		2.6
Fuel Type,		LP

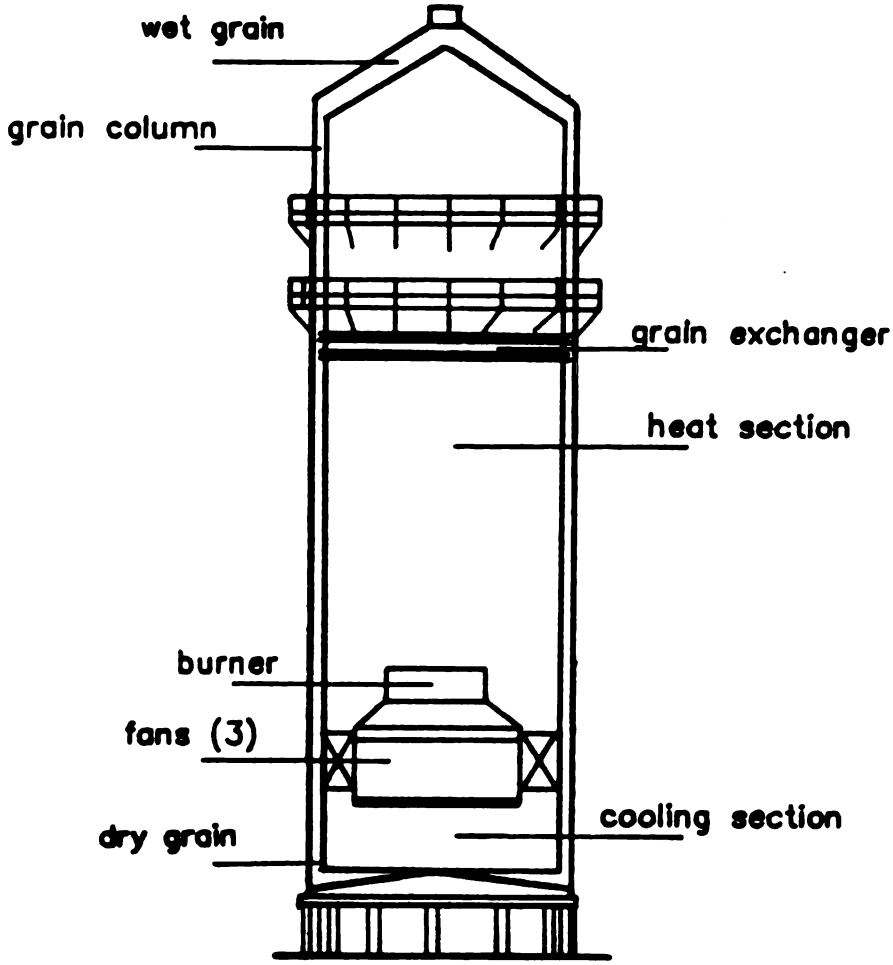

Figure 5.2: Schematic of the Zimmerman ATP 5000 crossflow dryer.

Table 5.2: Zimmerman ATP 5000 crossflow dryer specifications.

PARAMETER		VALUE
Airflow rate, [m/min]	heat section	18.6
	cooling section	33.8
Static Pressure, [Pa]	heat section	373.7
	cooling section	373.7
Grain flow rate, [m/hr]	at 5 points moisture removal	27.0
Drying Temperature, [°C]	recommended	82.2
Dryer Dimensions [m]		
	length of drying section	29.4
	length of cooling section	5.6
	columns widths	0.3
	outside dryer diameter	7.1
Column Cross Sectional Area, [m^2]		5.8
Rated Capacity, [tonne/hr]	20%-15% MC	127.0
Retention Time, [hr]		1.0
Burner Capacity, [W]x10^6		15.9
Fuel Type,		natural gas

5.1.2) Control System

A schematic of the adaptive control system for the continuous-flow crossflow dryers is illustrated in Figure 5.3. The system consists of (Eltigani, 1987):

(1) a microcomputer with 128K memory;

(2) a tachometer;

(3) a moisture meter;

(4) A/D and D/A converters;

(5) system software:

- BASIC;
- data collection and control algorithm.

The heart of the system is an Apple IIe microcomputer with 128K RAM and floating-point Basic Language in read-only-memory (ROM). A hard copy of the collected data is provided by a printer.

The inlet and outlet grain moisture contents are automatically measured every 6 min by a semi-continuous, capacitance based, moisture meter (Shivvers, Inc.). A microprocessor built into the moisture meter collects the moisture content data, and periodically transfers the information to the microcomputer.

The moisture meter is calibrated with the use of a standard moisture meter (Motomco moisture meter). The calibration adjustment is stored in the moisture meter microprocessor memory for adjustment of each moisture content measurement. A comparison between moisture content values obtained with the Shivvers moisture meter (Comp-U-Dry), a Motomco moisture meter and the air-oven showed good agreement (Eltigani, 1987). The difference in the outlet moisture content measured with the Shivvers moisture meter and with the Motomco is about 0.71%, and with the air

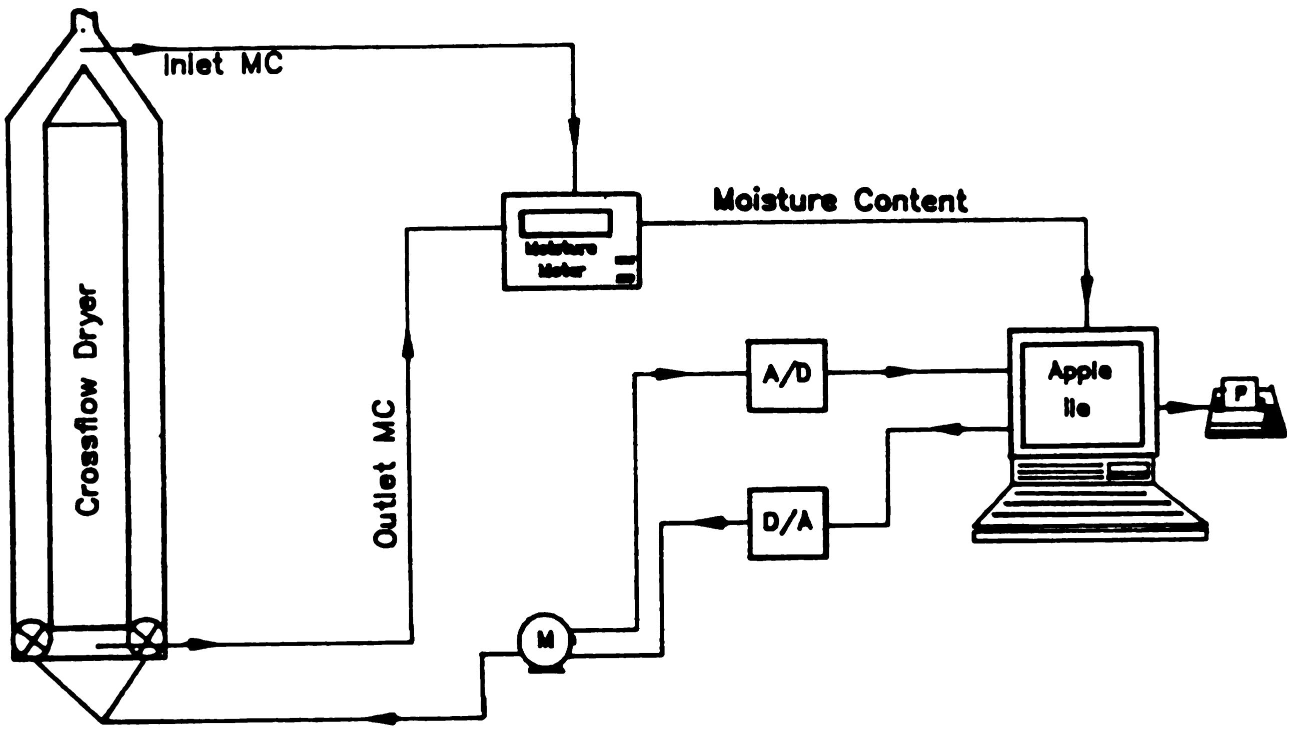

Figure 5.3: Schematic of the adaptive control system for a crossflow dryer.

-oven about 1.01%. In measuring the inlet moisture content, the Shivvers and the Motomco moisture meters show good agreement, i.e., only 2% difference, but 2-3 points lower than the value obtained with the oven method. The error in measuring the inlet moisture content is not as serious as the error in measuring the outlet moisture content because of the ability of the control system to account for the error through the dryer model parameters.

An AD/DA interface card is used in conjunction with the microcomputer. It is able to collect data from instruments that measure voltage as input and send voltage as output. The card contains 12 bit analog to digital (A/D) and digital to analog (D/A) conversion with an overall accuracy of 0.1%. The A/D and D/A converters can send or accept a voltage up to 4 volts. The specifications for the data acquisition system components are explained in detail in Eltigani (1987).

An incremental optical encoder measures the discharge auger rpm. The encoder outputs 500 cycles per revolution, and is powered by 5 volt supplied by the microcomputer.

The auger rpm is read continuously by a tachometer, and is calculated in terms of residence time (and dryer capacity) by the software of the microcomputer. The desired residence time of the dryer is achieved by sending a voltage to the unload auger. The relationship between the auger rpm and the residence time varies with dryer design.

5.1.3) Procedure

The following parameters are measured by the dryer control system:

(1) the grain inlet moisture content

(2) the grain outlet moisture content

(3) the discharge-auger rpm.

The values of the inlet and outlet moisture contents and of the rpm are transmitted intermittently to the microcomputer.

The controller equations used in the first part of this study are: Eqn.(4.33), Eqn.(4.36) and Eqn.(4.55). Therefore, the control input (auger rpm or residence time) is obtained by using one of the following three equations:

i) For the MV-feedback controller:

$$rpm(k+1) = -[q_0*e_w(k)+q_1*e_w(k-1)+...+q_m*e_w(k-m+1)+$$
$$r_1*rpm(k)+r_2*rpm(k-1)+...+r_m*rpm(k-m+1)] \qquad ....(5.1)$$

ii) For the MV-feedback/feedforward controller:

$$rpm(k+1) = -[q_0*e_w(k)+q_1*e_w(k-1)+...+q_m*e_w(k-m+1)+$$
$$d_0*\Delta mi(k-\tau')+d_1*\Delta mi(k-\tau'-1)+...+d_m*\Delta mi(k-m-\tau'+1)+$$
$$r_1*rpm(k)+r_2*rpm(k-1)+...+r_m*rpm(k-m+1)] \qquad ....(5.2)$$

iii) For the PP-controller:

$$t_r(k+1) = \frac{H*\hat{W} - H*MO(k) - E*\Delta MI(k) - J}{1+\beta} \qquad ......(5.3.1)$$

$$J = \{T_r(k-1) - T_r(k)*[L(1)/Z(1)]\} \qquad ......(5.3.2)$$

Eqns. (5.1) and (5.2) are obtained by substituting the controller parameters (Q and R) into Eqn.(4.33) and Eqn.(4.36), respectively. Eqns.(5.3) are obtained by replacing the controller parameters L, Z, E, H, and J (defined in section 4.1) into Eqn.(4.55).

In implementing the control system, the first attempt was to use the direct value of the measured discharge auger rpm as a control input [see Eqns.(5.1) and (5.2)]. In Eqn.(5.3) the discharge auger rpm is used indirectly, since the residence time t_r is inversely proportional to the rpm.

The residence time of the grain in the dryer is achieved by sending a voltage, corresponding to the specific residence time, to the discharge auger. The relationships between the residence time and the auger rpm, the auger rpm and voltage for the Meyer-Morton 850 dryer were determined experimentally:

$$T_r = \frac{1226.3}{RPM} \qquad \text{........(5.4)}$$

$$RPM = \frac{1226.3}{T_r} \qquad \text{........(5.5)}$$

$$\text{Voltage} = 0.5653 + 0.002543*RPM \qquad \text{........(5.6)}$$

The linear regression method was used to determine Eqns.(5.4)-(5.6) by fitting the experimental data to the predicted curves. In Appendix B the experimental data for the Meyer-Morton crossflow dryer is presented, and the method used to determine Eqn.(5.4) is explained in detail.

The sample strategy used in this study (see Section 4.1.3) requires a moisture meter which is capable of sending the measured data every time it is required by the microcomputer. However, the Shivvers moisture meter only measures the moisture content data approximately every 6 minutes. One way of overcoming this problem, and still be capable to use the fixed-distance sample strategy, was to limit the minimum sample time to 6 minutes, i.e., to limit the minimum interval of time between two samples to 6 minutes. This value is obtained by determining the maximum allowed auger rpm for the dryer. The expression for the sample time is obtained by dividing Eqn.(5.4) by the number of layers in the dryer. Therefore, the sample time for the Meyer-Morton 850 dryer is equal to:

$$t_r = \frac{1226.3/n}{RPM} = \frac{122.63}{RPM} \qquad \text{........(5.7)}$$

where t_r is in hour and the number of layers (n) in the dryer is 10. For the Meyer-Morton, the maximum discharge auger speed value is 1200 rpm.

The relationships between the residence time and the auger rpm, and the auger rpm and voltage for the Zimmerman ATP 5000 dryer are:

$$T_r = \frac{7200.}{7.95*RPM-6390.} \qquad \text{........(5.8)}$$

$$RPM = \frac{6390.*T_r+7200.}{7.95} \qquad \text{........(5.9)}$$

$$\text{Voltage} = 0.0097*\text{RPM}^{0.7943} \qquad \text{.......(5.10)}$$

The sample time is equal to:

$$t_r = \frac{7200./n}{7.95*\text{RPM}-6390.} = \frac{600.}{7.95*\text{RPM}-6390.} \qquad \text{.......(5.11)}$$

with n=12 layers. For the Zimmerman dryer, the maximum allowed discharge auger speed was 1800 rpm.

The voltage to be send to the SCR is converted to its digital equivalent by Eqn.(5.12), and then input to the D/A converter which sends it to the SCR in the dryer controller. The SCR then adjusts the auger rpm accordingly (Eltigani, 1987):

$$\text{VT} = \text{Volt}*(2047.)/4 \qquad \text{.......(5.12)}$$

where:

Volt = analog voltage

VT = digital equivalent Volt

The following procedure was followed in conducting the controller tests:

(1) the dryer is manually started for a period of time equal to the residence time equivalent to the initial rpm. During this period, moisture content and rpm data are continuously collected by the computer to be used by the control system during subsequent automatic control;

(2) after the start-up period has ended, the control system is switched to automatic (the length of a test varied from 5-8 hours);

(3) at the end of each test the data are analyzed.

5.2) CONTROL OF MULTI-STAGE CONCURRENTFLOW GRAIN DRYERS

Like in a crossflow dryer, the drying time in a concurrentflow dryer is determined by the rate at which the grain is discharged from the dryer. Feed-roll augers are used to regulate and control the grain flow. In multi-stage dryers, the discharge auger is located at the outlet of the last stage and thus the grain flow rate is the same throughout the dryer.

Therefore, the same control strategy used to design the control system for a crossflow dryer is considered in the design of the two-stage CCF corn dryer control system. The discharge rate (GFR) is the input to the process, the grain outlet moisture content is the output, and the grain inlet moisture content is the main disturbance. Neither the inlet air temperature nor the air flow rate is adjusted in the two dryer stages during the course of drying.

One of the objectives of this study in automatic control of continuous-flow grain dryers is to develop a control system which can be employed in both dryer types (crossflow and concurrentflow). Because the grain velocity is the same throughout a two-stage CCF dryer, the control system for this dryer type can be designed by considering the dryer as a one-stage drying process. The main goal is to demonstrate that a two-stage CCF dryer can be modeled as a one-stage dryer using a simple linear model.

The following is the description of the two-stage CCF corn dryer used in the simulation study.

5.2.1) Two-Stage Concurrentflow (CCF) Dryer

The two-stage Blount/ccd CCF dryer consists of two concurrentflow drying beds and a counterflow cooler. Between the first and the second drying stages, the grain flows through a tempering or steeping zone. The dryer is schematically shown in Figure 5.4. In Table 5.4 the specifications of the dryer are presented. The dryer is 12.83 meters in height. The length of the first and second drying stages is 0.76 meters. The tempering zone is 5.18 meters in height, and the cooling section measures 1.5 meters. The dryer cross-section area is 9.0 meters. The rated capacity is 34.0 tonnes of wet corn per hour at 5 points moisture removal.

5.2.2) Procedure

The same adaptive control system as shown in Figure 5.3 and described in Section 5.1.1 is considered for the concurrentflow dryer.

The following parameters are employed in the two-stage concurrentflow dryer control system:

(1) the grain inlet moisture content

(2) the grain outlet moisture content

(3) the discharge auger rpm.

In the second part of this study, the residence time is considered as the control input [U(k)] instead of the rpm [see Eqns. (4.2), (4.3) and (4.4)]. This procedure results in a linearization of the drying process (Nybrant and Regnér, 1985). The following is a

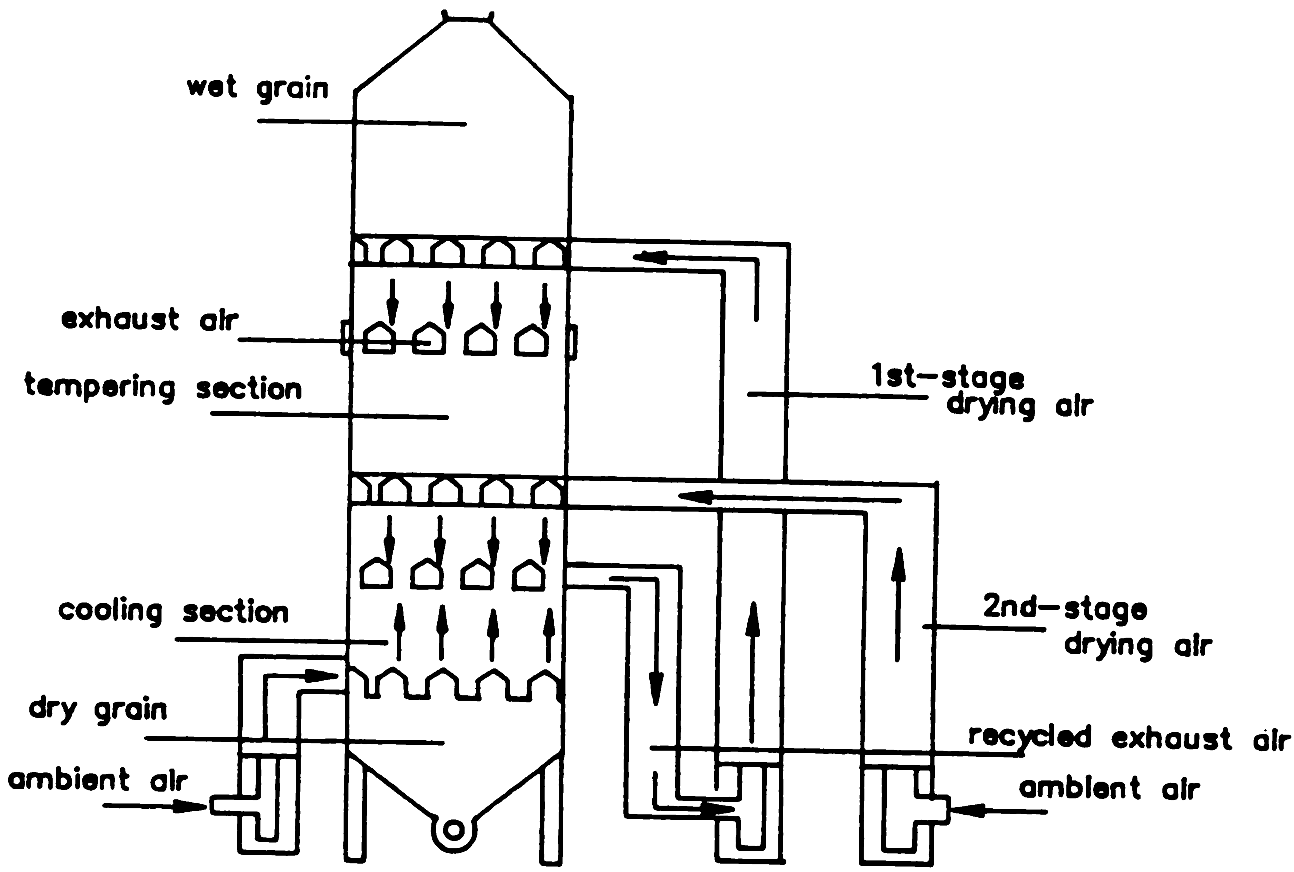

Figure 5.4: Schematic of a two-stage CCF dryer.

Table 5.3: Blount/cdd two-stage CCF dryer specifications.

PARAMETER		VALUE
Airflow rate, [m/min]	1st drying section	42.7
	2nd drying section	42.7
	cooling section	42.7
Static Pressure, [Pa]	1st drying section	2100.0
	2nd drying section	2100.0
Grain flow rate, [m/hr]	at 5 points moisture removal	12.4
Drying Temperature, [°C]	recommended	232.2
Dryer Dimensions [m]		
1st drying section		0.76
2nd drying section		0.76
cooling section		1.5
tempering		5.2
Dryer Cross Sectional Area, [m^2]		9.0
Rated Capacity, [tonne/hr]	20%-15% MC	34.0
Retention Time, [hr]		1.2
Fuel Type,		natural gas

detailed description of the linearization method.

The output of a continuous-flow grain dryer (moisture content) is approximately a linear function of the grain residence time T_r in the drying section [for example, the linear Eqn.(4.6)]. For a constant discharge rate, the residence time of the grain in the dryer is:

$$T_r = \frac{\ell_1}{GFR} \qquad ....(5.13)$$

where ℓ_1 is a constant depending on the same factors as ℓ [see Eqn. (4.5.1)]. Thus, if the GFR (i.e., rpm) is directly used as the control input, a linear system can not be expected. However, if

$$U = \frac{\ell_2}{GFR} \qquad ....(5.14)$$

is regarded as input, the dryer model can be linearized (Nybrant, 1986). When the control input U is used together with the sampling method [Eqn.(4.5.3)], ℓ_1=ℓ and the sample interval t_r will be equal to the control input U.

The two linearizations represented by Eqn.(4.5.3) and Eqn.(5.14) are employed for the automatic control design of a two-stage CCF dryer; this means that the sampling is performed with respect to the grain displacement in the dryer, and with the control input equal to the sample interval measured in time.

The controller equations in the automatic control of a two-stage CCF dryer are: Eqn.(4.32), Eqn.(4.35), Eqn.(4.36), Eqn.(4.55), and

Eqn.(4.57). Therefore, the control input (residence time) is obtained by using one of the following five equations:

i) For the MV-feedback controller:

$$t_r(k+1) = -[q_0*e_w(k)+q_1*e_w(k-1)+...+q_m*e_w(k-m+1)+$$
$$r_1*t_r(k)+r_2*t_r(k-1)+...+r_m*t_r(k-m+1)] \qquad ....(5.15)$$

ii) For the MV-feedforward controller:

$$t_r(k+1) = -[q_0*\Delta MI(k)+q_1*\Delta MI(k-d'-1)+...+q_m*\Delta MI(k-d'+1)+$$
$$r_1*t_r(k)+r_2*t_r(k-1)+...+r_m*t_r(k-m+1)] \qquad ....(5.16)$$

iii) For the MV-feedback/feeforward controller:

$$t_r(k+1) = -[q_0*e_w(k)+q_1*e_w(k-1)+...+q_m*e_w(k-m+1)+$$
$$d_0*\Delta MI(k-d')+d_1*\Delta MI(k-d'-1)+...+d_m*\Delta MI(k-m+1)+$$
$$r_1*t_r(k)+r_2*t_r(k-1)+...+r_m*t_r(k-m+1)] \qquad ....(5.17)$$

iv) For the PP-controller:

$$t_r(k+1) = \frac{H*W - H*MO(k) - E*\Delta MI(k) - J}{1+\beta} \qquad .....(5.18.1)$$

$$J = \{T_r(k-1) - T_r(k)*[L(1)/Z(1)]\} \qquad .....(5.18.2)$$

v) For the MB-controller:

$$T_r(k+1) = [\ln(M_{ps}(k)/\hat{W})]/b' \qquad \text{.......(5.19)}$$

with,

$$M_{ps}(k) = \kappa_1 *MI(k)+\kappa_2 *MI(k+1)+...+\kappa_i (k+i) \qquad \text{.......(5.20)}$$

and $\kappa_1 ... \kappa_i$ as defined by Eqns.(4.58) and (4.59) and b' by Eqn.(4.56).

Eqn.(5.15) and Eqn.(5.17) are obtained by replacing the controller variables Q and R into Eqns.(4.32) and (4.36), respectively; Eqn.(5.16) by replacing the controller variables Q" and R" into Eqn.(4.33); Eqn.(5.18) by replacing the controller variables L, Z, E, H and J into Eqn.(4.55) and, Eqn.(5.19) by replacing the controller variable b' into eqn.(4.57).

The values of the resident time and the auger rpm for a two-stage CCF dryer were obtained from a commercial CCF dryer brochure (Blount Inc., Montgomery, AL). The relationship between the residence time and the auger rpm was determined by linear curve-fitting, and was found to be:

$$T_r = \frac{1700.}{12.49+46.4*RPM} \qquad \text{.......(5.21)}$$

$$RPM = \frac{1700.-12.49*T_r}{46.4} \qquad \text{.......(5.22)}$$

For the control study of a two-stage CCF dryer, it was assumed that the moisture meter can send the input data to the microcomputer each minute instead of each 6 minutes. This procedure decreases the computer time for the simulation.

The sample time was found to be equal to:

$$t_r = \frac{1700./n}{12.49+46.4*RPM} \qquad ....(5.23)$$

with n=23 layers. For the two-stage CCF dryer, the maximum allowed discharge auger speed is 48 rpm.

5.3) NUMERICAL IDENTIFICATION

Experimental data obtained with the Meyer-Morton and the Zimmerman crossflow dryers were used to test the empirical models, i.e., Eqns.(4.2) and (4.4), and Eqn.(4.6), respectively. Simulation results obtained with the partial differential equations model (CCF dryer) provided data to test the suitability of the empirical models [Eqns(4.2), (4.3), (4.4), (4.6) and (4.7)] in describing the dynamics of the drying process.

A statistical test was employed to determine the model orders. For example, for Eqn.(4.2), to test if the model is of first order, the following hypothesis is considered:

$$H_0 = (a_2^o = b_1^o = c_2^o = 0) \qquad ....(5.24)$$

By assuming that the asymptotic theory can be applied, the statistic (Åstrom, 1970):

$$\vartheta = \frac{LF_1 - LF_2}{LF_2} * \frac{N-6}{3} \qquad ....(5.25)$$

has a $F_{1-\alpha}(3,N-6)$ distribution under the null hypothesis [Eqn.(5.24)]. The symbol LF_1 denotes the minimal value of the loss function for the first-order model, LF_2, the minimal value for the second-order model, and N the number of input-output pairs.

In using the statistic ϑ, the hypothesis (5.24) is tested at the α level of significance by comparing ϑ with the critical value $F_{1-\alpha}(3,N-6)$. If this critical value is exceeded, the hypothesis that the model is first-order is rejected. See Neter and Wasserman (1974) for an F table.

In summary, the implementation of the control algorithms [Eqns.(4.32), (4.33), (4.36), (4.55) and, (4.57)] to continuous-flow grain dryers has been presented. The calculation of the sample time, i.e., Eqn.(4.5.3), has been treated in detail.

For the implementation of the GMV controller it was suggested that the residence time (T_r) be used as the control input instead of the rpm because this procedure leads to a linearization of the drying process.

For the numerical identification of the drying process, a method for the selection of the order of the model (4.2) has been presented. The basic approach is to compare the performance (loss function) of the model of first and second order, and to test if the higher-order model is required.

CHAPTER 6

RESULTS AND DISCUSSION

The experimental results of the automatic control of the two crossflow dryers and the simulation results of a two-stage CCF dryer are presented and analysed in this chapter. In the first part, the empirical models are verified and their suitability assessed to describe the dynamics of the crossflow drying process; then, the experimental control data obtained with the Meyer-Morton 850 and the Zimmerman ATP 5000 crossflow dryers are presented. In the second part, the unsteady-state model is compared to the steady-state CCF dryer model; then, the empirical models are verified and their suitability determined to simulate the dynamics of the CCF drying process. Finally, the automatic control simulation results are presented, and the control behavior of the control system is evaluated based on several performance measures.

6.1) CROSSFLOW DRYING PROCESS

6.1.1) Model Identification Results

The dryer model is determined directly from measurements (inlet-outlet moisture contents, rpm) on the drying process. In general, the control variable (rpm) is perturbed and the resulting variations in the output (outlet moisture content) are observed. On the basis of the recorded rpm-outlet and/or inlet moisture content pairs, a model of the process and the disturbances is determined. In this particular case, the identification experiments could not be performed with the commercial dryers due to economical reasons. Instead, experimental data obtained during a normal operation test were used. The selected tests were chosen based on the inlet moisture content, grain flow rate and outlet moisture content variations. It is assumed that the length of the drying tests is sufficient to give the necessary information about the dynamics of the process.

The experimental data obtained with the crossflow dryers in 1986 were used to test the empirical models [Eqns.(4.2), (4.4) and (4.6)]. The recursive predicted error program (section 4.2.1) was adapted for off-line study. The objective of the first part of this section is to test if the empirical models used in the MV-feedback and MV-feedback/feedforward and PP controllers are suitable for on-line calculations.

6.1.1.1) Numerical Identification of the Meyer-Morton Dryer

Results of more than 10 hours run with the Meyer-Morton crossflow dryer (Eltigani, 1987) were employed to estimate the parameters of Eqn.(4.2) and Eqn.(4.4). Figure 6.1 shows the experimental data. The results are shown in Table 6.1.

To test the hypothesis that model I is of the first order (see Section 5.3), it is assumed that the the asymptotic theory can be applied (Åstrom, 1970). The null hypothesis is:

$$H_0: (a_2^0 = b_1^0 = c_2^0 = 0)$$

In this particular case, $\vartheta = 1.07$. At risk level of 5%, $F_{0.95}(3,64)$ is

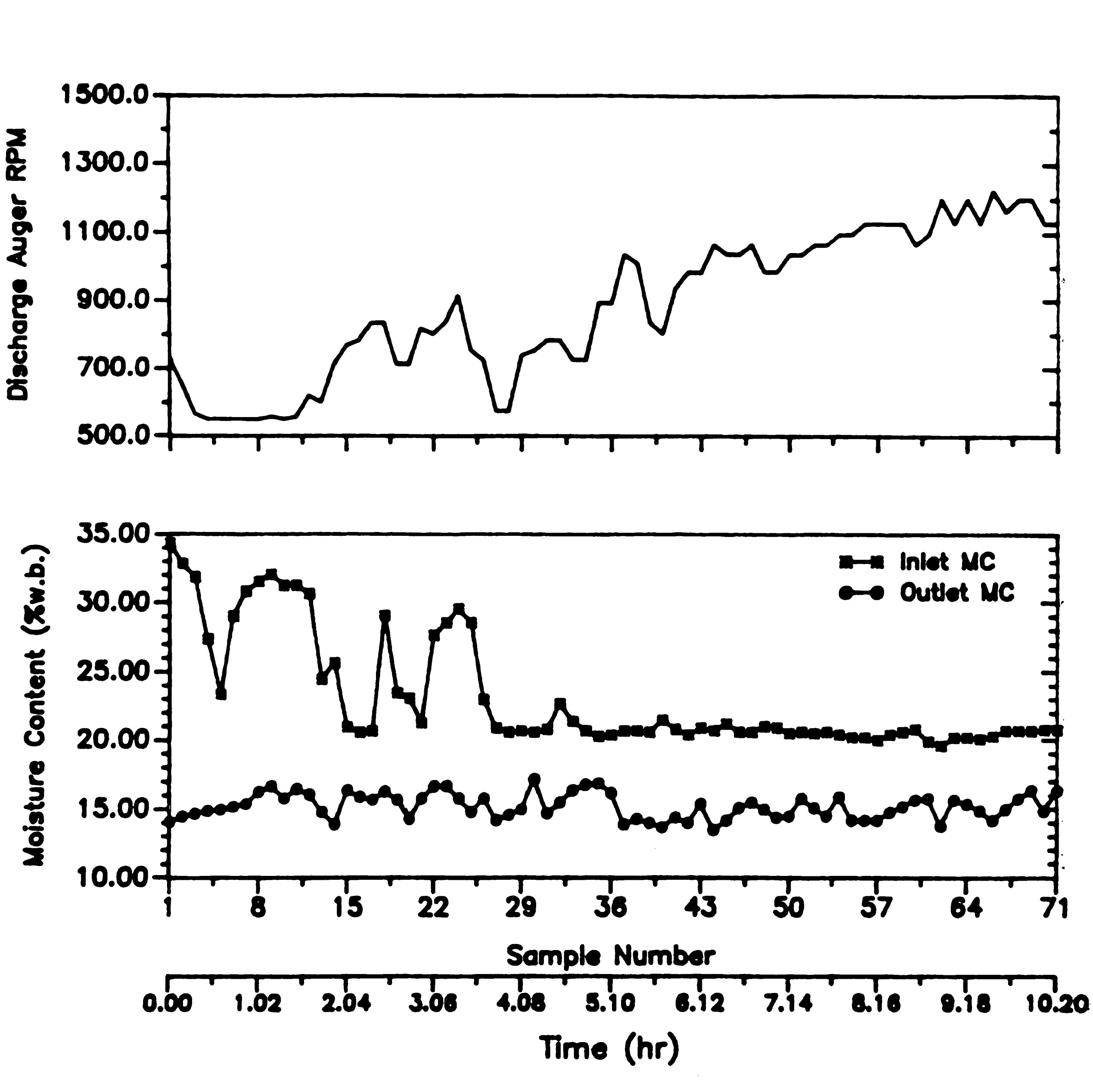

Figure 6.1: Meyer-Morton experimental data employed to obtain the parameters of model I and model II-b (10/29/86).

Table 6.1: Parameters values for the models I and II-b of the Meyer-Morton dryer.

		MODEL		
PARAMETERS		MODEL I		MODEL II-b
		1st-order	2nd-order	
a_1	=	-0.99±0.01	-1.41±0.06	-0.80±0.06
a_2	=		0.42±0.07	
b_1	=	0.00026±0.001	0.0020±0.0002	0.0015±0.002
b_2	=		0.00061±0.001	
c_1	=	-0.39±0.09	-0.67±0.01	0.088±0.08
c_2	=		-0.12±0.07	
d_1	=			-0.25±0.5
LOSS FUNCTION		54.50	51.89	58.02

2.76, and the null hypothesis (i.e. that the system is first order) has to be accepted.

Figure 6.2 illustrates the identification of the first-order model I. The estimated values show how well the observed outlet moisture contents can be predicted by the model.

The identification procedure was based on the assumption that the residuals $[mo(t)-\hat{mo}(t)]$ are normal and uncorrelated. As Figure 6.2 shows, these assumptions are not violated.

Figure 6.3 shows the outlet moisture contents predicted by the second-order model I. Predicted and observed output moistures are in good agreement. The residuals do not show any violation of the assumed assumptions.

Figure 6.4 shows a plot of the outlet moisture contents predicted by the 1st-order model II-b. The outlet moisture contents predicted by the model agree well with the observed data. The residuals plot does not show a violation of the assumptions.

6.1.1.2) <u>Numerical Identification of the Zimmerman Dryer</u>

Experimental results obtained with the Zimmerman dryer (Etigani, 1987) were used to analyze the linear model [Eqn.(4.6)] in describing the dynamics of the drying process. The identifications is based on 130 pair of input-output data. Figure 6.5 shows the experimental data. The results of the identification are summarized below:

$b = -0.031 \pm 0.007$ Loss Function = 50.27

$f = 0.93 \pm 0.03$

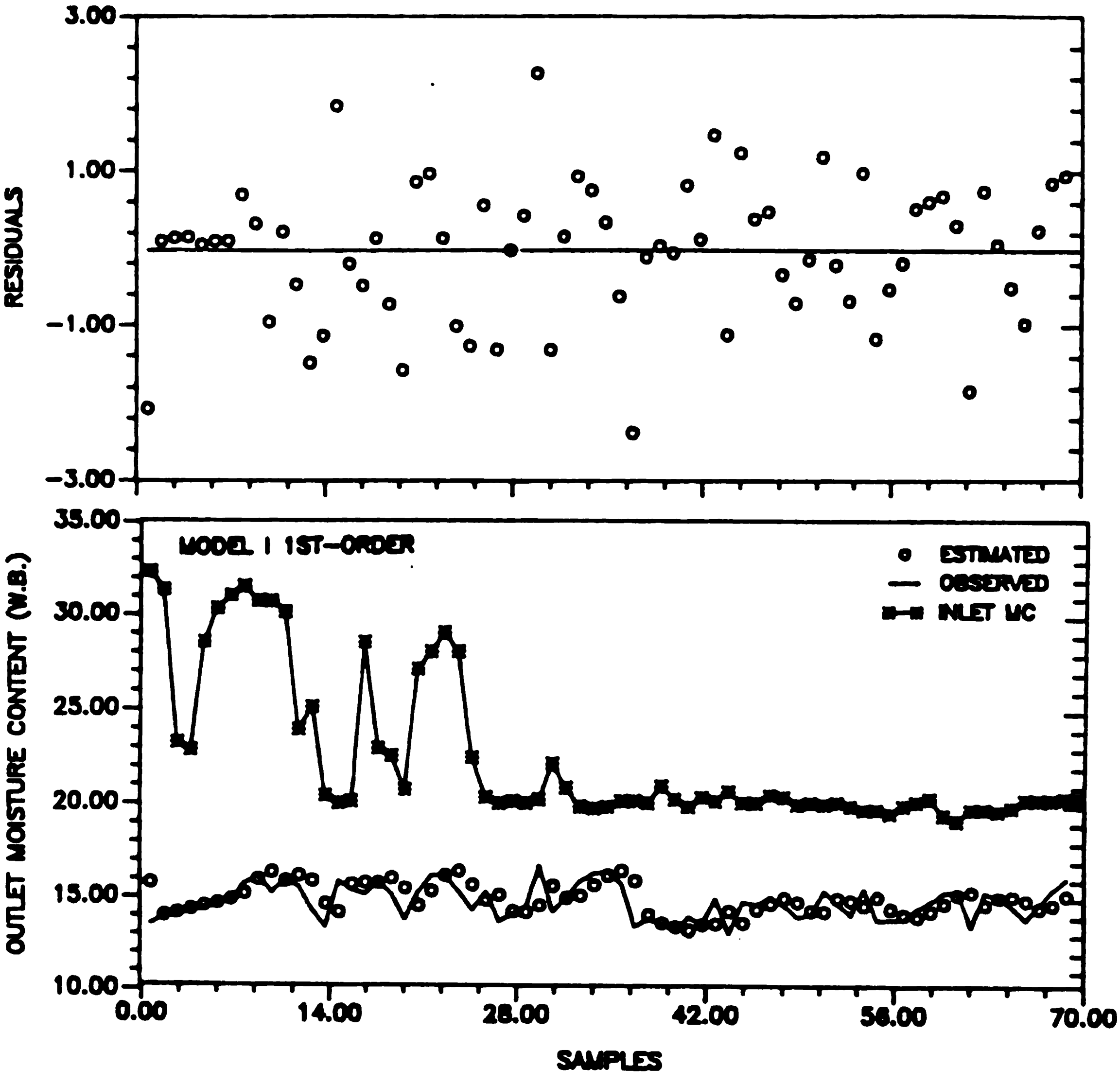

Figure 6.2: Identification results with the first-order model I for the drying of corn in the Meyer-Morton 850 dryer.

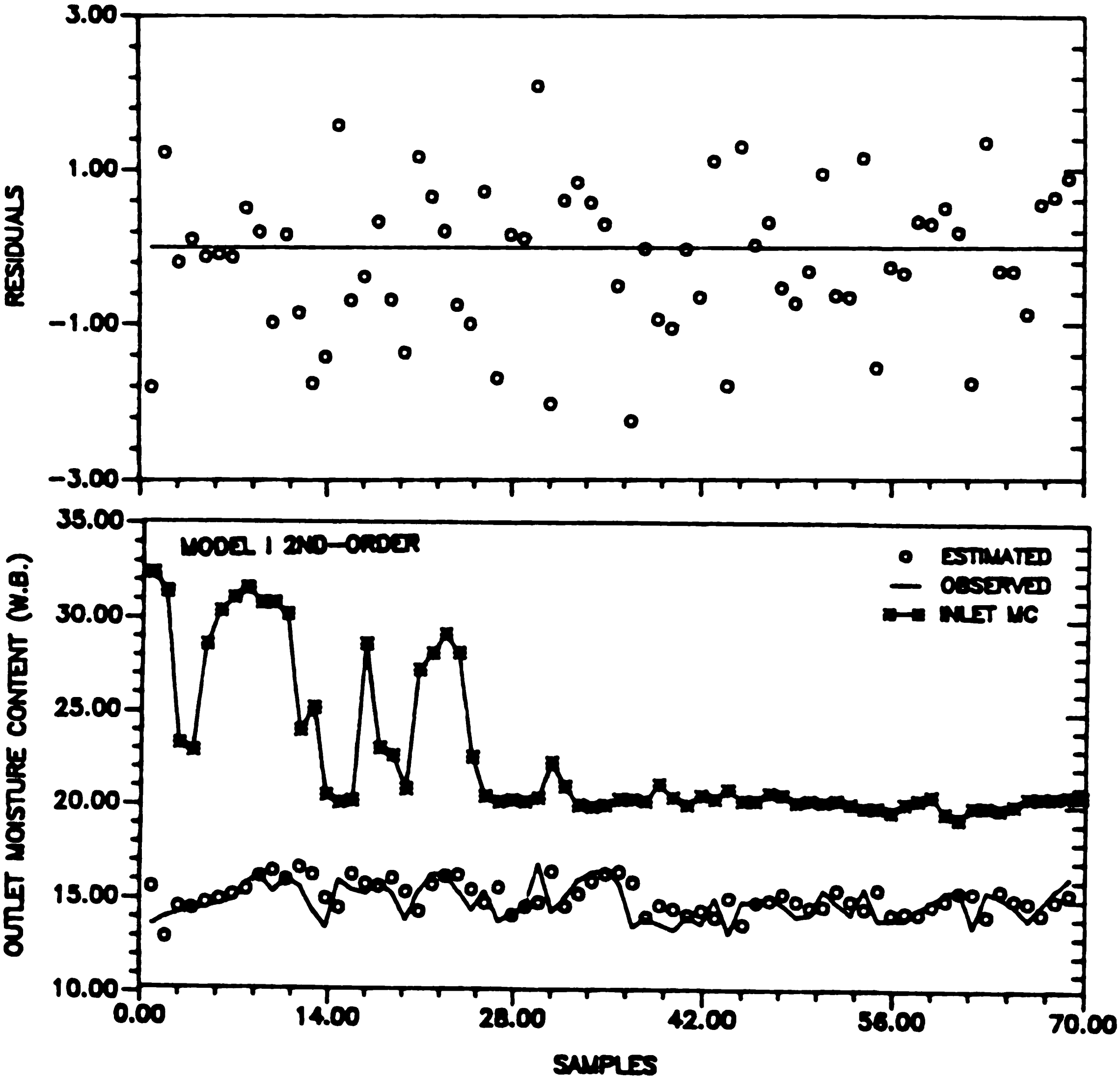

Figure 6.3: Identification results with the second-order model I for the drying of corn in the Meyer-Morton 850 dryer.

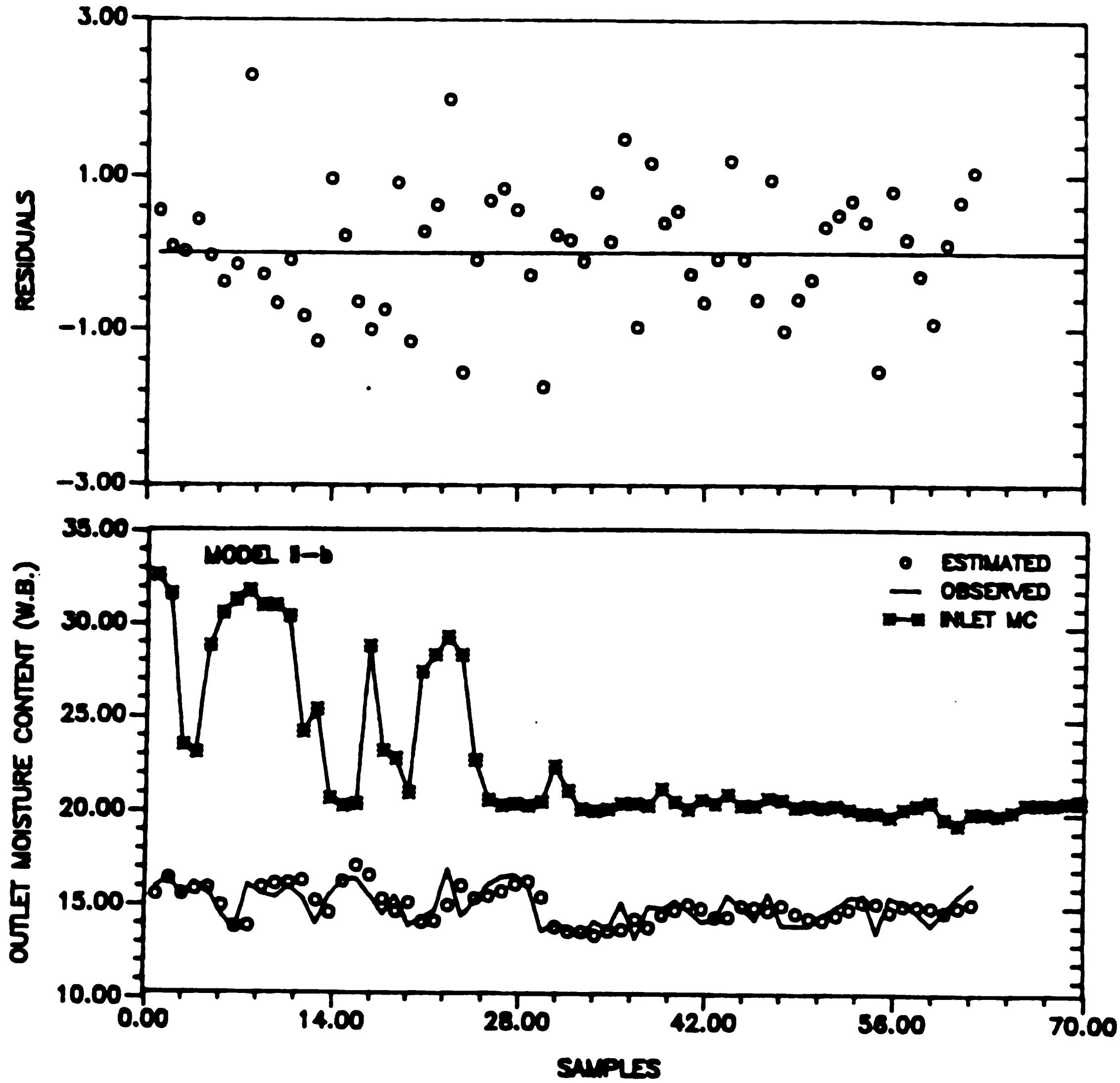

Figure 6.4: Identification results with the first-order model II-b for the drying of corn in the Meyer-Morton 850 dryer.

Figure 6.6 shows a plot of the outlet moisture content predicted by the linear model vs. the observed values, and a plot of the residuals. The predicted values agree well with the observed values. The standard assumption of normal measurement errors seems reasonable in Figure 6.6. A check to see if the residuals are approximately independent is based on the number of runs, i.e., the number of changes in the signals of the residuals plus one (Beck and Arnold, 1977). For N independent errors, the number of runs must be approximately equal to $(N+1)/2$. The residuals of Figure 6.6 exhibit 50 runs compared with $(N+1)/2 = 63$. Thus, there is no reason to question the independence of the residuals.

In conclusion, the three empirical models evaluated in this section are simple in their formation, and therefore efficient for on-line calculation. As is observed in Figure 6.4, model II-b shows the lowest difference value between the predicted and measured outlet moisture content, i.e., less than ±2% as compared with model I. As was discussed in Chapter 4, the model II-b has the inlet moisture content variable which makes this model a more realistic representation of the drying process. The linear model [Eqn.(4.6)] appears to have the advantage of requiring fewer parameters.

6.1.2) <u>Control Results</u>

Drying tests conducted with the automatic controller on the two commercial crossflow dryers are discussed in this section.

6.1.2.1) <u>Meyer-Morton 850 Dryer</u>

During the fall of 1986 four tests were conducted with the

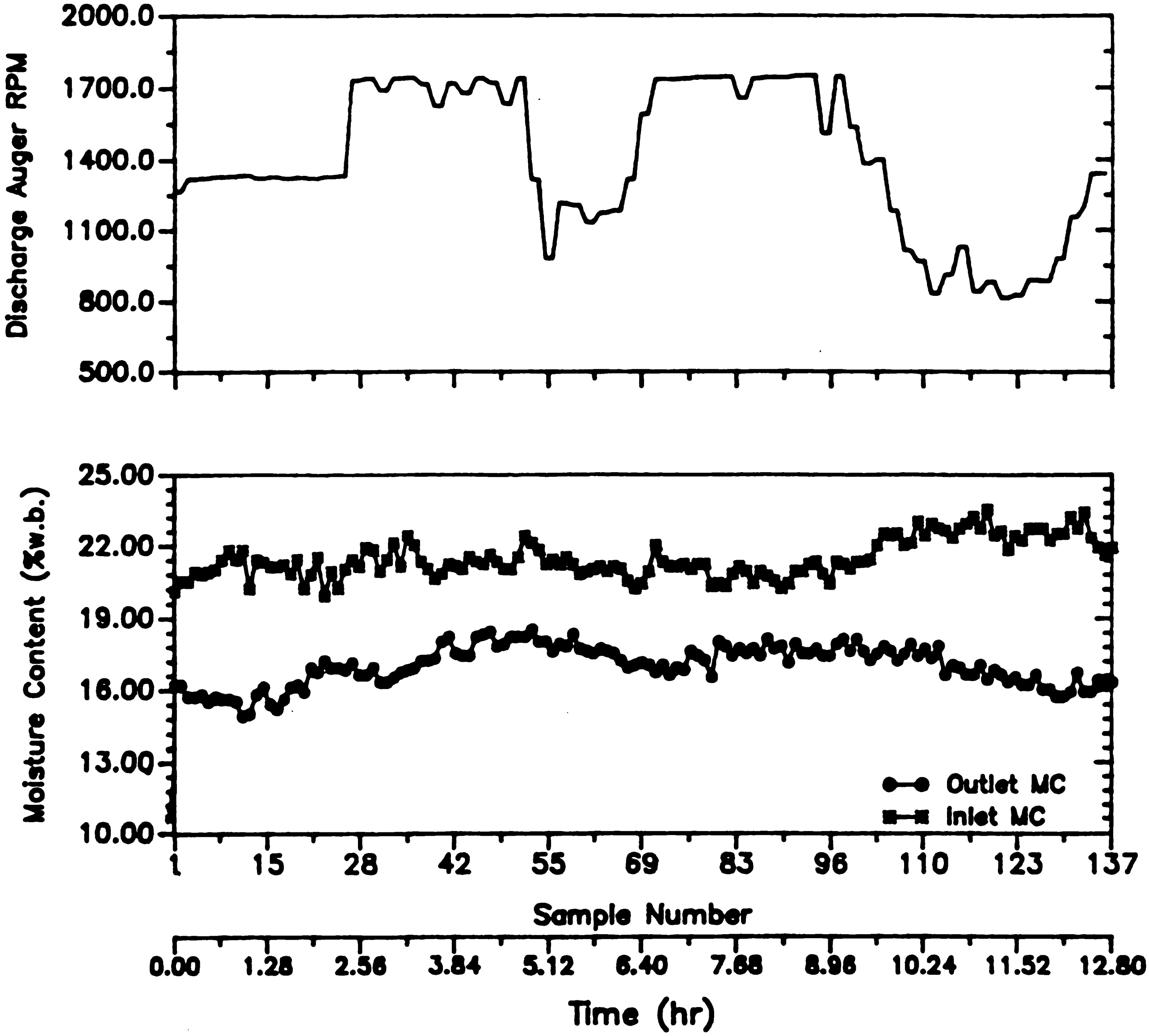

Figure 6.5: Zimmerman experimental data employed to obtain the parameters of the linear model (12/15/86).

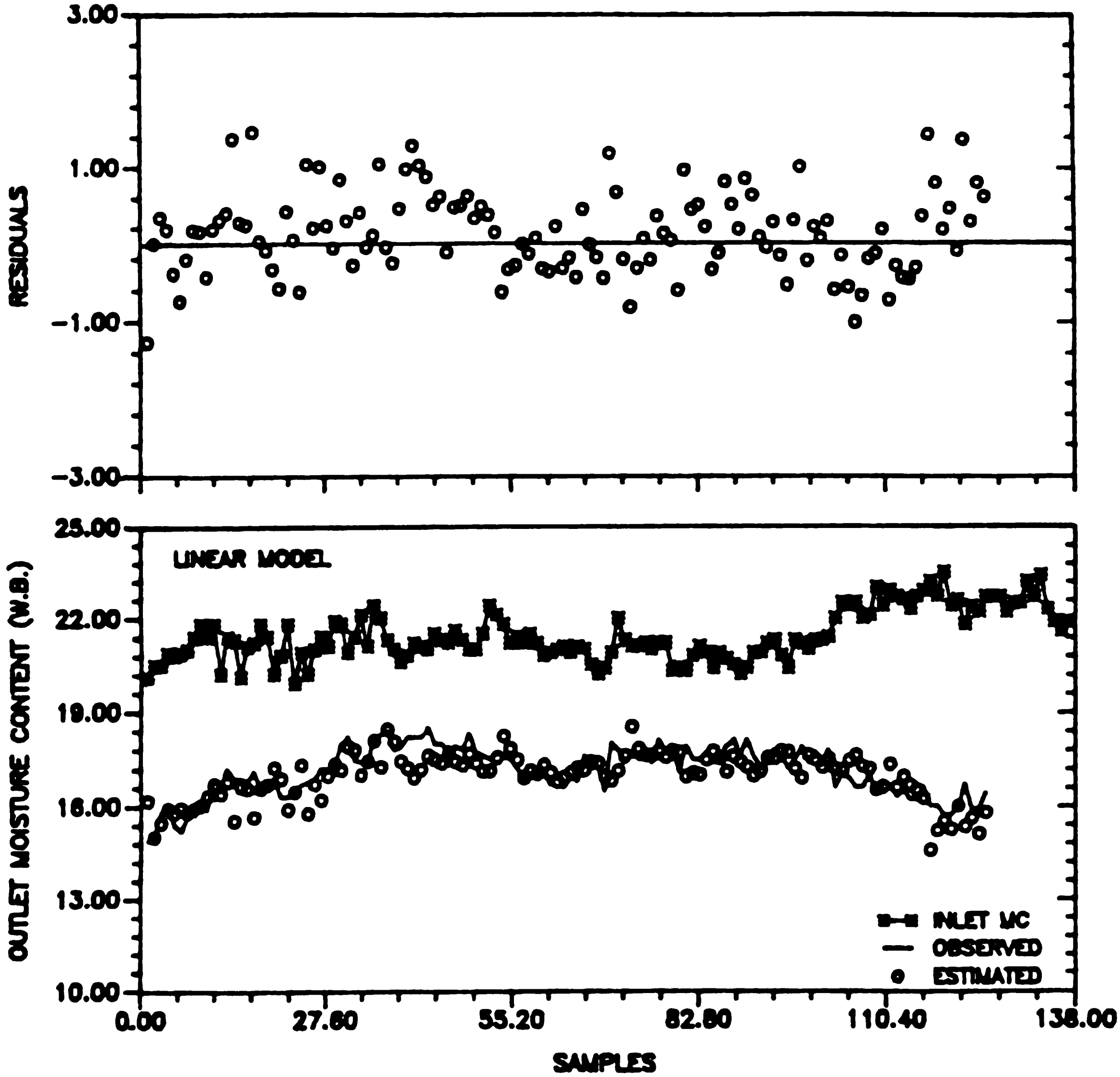

Figure 6.6: Identification results with the linear model (Eqn.4.6) for the drying of corn in the Zimmerman ATP-5000 dryer.

Meyer-Morton dryer. Figures 6.7 through 6.12 show the experimental results obtained during drying of corn.

Figure 6.7 illustrates the outlet moisture content variation which is typically obtained by **manual control** of the crossflow dryer. It shows the variation of the inlet moisture content, outlet moisture content, and the discharge auger rpm as a function of time. For a set-point of 14.5%, the average outlet moisture content during nine hours of drying was 13.6% (w.b). Overdrying by 0.9% point occurred which is characteristic of manual dryer control. During the nine hours of drying, the rpm was changed only three times by the operator; it was insufficient to prevent the overdrying. The variation in the corn inlet moisture content is typical for an on-farm dryers in Michigan.

A second example of **manual control** of the Meyer-Morton 850 dryer is shown in Figure 6.8. The average outlet moisture content was 0.7% below the setpoint. Note the large variation in the outlet moisture content in comparison with the inlet moisture content. Even for the best operator, it is difficult to control the dryer adequately due to the limited information an operator has during the drying process.

The **automatic dryer control** of the Meyer-Morton is illustrated in Figure 6.9. The MV-feedback controller was used. The auger rpm was limited between 900 and 1200. The value of the input penalty (ρ) was 0.6. The average inlet moisture content in Test1 was 20.4% with a standard deviation of 1.1%, the outlet moisture content 14.6% with a standard deviation 0.9%; the desired outlet moisture content 14.5%. The controller kept the outlet moisture content close to the setpoint.

In Figure 6.10 Test2 is shown; the MV-feedback algorithm was used. Large variations in inlet moisture content occured. The grain

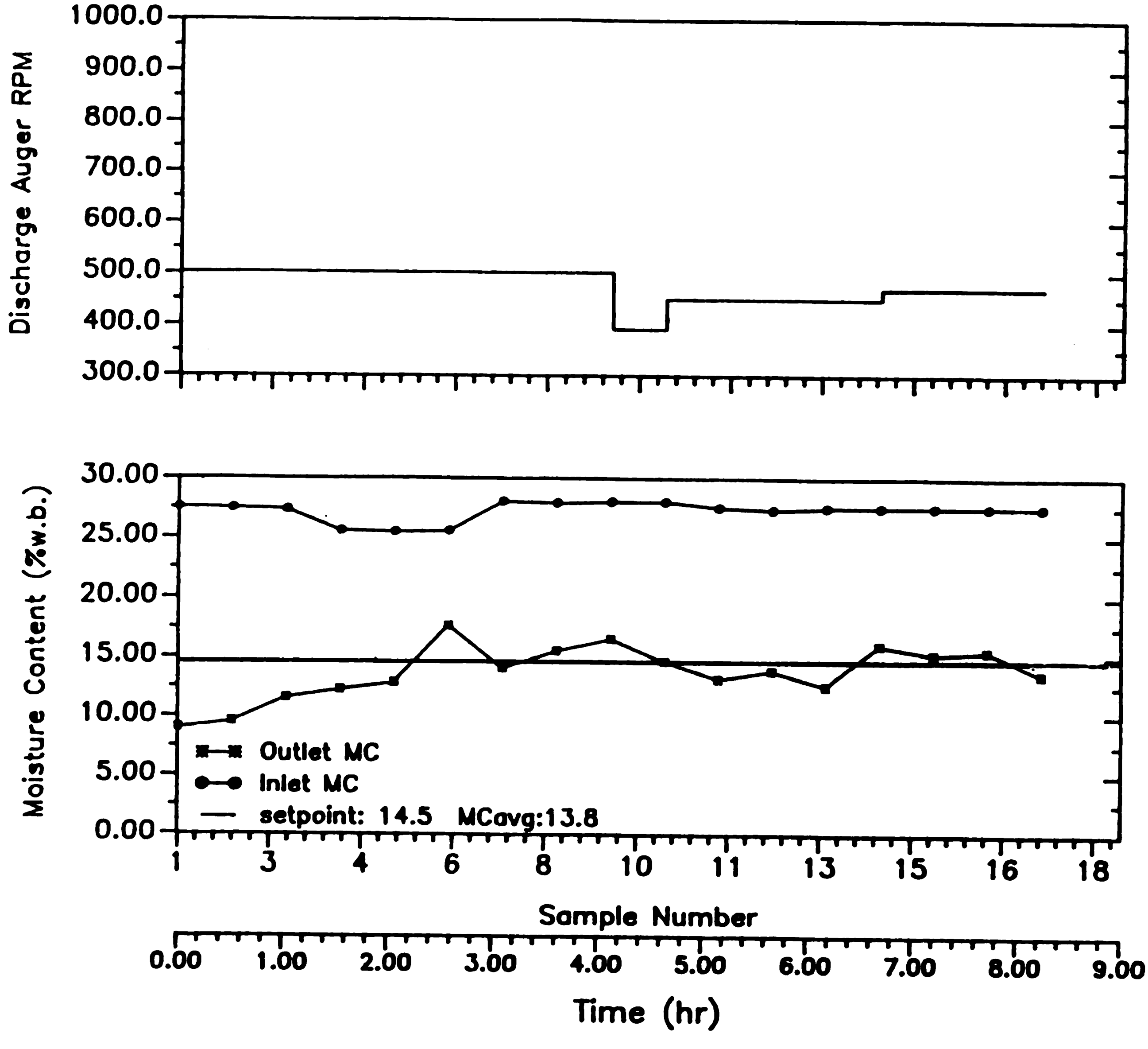

Figure 6.7: Results obtained during manual control of the Meyer-Morton 850 dryer (1984).

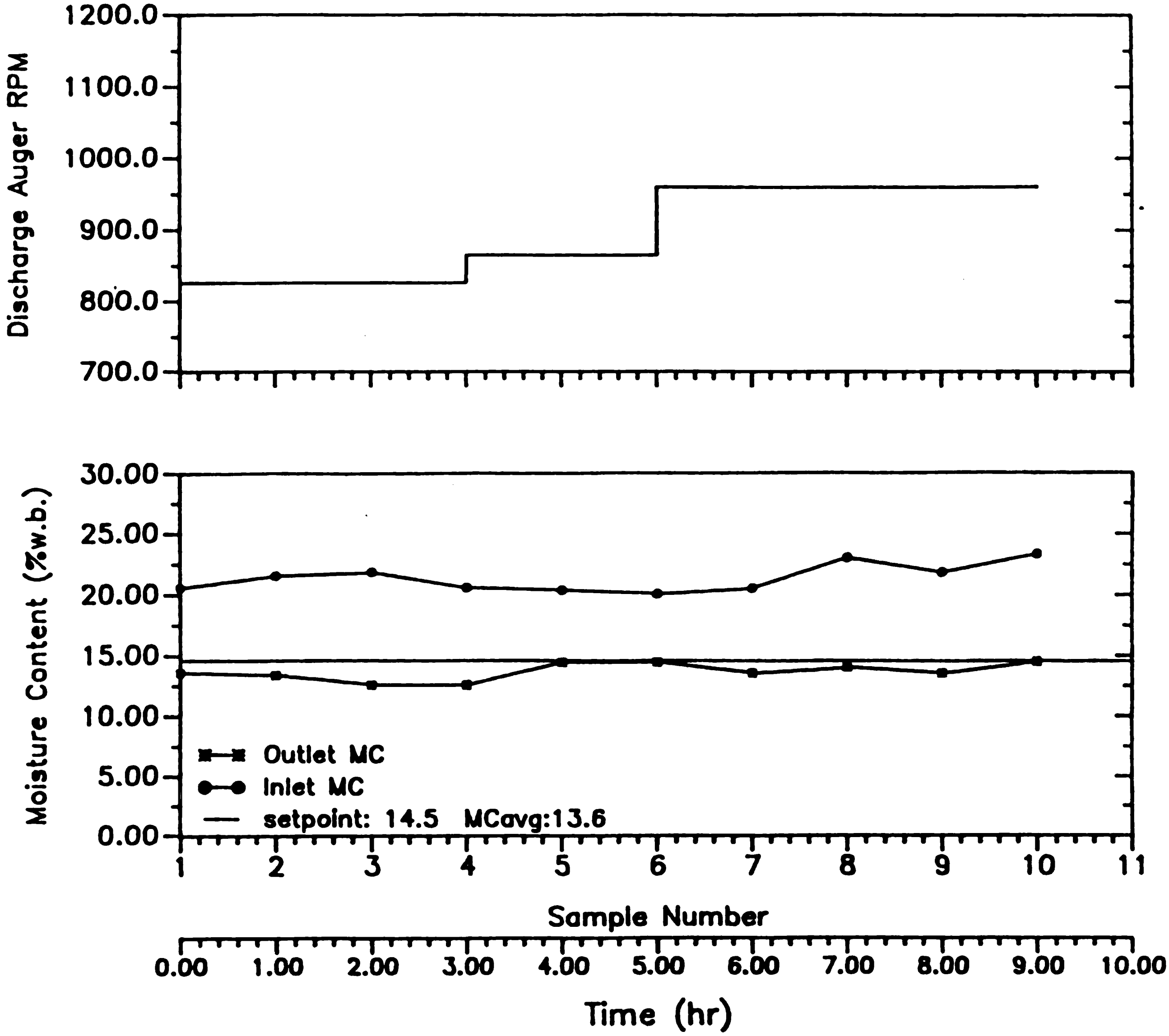

Figure 6.8: Results obtained during manual control of the Meyer-Morton 850 dryer (1985).

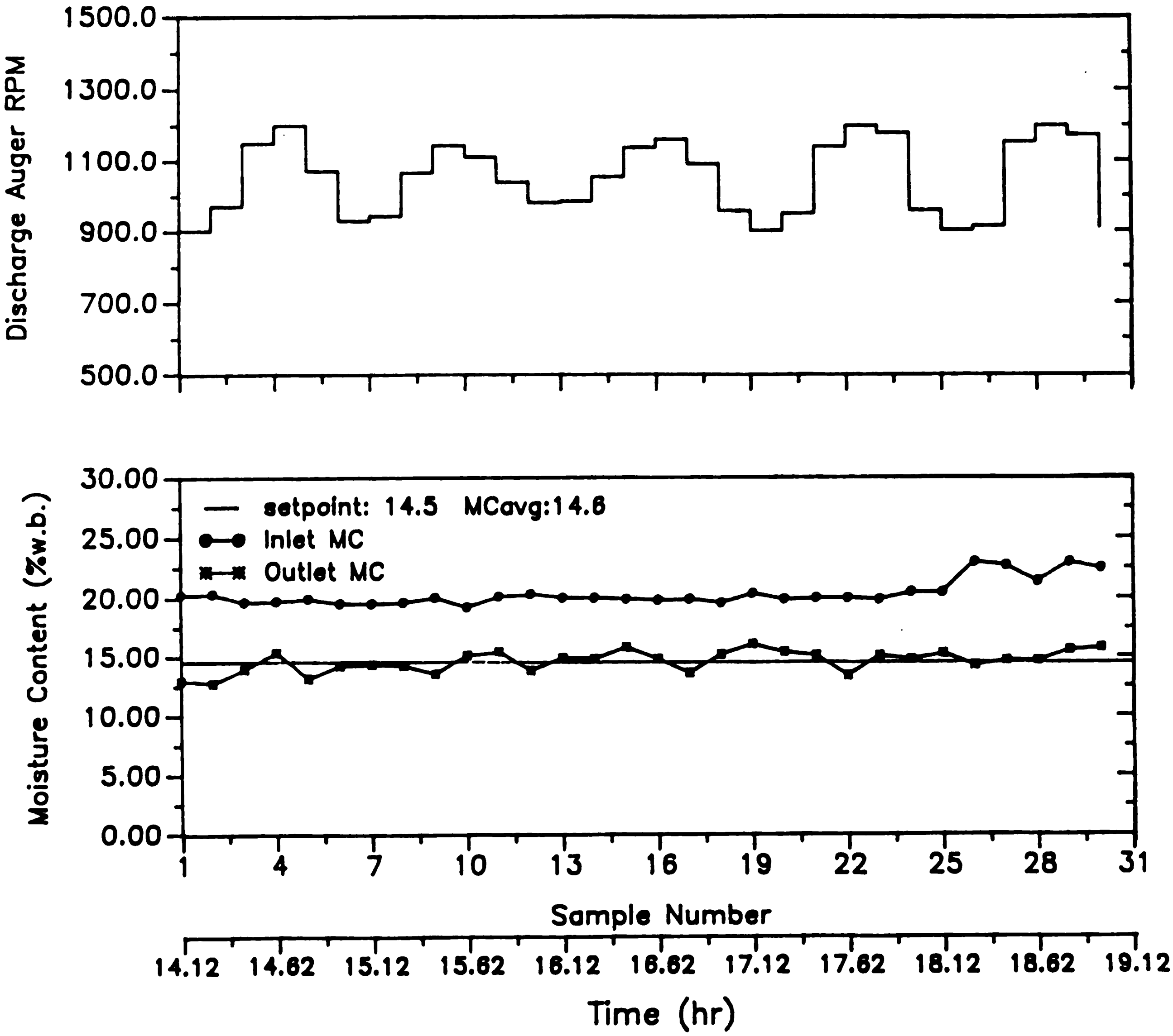

Figure 6.9: Results of Test1 obtained during automatic control of the Meyer-Morton 850 dryer with the MV-feedback controller (ρ=0.6).

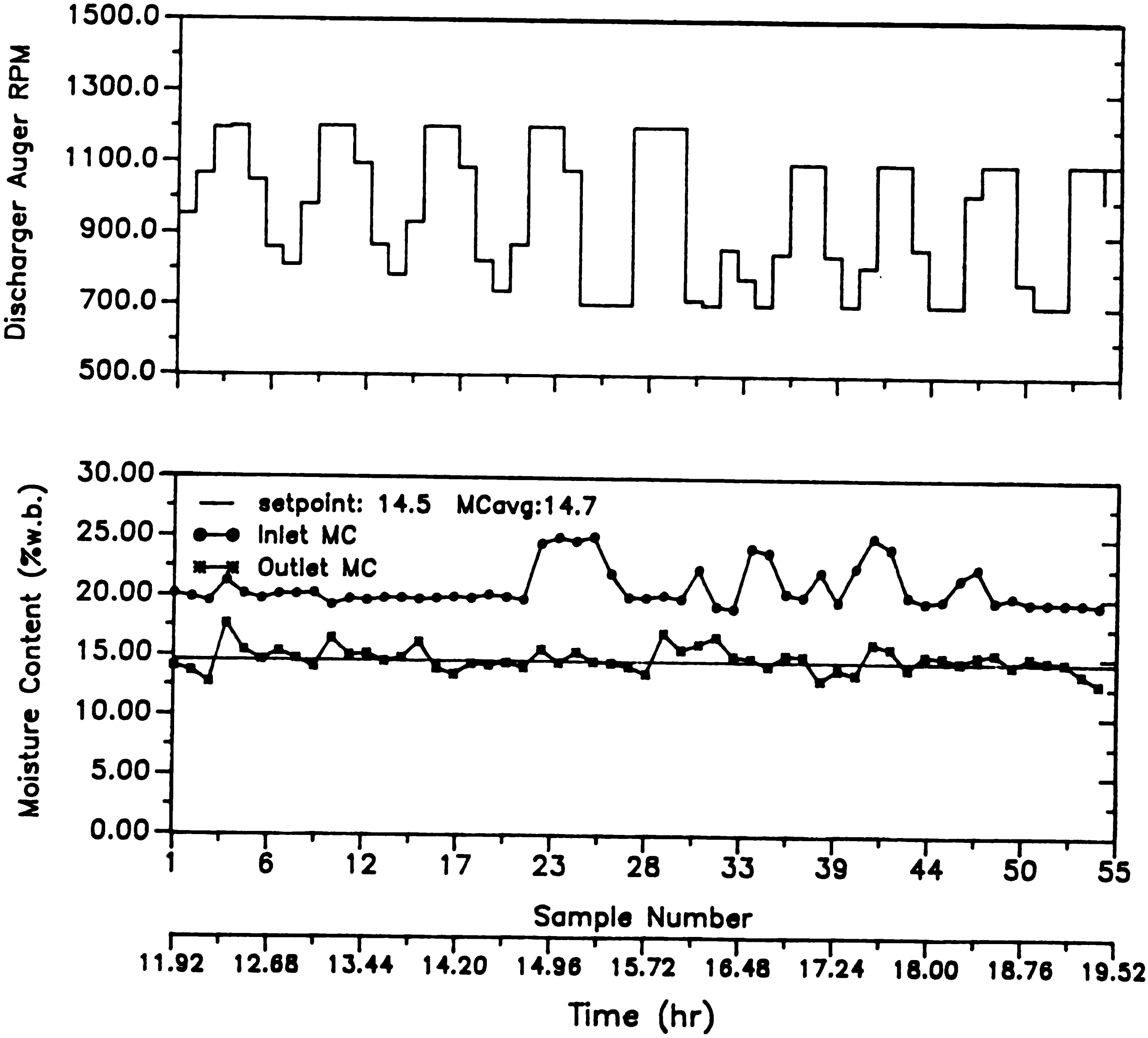

Figure 6.10: Results of Test2 obtained during automatic control of the Meyer-Morton 850 dryer with the MV-feedback controller (ρ=0.6).

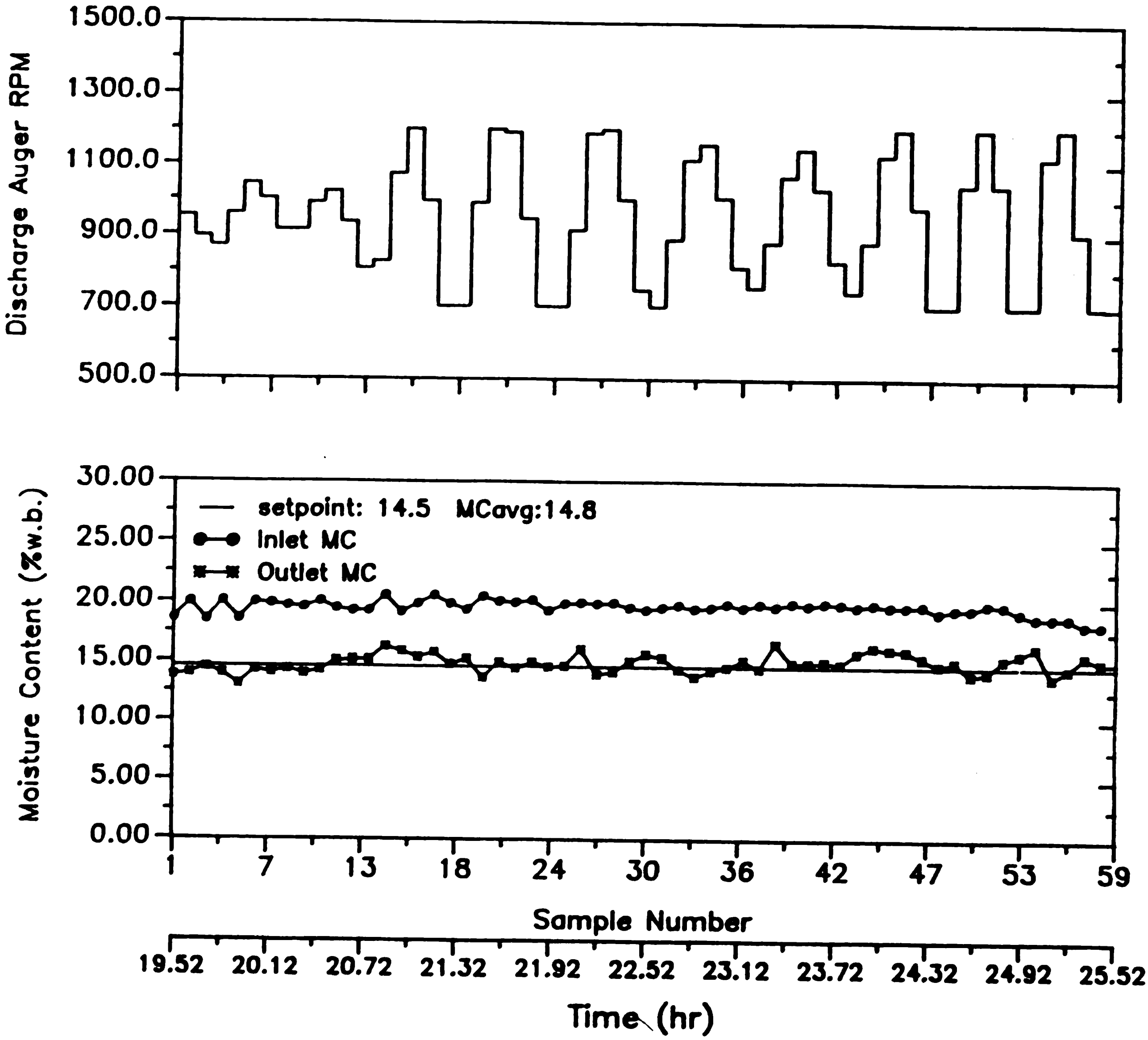

Figure 6.11: Results of Test3 obtained during automatic control of the Meyer-Morton 850 dryer with the MV-feedback/feedforward controller (ρ=0.008).

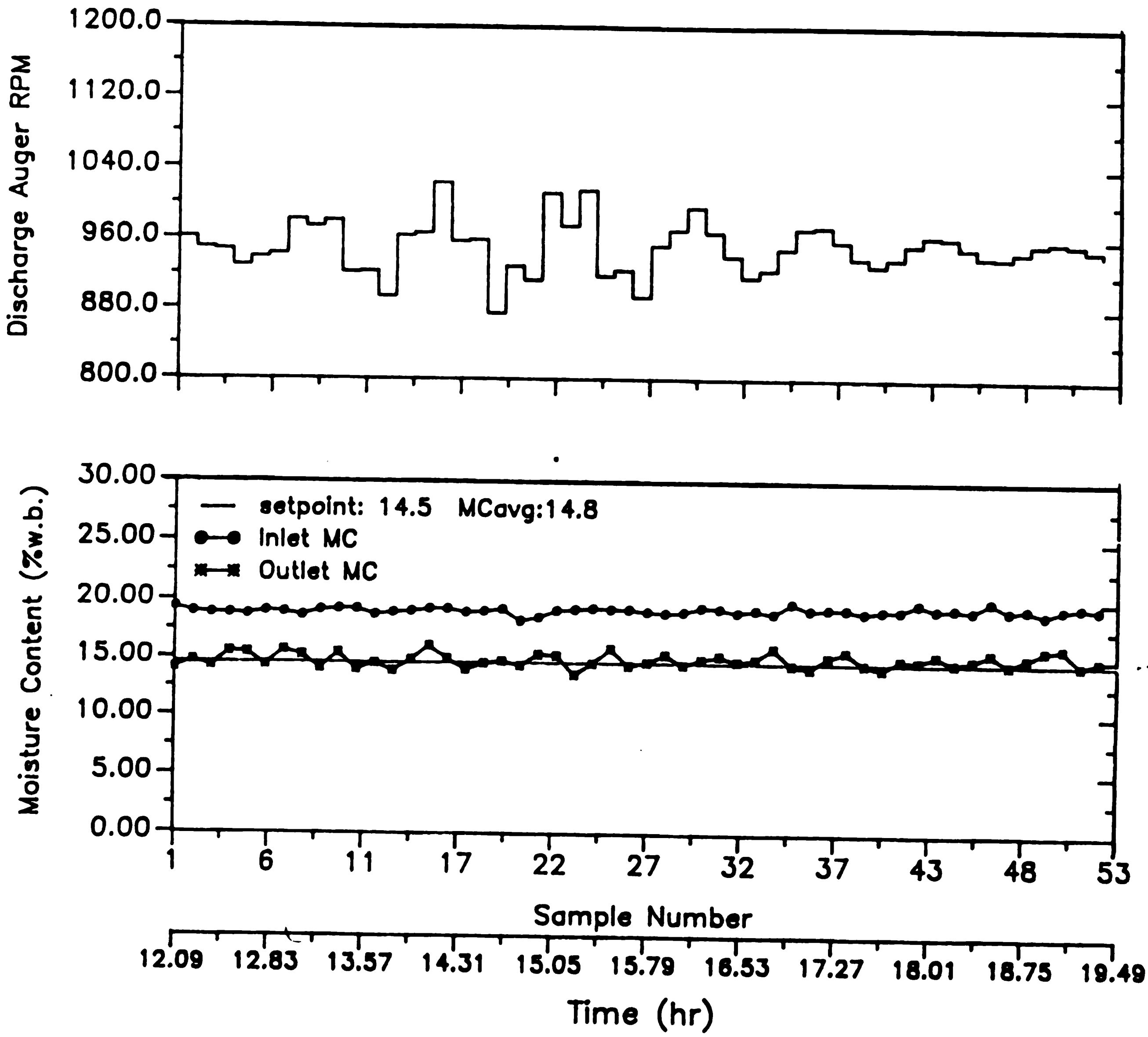

Figure 6.12: Results of Test4 obtained during automatic control of the Meyer-Morton 850 dryer with the MV-feedback/feedforward controller (ρ=0.01).

inlet moisture content varied from 25% to 19%. The auger rpm varied from 700 to 1200. In order to accommodate the large changes in the inlet moisture content, the rpm limits were changed at 16.30 hours. The controller performance can be described as excellent based on the average outlet moisture (14.7%) achieved with the large variation in the inlet moisture content.

A general drawback of a controller which just employs feedback is that a large change in inlet moisture content is corrected late if only the outlet moisture content is measured.

Figures 6.11 and 6.12 show the results of Test3 and Test4, respectively. The controller employed feedback from the outlet moisture content and feedforward from the inlet moisture content (MV-feedback/feedforward controller). The value of ρ in Test3 (Figure 6.11) was 0.008; the objective was to decrease the output variation. Although the variation in inlet moisture content was small, the controller auger rpm varied from 700 to 1200 in order to keep the corn outlet moisture content close to the setpoint. The small value of the penalty factor ρ resulted in a large variation in the control input signal. Note that the controller does not only react to the inlet moisture content variation, the main reaction is to the outlet moisture content deviation from the setpoint.

In Figure 6.12, the response of the auger rpm using ρ=0.01 was much better. However, the average outlet moisture content was still 0.3% of the setpoint although only a small variation (standard deviation of 0.3%) in the grain inlet moisture content occurred. Again, it is observed that the control reaction is due to the outlet moisture content variation. These deviations can be caused by internal and/or external disturbances which affect the drying process during a test.

With the GMV method, the value of ρ (the input penalty factor) can be tuned on line in order to match the input variance to the actual working conditions. Since the working conditions change from test to test, a way of automatically estimating ρ should be incorporated in the control software. Isermann (1981) describes a simple method of determining the penalty factor. It consists of continuosly calculate the input (U) and the output (Y) variances and adjust ρ according to these variances.

The summary of the results obtained from the tests conducted with the Meyer-Morton dryer is shown in Table 6.2. Due to the small values of the standard deviation in the inlet moisture content during the tests, the performance of the controllers can not be fully evaluated. However, the performance of the MV-feedback controller can be considered excellent for Test1 and Test2; the average final moisture content was kept close to the desired values and the standard deviation was lower than that for the inlet moisture content. Test3 and Test4 show that with the additional feedforward action in the MV-controller (MV-feedback/ feedforward) the control performance is not improved when the variation in the inlet moisture content is small. In general, the results are excellent, manual control can not duplicate these results as is shown in Figures 6.7 and 6.8.

6.1.2.2) Zimmerman ATP 5000 Dryer

During the fall of 1987 two tests were conducted with the Zimmerman dryer. Figures 6.13 through 6.16, show the experimental results obtained during the drying of corn.

Table 6.2: Summary of the results obtained from the different control tests with the Meyer-Morton 850 dryer.

	TEST NUMBER			
	1	2	3	4
1986	11/16	11/25	12/11	12/14
	Inlet Moisture Content (%w.b.)			
Average	20.4	20.8	19.5	19.1
Minimum	19.5	19.0	18.1	18.2
Maximum	23.0	25.0	20.5	20.0
Standard Deviation	1.1	1.8	0.5	0.3
	Outlet Moisture Content (%w.b.)			
Average	14.6	14.7	14.8	14.8
Minimum	12.7	12.7	13.0	13.5
Maximum	16.1	17.6	16.5	16.0
Standard Deviation	0.9	1.0	0.8	0.6
	Discharge Auger RPM			
Average	1048.0	958.0	941.0	950.0
Minimum	900.0	700.0	700.0	847.0
Maximum	1200.0	1200.0	1200.0	1023.0
Standard Deviation	106.3	185.4	168.4	28.2

Setpoint = 14.5% w.b.

Test1 = MV-feedback controller
Tets2 = MV-feedback controller
Test3 = MV-feedback/feedforward controller
Test4 = MV-feedback/feedforward controller

Figure 6.13 illustrates the controlability of **manual control** of the Zimmerman dryer. The average outlet moisture content obtained was 16% (standard deviation 0.97%) for a setpoint of 17%. The large oscillation in the inlet moisture content (15% to 26% and a standard deviation of 1.68%) resulted in a difficult control problem.

In general, the operator controlled the drying process reasonably well considering the large variation in the inlet moisture content during the test. It must be emphasized that the dryer operator had information about the drying process supplied by the moisture meter (inlet, outlet and intermediary moisture content every 6 minutes), which helped to control the dryer.

Figure 6.14 shows the result of the automatic control of Test5 performed with the Zimmerman dryer using the PP-controller described in Chapter 4. The value of β used was 50; simulation studies with different values of β showed that β=50 would give small rpm values. The average outlet moisture content during the test was 16.5% (standard deviation 0.7%); the setpoint was 16.5%. Based on the average outlet moisture content, the controller was successful in controlling the drying process. The discharge auger rpm changed from 1212 to 1608 during the test due to the variation in inlet moisture content which varied from 18.5% and 21.5%.

Figure 6.15 shows the results of Test6. The inlet moisture content ranged between 15.9% and 21.4%. The average grain outlet moisture content was 16.6% (standard deviation 0.5%), only 0.1% above the setpoint. The auger rpm varied between 1058 and 1595 in response to the changes in inlet and outlet moisture content.

The summary of the results obtained from the tests conducted

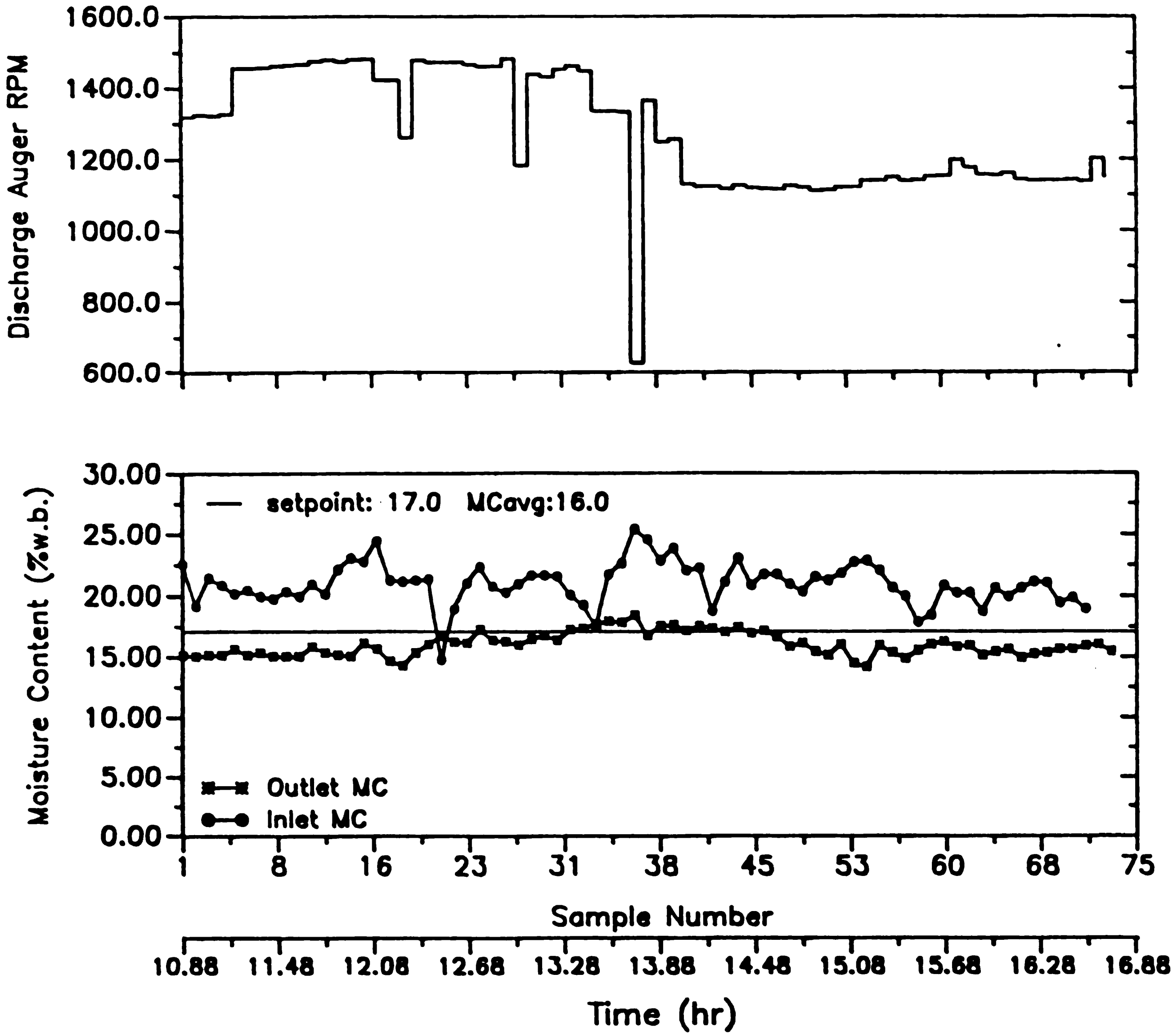

Figure 6.13: Results obtained during manual control of the Zimmerman ATP 5000 dryer (1987).

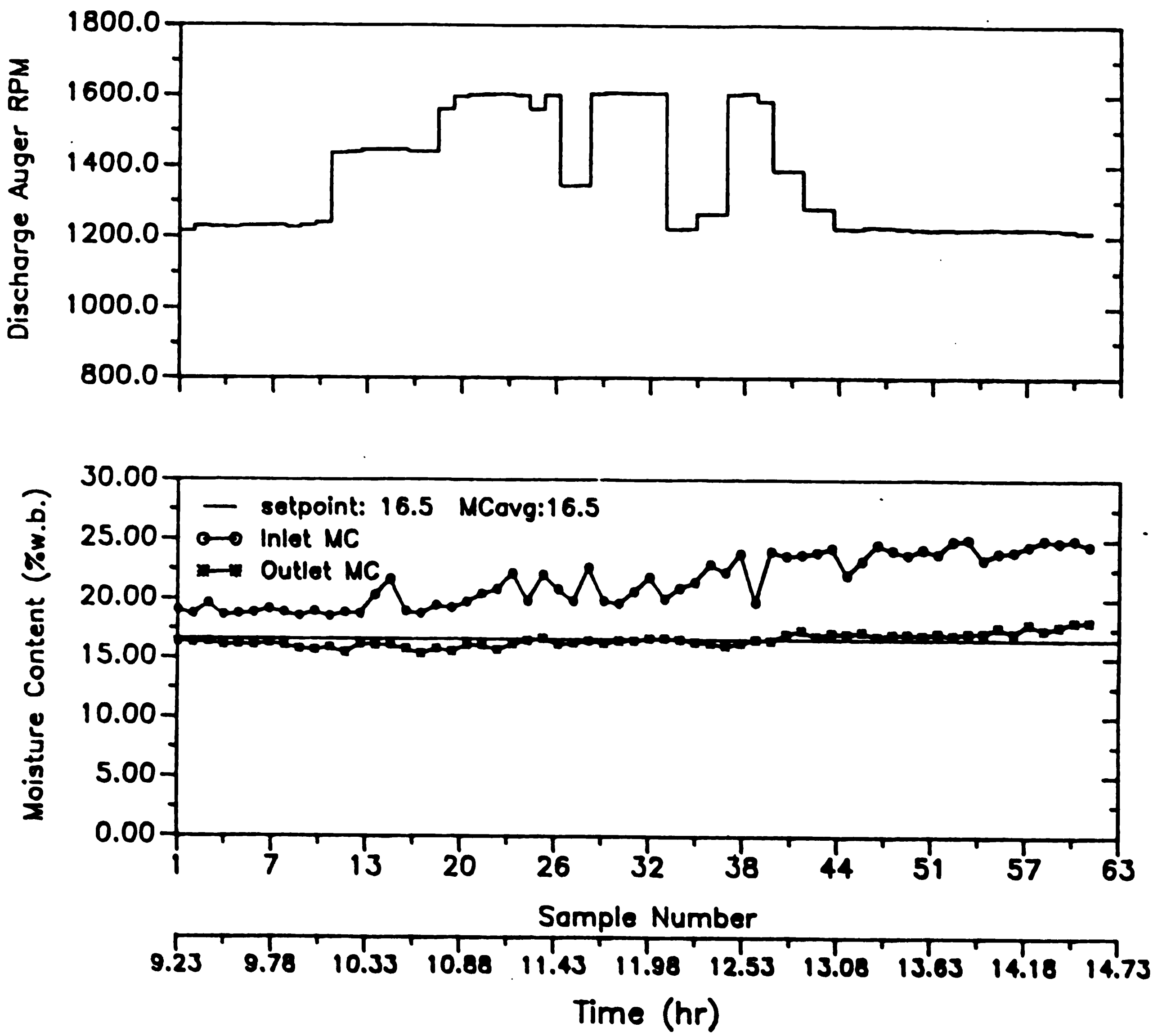

Figure 6.14: Results of Test5 obtained during automatic control of the Zimmerman ATP 5000 dryer with the PP-controller (β=50).

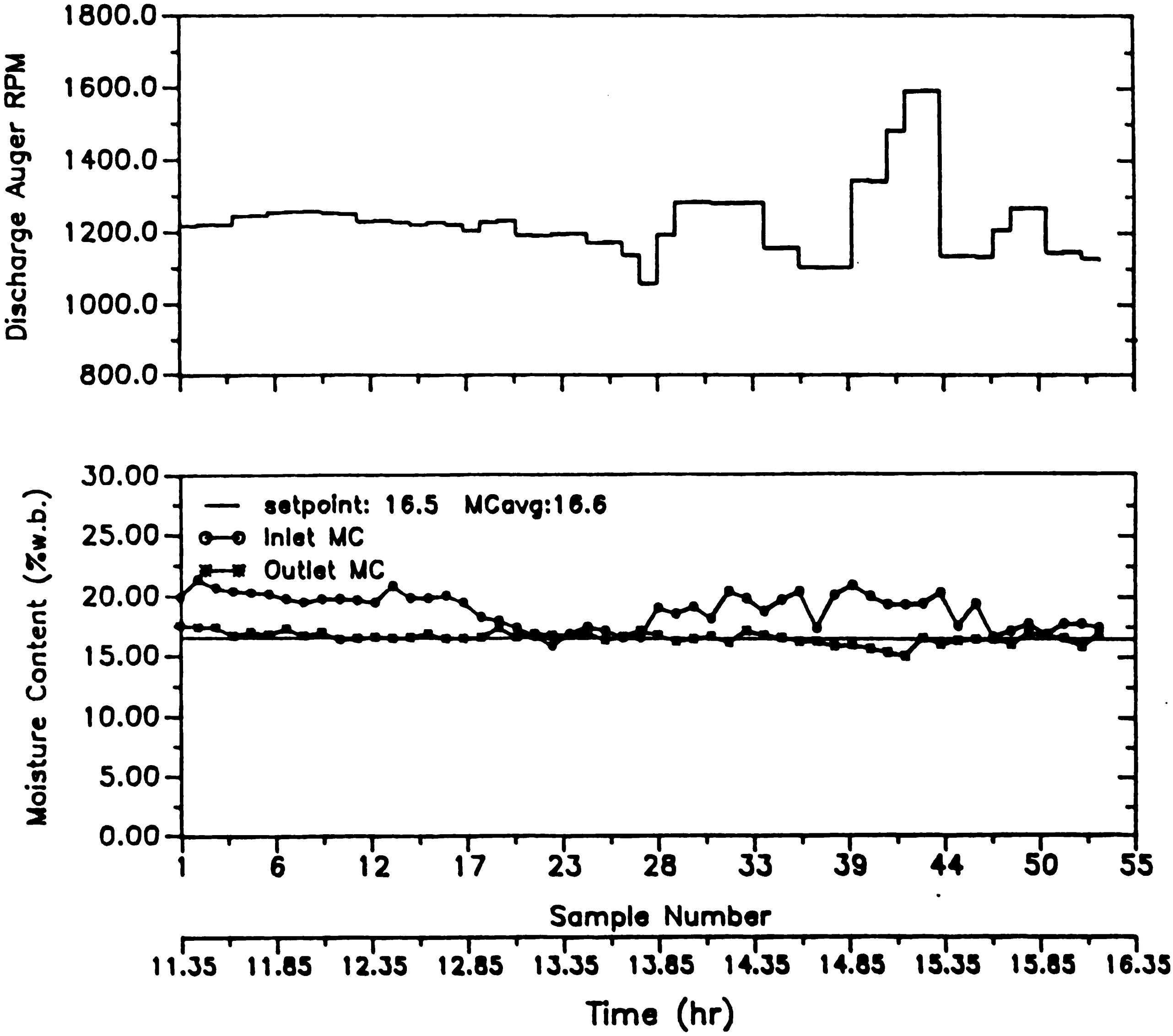

Figure 6.15: Results of Test6 obtained during automatic control of the Zimmerman ATP 5000 dryer with the PP-controller (β=50).

with the Zimmerman dryer is shown in Table 6.3. The results of the two tests can be considered excellent based on the average final moisture content and on the standard deviations of the outlet moisture content. In both tests a large variation in inlet moisture content was experienced. The controller was capable of maintaining the final moisture content close to the setpoint by reducing the deviation of the moisture content.

In general, it is difficult to evaluate the performance of the control in practice, and in particular it is difficult to compare different control laws. The main reason for this is that there are variations in the disturbance level. This implies that in order to evaluate the different control strategies it is necessary to test periods of considerable length.

A series of successful tests were conducted with the MV and PP controllers on two commercial dryers over a period of two drying seasons. The pole placement controller (PP) appears to be stable and accurate. It controls the outlet moisture content well even for large variations in the inlet grain moisture content. However, more tests need to be performed in order to fully evaluate the controller. The influence of β on the variation of the auger rpm must also be evaluated.

In conclusion, it is shown that a simple model can be used for on-line calculations. The GMV and the PP controllers can be used for the control of continuous-flow grain dryers. Compared with the MB-controller described in Eltigani (1987), the PP-controller has the potential to be used in different dryer designs, and can be employed for any class of input-output signals. The last advantage is important when designing a control system for a multi-stage CCF rice dryer.

Table 6.3: Summary of the results obtained from the different control tests with the Zimmerman ATP 5000 dryer.

	TEST NUMBER	
	5	6
1987	11/25	12/02
	Inlet Moisture Content (%w.b.)	
Average	21.5	18.9
Minimum	18.5	15.9
Maximum	25.0	21.4
Standard Deviation	2.3	1.4
	Outlet Moisture Content (%w.b.)	
Average	16.5	16.6
Minimum	15.3	15.1
Maximum	18.1	17.5
Standard Deviation	0.7	0.5
	Discharge Auger RPM	
Average	1608.0	1228.0
Minimum	1358.0	1058.0
Maximum	1606.0	1595.0
Standard Deviation	160.4	102.1

Setpoint = 16.5%

Test5 = PP-controller
Test6 = PP-controller

Eltigani's controller showed to be excellent for a small variation in the inlet moisture content. However, his controller converges slowly when large variations in the inlet moisture content occurs.

6.2) CONCURRENTFLOW DRYING PROCESS

Since no experimental data were available for this part of the study, the steady state CCF dryer model developed by Bakker-Arkema et al. (1974) was used to check the transient model.

The parameters employed in the simulation of a two-stage CCF dryer are listed in Table 6.4.

Table 6.4: Simulation input parameters for the single-stage CCF dryer*.

BED DEPTH (m)	Min (%w.b.)	θin (°C)	G_p (kg/hr-m²)	Tin (°C)	Win (kg/kg)	G_a (kg/hr-m²)
0.76	20.	7.22	4,410.	232.22	0.006	3,137.
0.76	20.	7.22	5,140.	232.22	0.006	3,137.
0.76	20.	7.22	6,410.	232.22	0.006	3,137.

*see Table (4.1) for air, grain and bed parameters used.

Figures 6.16 and 6.17 illustrate the temperature and moisture profiles results obtained from the steady-state (SS) and unsteady-state (USS) simulation models for a grain flow rate of 4,410 kg/hr-m² and 6,410 kg/hr-m², respectively. The values for the parameters used in the numerical calculation were Δx=0.168cm and Δt=1.145 & 0.716 sec, respectively. The solution was sensitive to time and distance step. A large distance step caused the solution to become unstable. The simulation results were compared to verify the accuracy of the USS model for use in the design of multi-stage control sytems. The results indicate good agreement between the two models. The grain moisture and the temperature profiles are essentially identical, while there is some difference in the air humidity at the higher grain flow rates.

Table 6.5 compares the values of T, θ, W and M at the inlet and midway through the dryer predicted by the SS and USS models for the second stage of a CCF dryer. The drying rates predicted by the USS model are within 2.8% of those predicted by the SS model. Air and grain temperature profiles are predicted within 8.4%. The exhaust air humidity (outlet) is predicted within 16%, while it is overestimated at the middle of the dryer by means of 24% for 5,140 and 6,410 kg/hr-m^2, respectively. The behavior of the air humidity inside the dryer is difficult to validate because of the lack of experimental data at those points. The most important parameter for the control is the outlet moisture content which is within 2.8% of the SS results. Therefore, the agreement between the simulation models is considered sufficient for the model to be used in the design of control-systems for concurrentflow corn dryers.

The USS model was used to simulate a single-stage steady-state drying of corn. The parameters used in the simulation of a single-stage CCF dryer are listed in Table 6.4. Table 6.6 shows the values of the differences between the simulation results at the dryer exit and midway through the dryer. The discrepancy among the values is primarily due to differences between the simulation models. The main differences are summarized in Table 6.7.

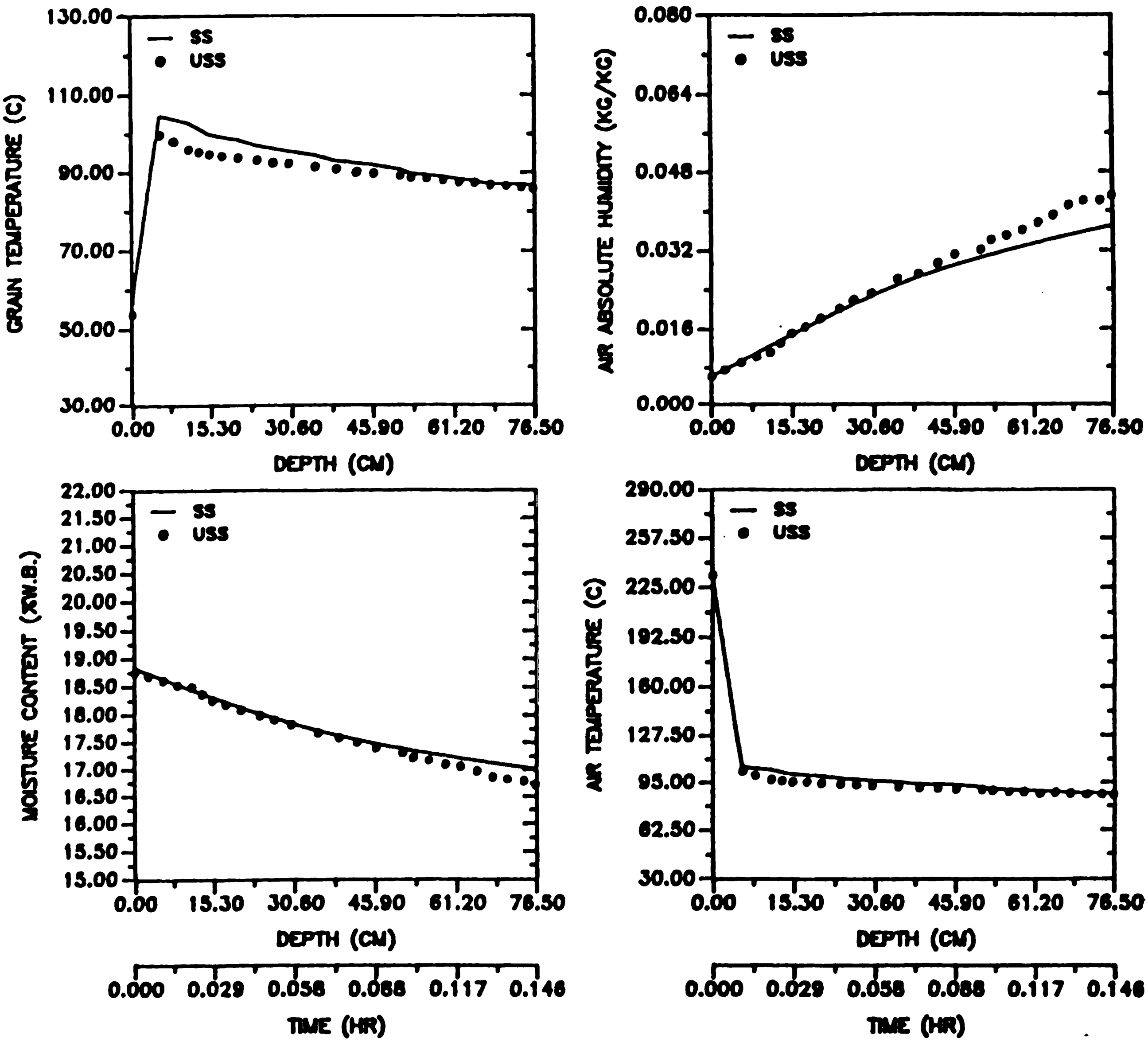

Figure 6.16: Steady-state temperature and moisture profiles for the second-stage of a CCF dryer predicted by the steady-state (SS) and unsteady-state (USS) models (G_p= 4,410 kg/hr-m²)

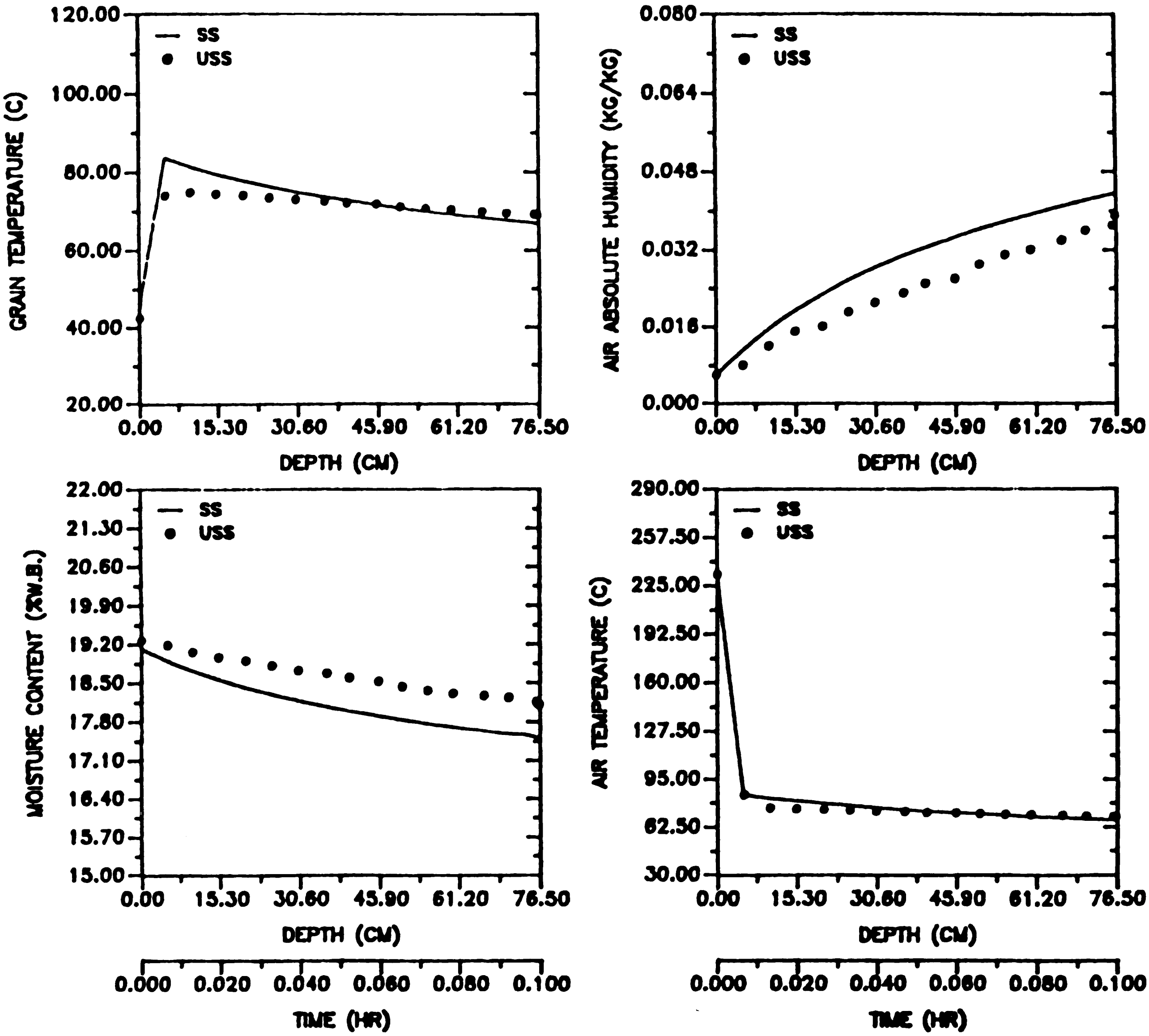

Figure 6.17: Steady-state temperature and moisture profiles for the second-stage of a CCF dryer predicted by the steady-state (SS) and unsteady-state (USS) models (G_p= 6,410 kg/hr-m²)

Table 6.5: Steady-state results for the two-stage of a CCF dryer predicted by the steady-state (SS) and unsteady-state (USS) models for different values of grain flow rates.

G_p(kg/hr-m²)	T(°C)		θ(°C)		M(%w.b.)		W(kg/kg)	
	SS	USS	SS	USS	SS	USS	SS	USS
4,410.								
outlet	86.7	85.9	86.6	85.7	17.0	16.7	0.0370	0.043
difference	-0.8		-0.9		0.3		0.006	
midway	94.5	91.1	94.3	91.3	17.7	17.6	0.0250	0.027
difference	-3.4		-3.0		-0.1		0.002	
5,140.								
outlet	72.2	78.8	72.1	78.7	16.9	17.4	0.0450	0.041
difference	6.6		6.6		0.4		-0.004	
midway	78.7	83.2	78.5	83.0	17.3	18.1	0.033	0.025
difference	4.5		4.5		0.8		-0.008	
6,140.								
outlet	66.8	69.1	66.7	68.9	17.7	18.1	0.0435	0.0374
difference	2.3		2.2		0.4		-0.0061	
midway	77.6	72.4	72.5	72.2	18.0	18.6	0.031	0.0233
difference	-0.2		-0.3		0.6		-0.0077	

difference = USS - US
midway = at 36.1 cm of the drying bed length
outlet = at 76.2 cm

Table 6.6: Steady-state results for the 1st-stage of a CCF dryer predicted by the steady-state (SS) and unsteady-state (USS) models.

G_p(kg/hr-m²)	T(°C)		θ(°C)		M(%w.b.)		W(kg/kg)	
	SS	USS	SS	USS	SS	USS	SS	USS
4,410.								
outlet	56.6	53.7	56.5	53.6	18.8	18.6	0.0270	0.0300
difference	-2.9		-2.9		-0.2		-0.003	
midway	61.3	56.7	61.2	56.6	19.2	19.3	0.0193	0.0210
difference	-4.6		-4.6		0.1		-0.0012	
5,140.								
outlet	48.6	48.7	48.6	48.7	18.8	19.0	0.0308	0.0285
difference	0.1		0.1		0.2		0.0023	
midway	53.2	50.1	53.0	50.9	19.2	19.4	0.0233	0.020
difference	-3.1		-2.1		0.2		0.0033	
6,140.								
outlet	44.8	42.3	44.8	42.2	19.1	19.3	0.0270	0.026
difference	-2.5		-2.6		0.2		0.001	
midway	48.6	45.7	48.5	44.0	19.4	19.6	0.0183	0.018
difference	-2.9		-4.5		0.2		-0.0003	

difference = USS - SS
midway = at 36.1 cm of the drying bed length
outlet = at 76.2 cm

Table 6.7: Differences between the SS and the USS simulation models.

PARAMETER	SS	USS
numerical method	Runge-Kutta	finite - difference
$\partial \cdot / \partial t$	0	calculated

The numerical method used to solve the SS model was the Runge-Kutta. The finete difference technique was chosen to solve the USS model. The numerical technique together with the assumption that the derivative term in ∂t is neglected for the SS model, are the main reasons why the results obtained with the SS and USS models are different. Considering the fact that the SS model can predict the performance of a single-stage CCF dryer to within 10% of the experimental data, there is no reason to question the accuracy of the USS model. Therefore, the USS model is accepeted for single-stage drying.

Figure 6.18 shows the results of a typical steady-state concurrentflow simulation using the unsteady-state model. Different grain flow rates are considered in order to analyze the response of the unsteady-state model to changes in discharge rates. The grain flow rates are representative of commercial CCF dryers. It requires about 11.68 second of CPU time for each of the runs on the Vax/VMS microcomputer system. As can be seen, the drying rate decreases with an increase in grain flow rates. Also, the air temperature cools faster if the corn moves faster through the dryer. The air humidity ratio increases at higher grain flow rate. In the CCF drying process, most of the moisture is removed during the first few minutes of drying. Basically, the

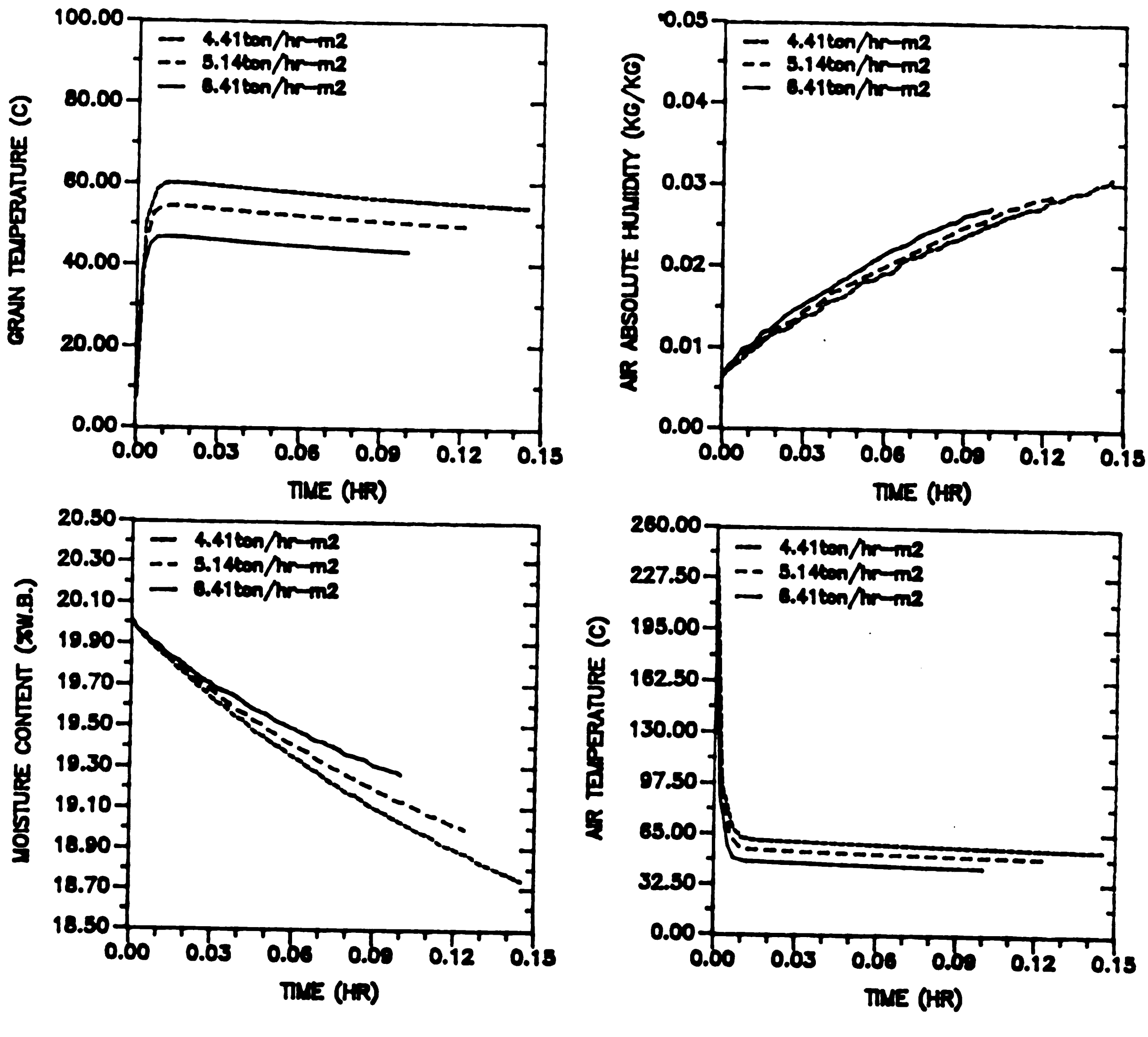

Figure 6.18: Steady-state temperature and moisture profiles for the 1st-stage of a CCF dryer predicted by the unsteady-state model for different grain flow rates (see Table 6.4 for input parameter values).

process consists of the grain losing moisture to the drying air which cools the air and the corn. As the grain loses moisture and the air cools, the humidity of the air increases and thus the equilibrium moisture content increases, which in turn slows down the rate of drying.

Figure 6.19 shows the temperature (air and corn) and the moisture content distributions in a two-stage CCF dryer. The input conditions are listed in Table 6.8.

Table 6.8: Simulation input parameters for the two-stage CCF dryer.

Parameters	1st-stage	2nd-stage
Temperature -Air	232.2	232.2
(°C) -Grain	7.2	53.6
Moisture (%w.b.)	20.0	18.7
Humidity (kg/kg)	0.006	0.006
Flow rate -Grain	4,410.0	4,410.0
($kg/hr\text{-}m^2$)-Air	3,137.0	3,137.0
Bed Depth (m)	0.76	0.76
Tempering length (m)	5.18	

With concurrentflow drying, the air and grain temperatures equilibrate in the first few centimeters of the drying bed, then both gradually decrease as the grain moves through the dryer. The tempering in a multi-stage CCF dryer increases the drying rate in the second stage. During the tempering process, the moisture concentration within the kernels is equalized. If insufficient tempering time is allowed between two drying stages, less drying is achieved in the second drying stage (Steffe and Singh, 1980).

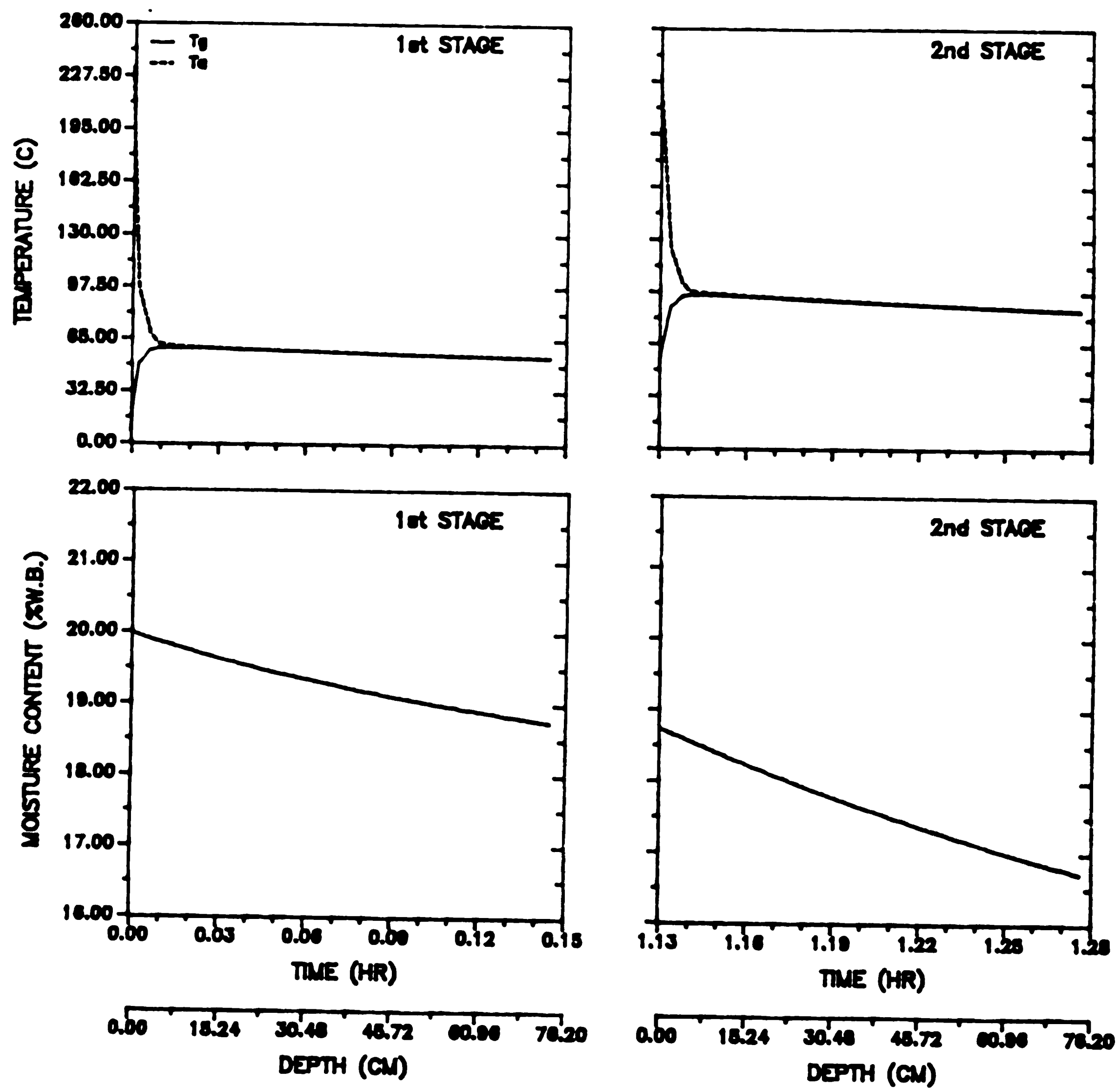

Figure 6.19: Steady-state temperature and moisture profiles for the two stages of a CCF dryer predicted by the unsteady-state model (see Table 6.4 for input parameter values).

Figure 6.20 and Figure 6.21 present a sample output of the unsteady-state two-stage CCF drying simulation for constant and varying grain flow rates, respectively. The figures show the relationship between the inlet moisture content, outlet moisture content and discharge auger rpm.

Figure 6.20 presents the simulation results when the discharge auger is constant and the inlet moisture content varies at random. It is observed that the outlet moisture content follows the same trend as the inlet moisture content within the corresponding time delay of about 1.8 hours.

When the input is pertubated, i.e., the discharge auger is randomly varied (see Figure 6.21), a change in trends is noticed due to the variation in the auger rpm. These results allow for an understanding of the process dynamics and permit the modeling of the drying process.

6.2.1) Model Identification Results

The unsteady-state differential equation model for concurrentflow drying was used to test the adequacy of the empirical models in describing the drying process of two-stage a concurrentflow dryer. The outlet moisture content and discharge auger rpm for a given moisture content generated by the unsteady-state model shown in Figure 6.21, are used in estimating the model parameters in the empirical equations discussed in Chapter 4.

Tables 6.9 and 6.10 show the values of the estimated parameters of model I, model II-a, model II-b, the linear model and the exponential model.

It can be seen that the value of the loss function for the

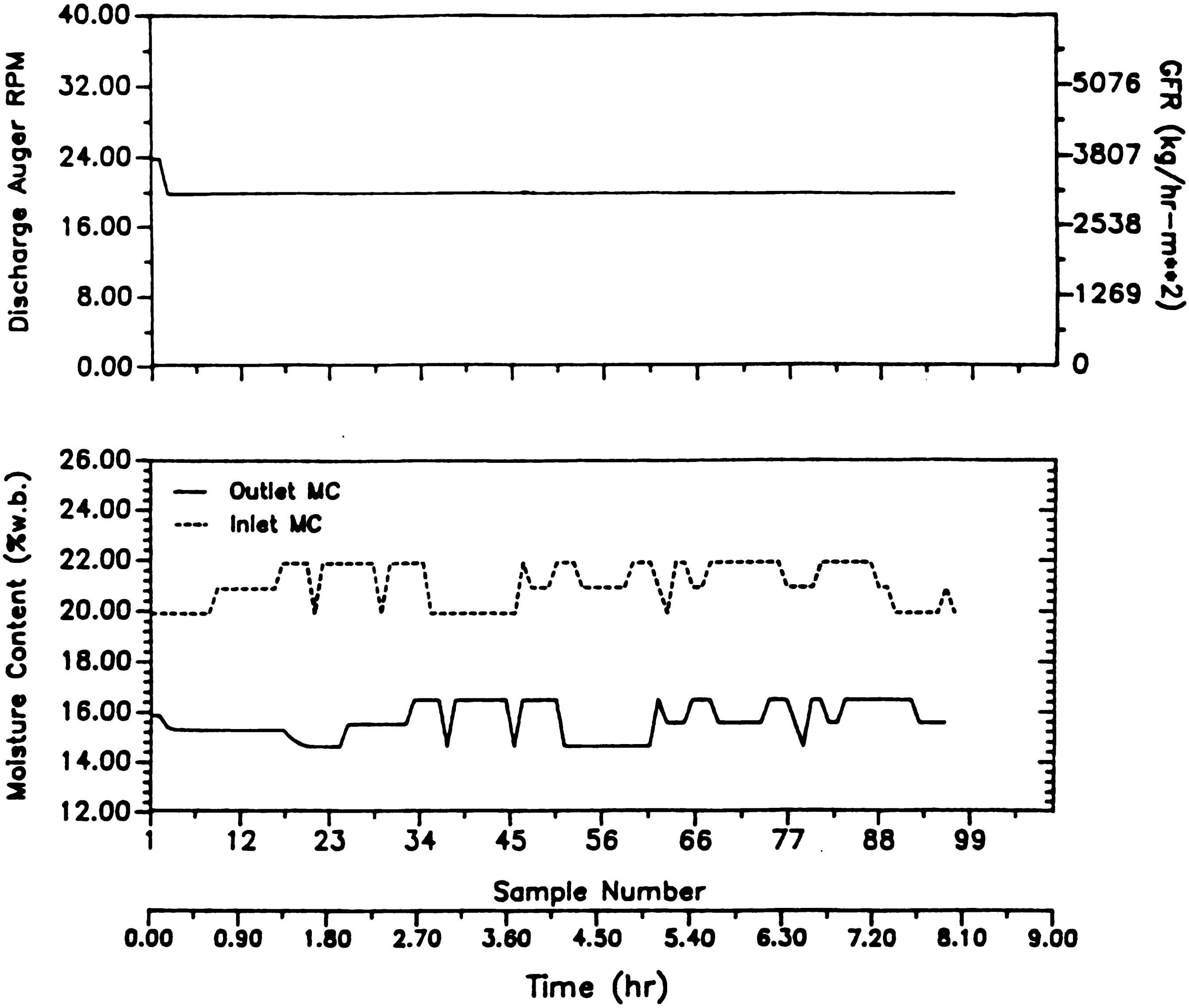

Figure 6.20: Unsteady-state moisture profile for the two stages of the CCF dryer using the USS model at constant GFR (Tin=232.2°C, θin=7.2°C).

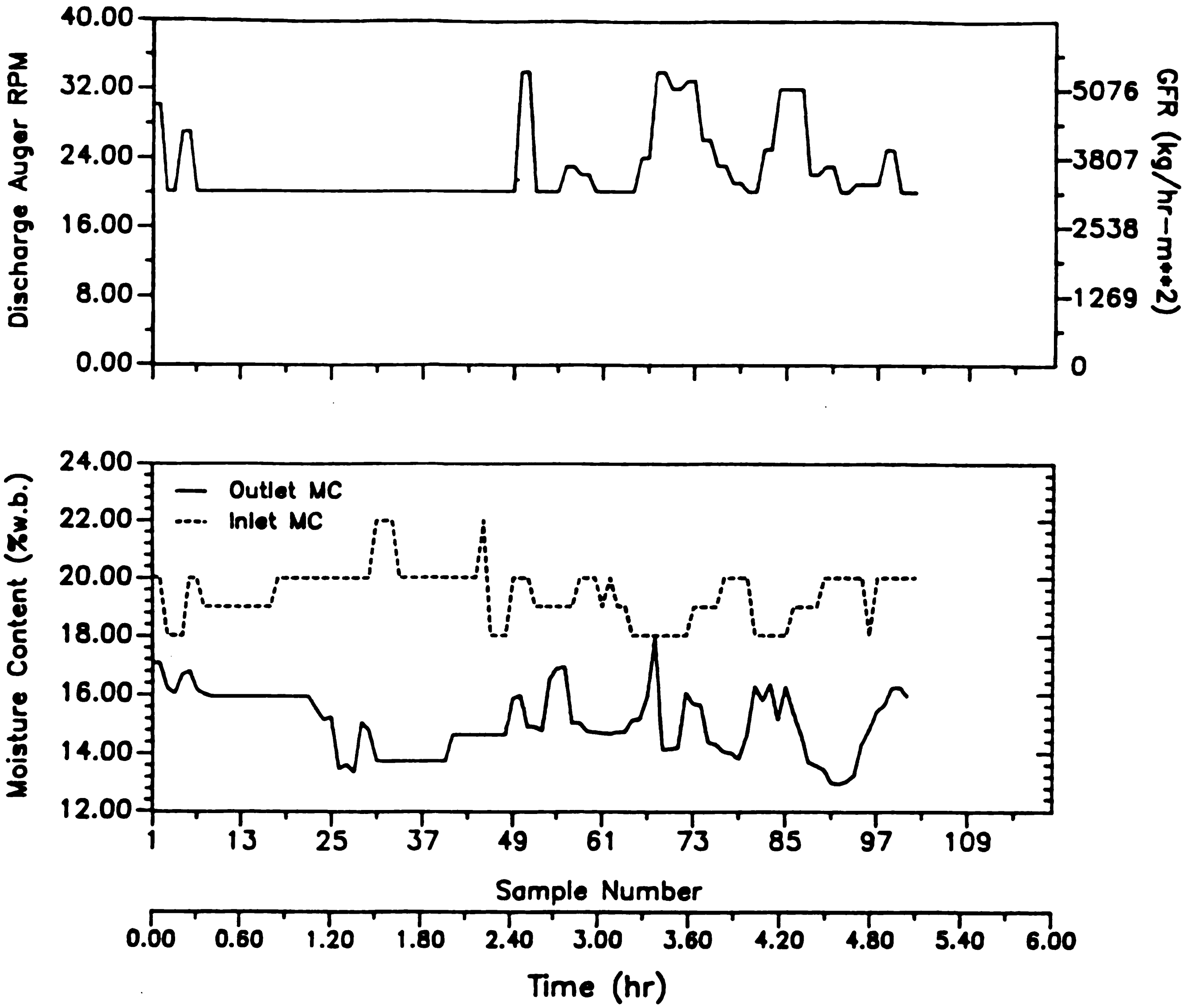

Figure 6.21: Unsteady-state moisture profile for the two stages of the CCF dryer using the USS model at varying GFR (Tin=232.2°C, θin=7.2°C).

model I decreases when the model order increases. However, a higher order was not tested because the objective is to obtain a simple model which adequately represents the dynamic of the drying process.

The null hypothesis that model I is of the first order was tested:

$$H_0: (\overset{o}{a}_2 = \overset{o}{b}_1 = \overset{o}{c}_1 = 0).$$

thus, θ is equal to 3.44 [Eqn.(5.25) for N=77]. At a risk level of 5%, $F_{0.95}(3,71)$ is 2.76. Thus the hypothesis that the model is first-order has to be rejected.

Figure 6.22 shows a plot of outlet moisture content predicted by the 1st-order model I. The model predicts the outlet content well. The residuals do not show any violation of the assumed assumptions (i.e., that the errors are normal and independent).

Similar results are obtained with the 2nd-order model I (Figure 6.23). The residuals are smaller than for the 1st-order model as can be seen in Table 6.7.

The values of outlet moisture content predicted by the model II-a (Figure 6.24) agree well with the unsteady-state predicted values. The residuals do not show a violation of the assumptions.

Figure 6.25 shows the outlet moisture contents predicted by the model II-b. The difference between the outlet moisture content predicted by the empirical and unsteady-state models are randomly distributed between ± 1%. The outlet moisture content predicted by the model II-b agrees well with the unsteady-state model.

Figures 6.26 and 6.27 show a plot of moisture content predicted by the linear model and the exponential model, respectively. Both models

Table 6.9: Estimates for the model I, model II-a, model II-b [Eqns.(4.2), (4.3) and (4.4), respectively].

PARAMETERS	MODEL			
	Model I		Model II-a	Model II-b
	1st-order	2nd-order		
a_1=	-0.77±0.06	-1.12±0.09	-0.17±0.03	0.098±0.03
a_2=		0.31±0.08		
b_1=	0.033±0.008	0.015±0.02	-0.043±0.003	-0.21±0.09
b_2=		0.012±0.02		
c_1=	0.00085±0.08	-0.34±0.004	0.85±0.03	0.87±0.1
c_2=		-0.0081±0.1		
d_1=				0.87±0.04
LOSS FUNCTION	41.02	35.82	11.47	7.38

Table 6.10: Estimates for the linear model and exponential model [Eqns.(4.6) and (4.7), respectively].

PARAMETERS	MODEL	
	Linear Model	Exponential Model
b =	-0.049±0.0084	-0.039±0.0083
f =	1.03±0.042	
LOSS FUNCTION	13.03	13.04

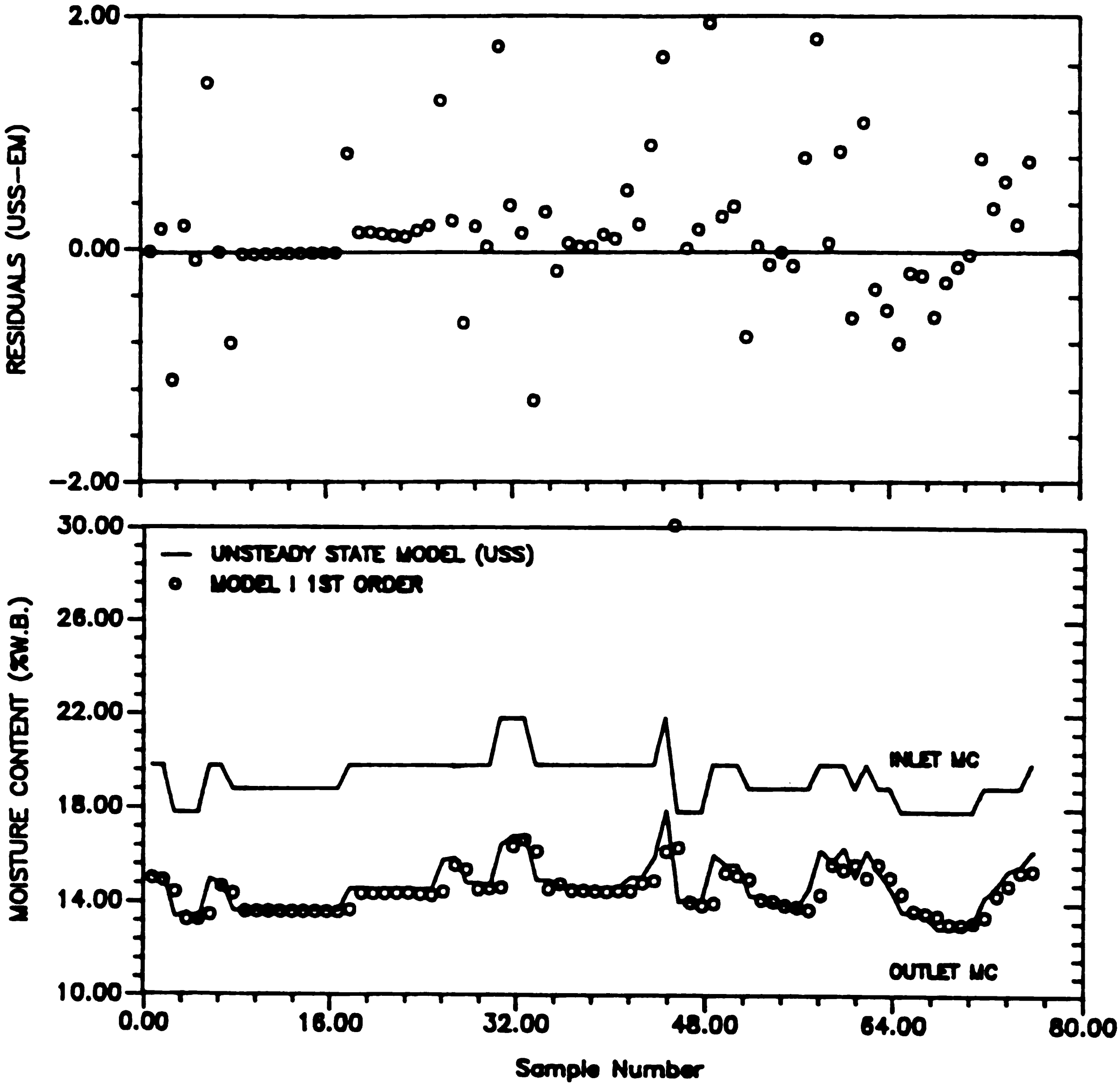

Figure 6.22: Identification results with the first-order model I for the drying of corn on a two-stage CCF dryer.

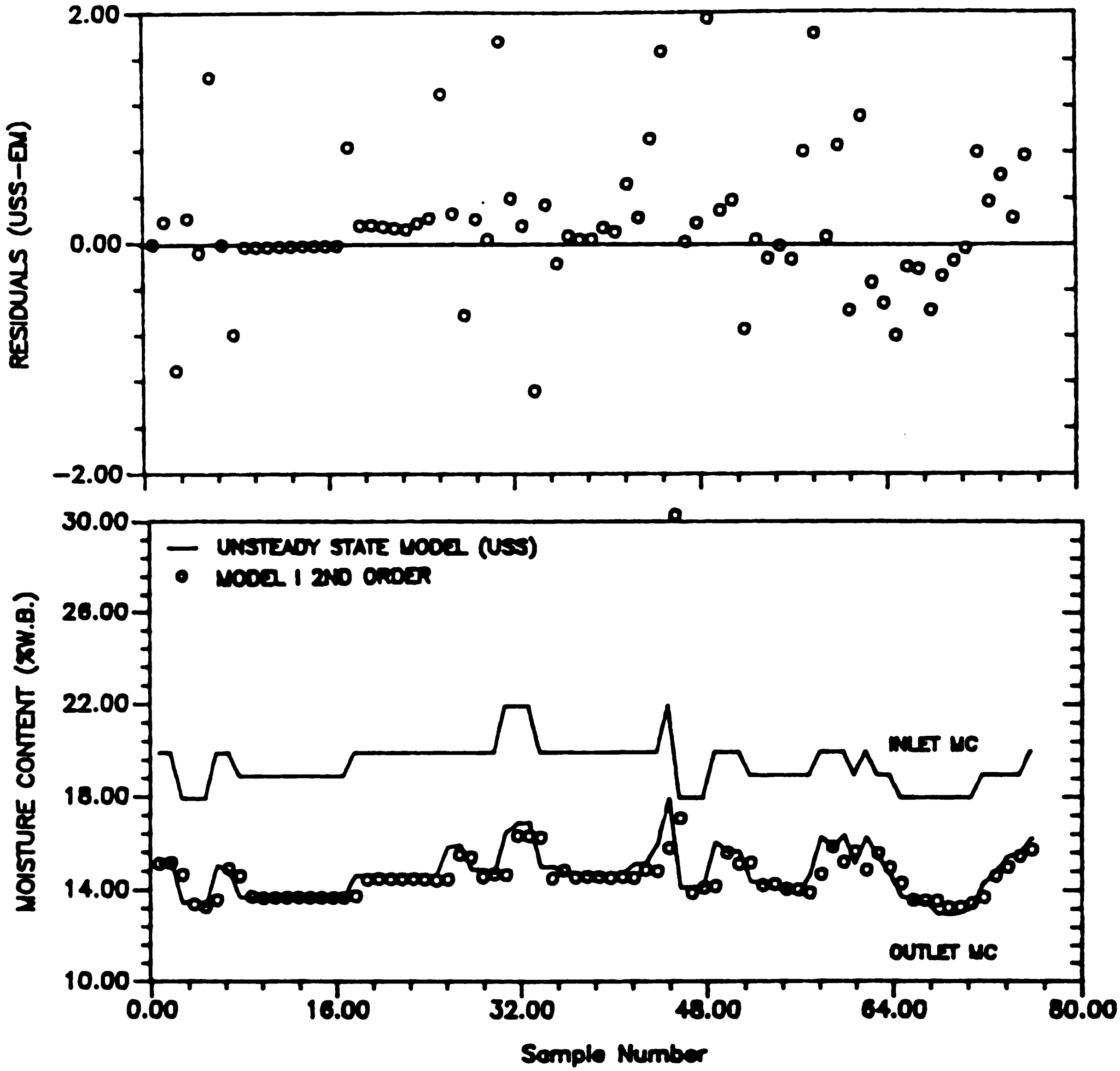

Figure 6.23: Identification results with the second-order model I for the drying of corn on a two-stage CCF dryer.

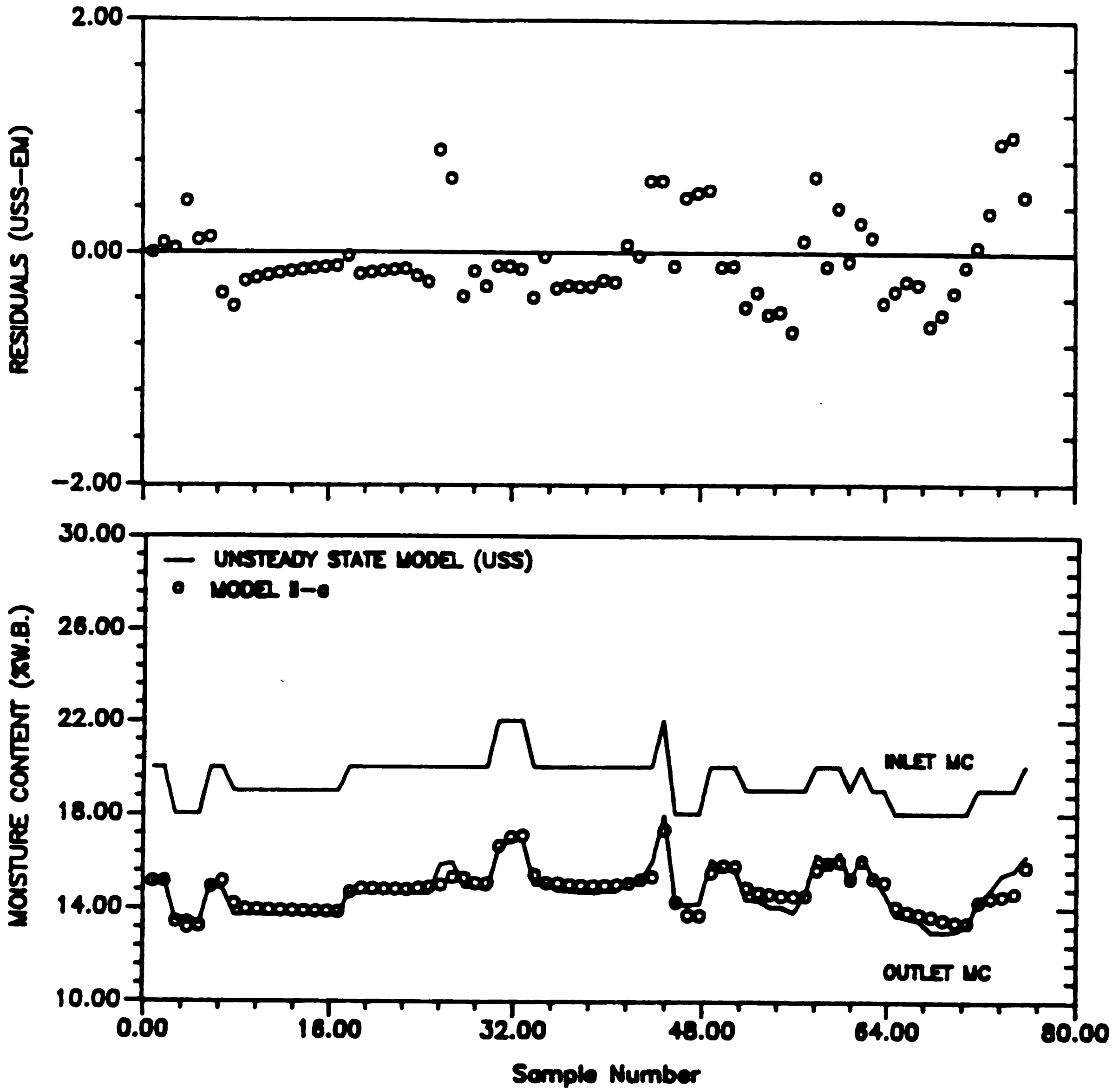

Figure 6.24: Identification results with the model II-a for the drying of corn on a two-stage CCF dryer.

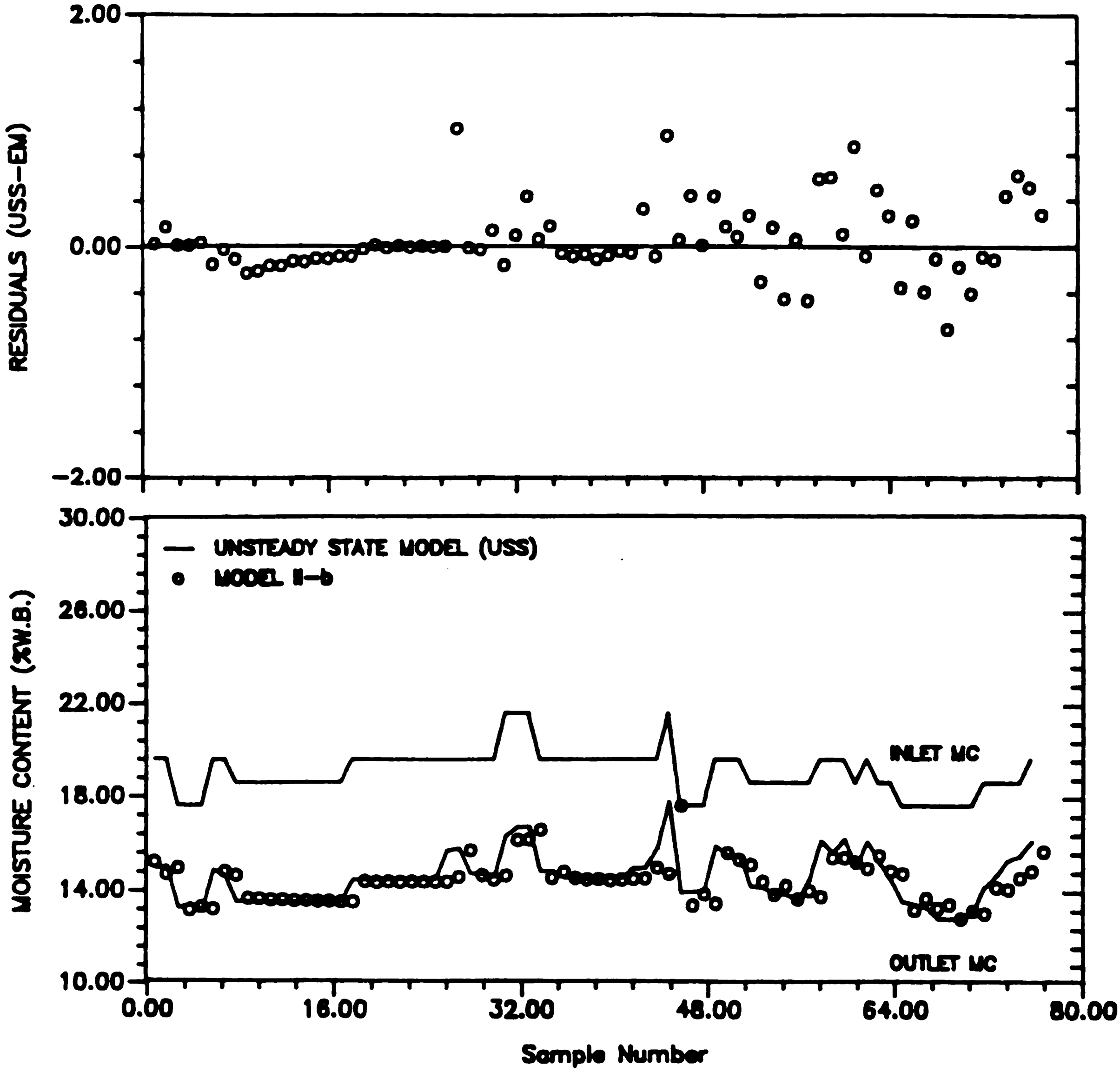

Figure 6.25: Identification results with the model II-b for the drying of corn on a two-stage CCF dryer.

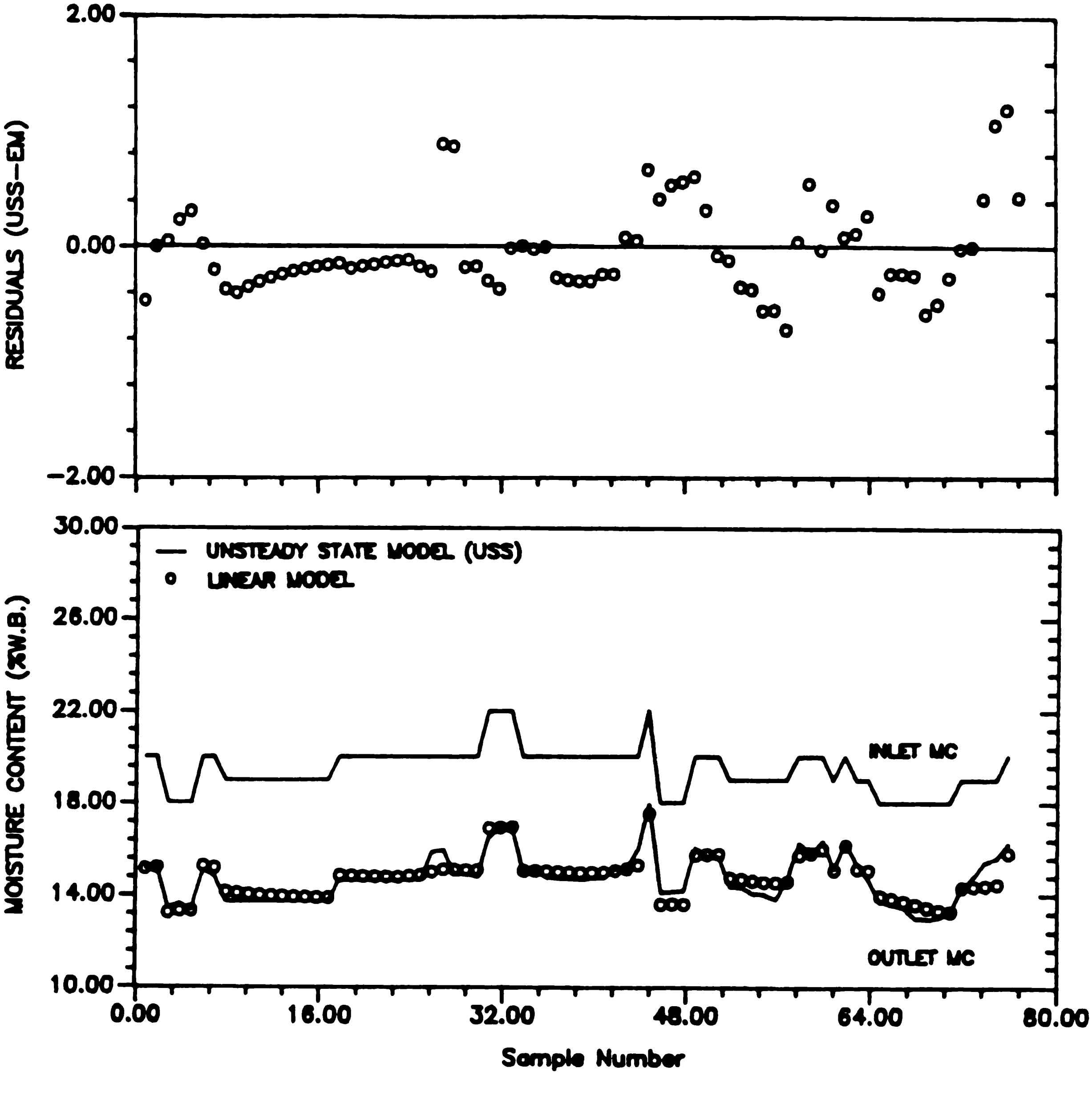

Figure 6.26: Identification results with the linear model for the drying of corn on a two-stage CCF dryer.

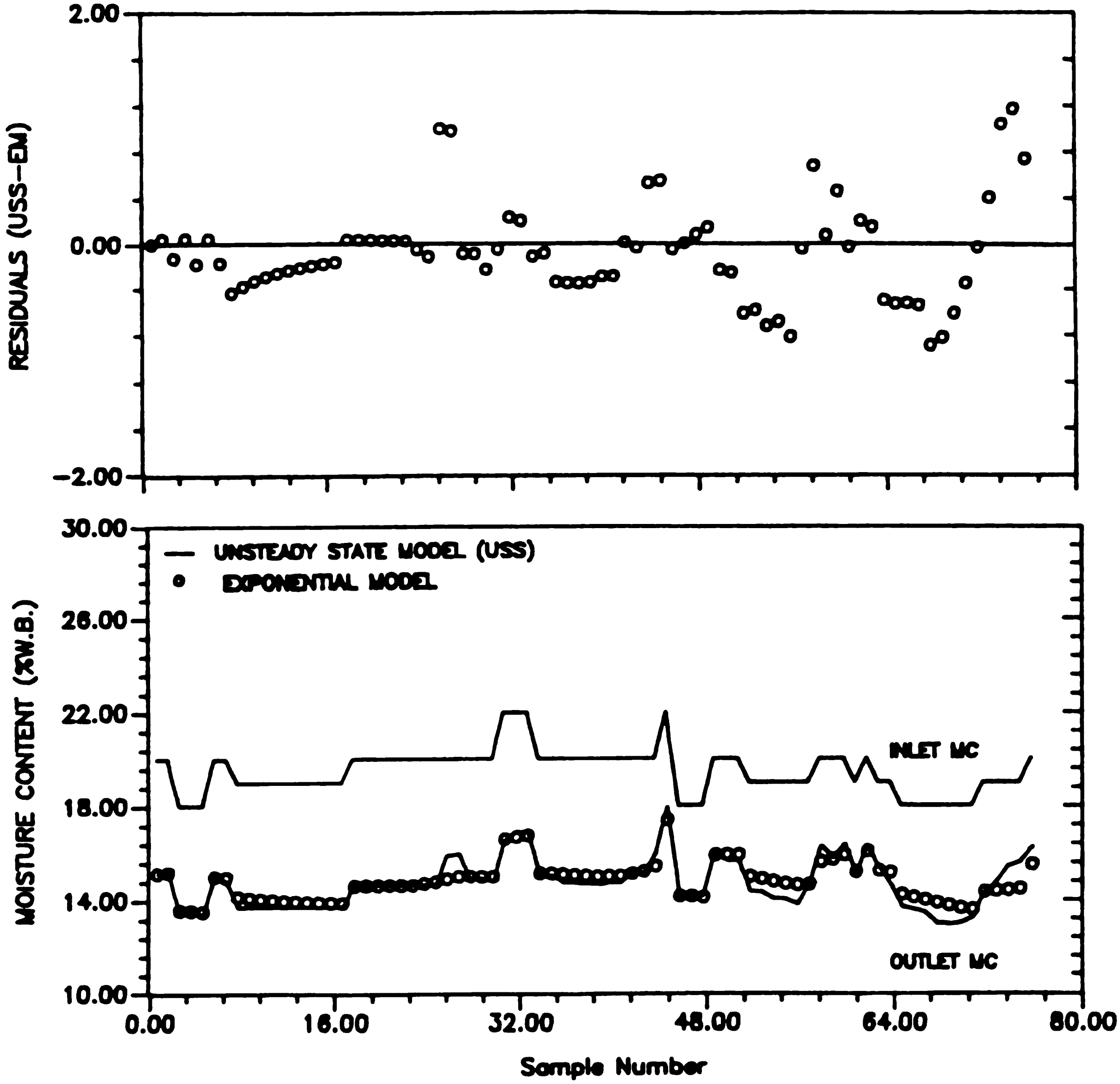

Figure 6.27: Identification results with the exponential model for the drying of corn on a two-stage CCF dryer.

predict the outlet moisture well. The residuals tend to randomly distribute around zero as the number of samples increases.

In conclusion, the five empirical models evaluated in this section are simple in their formation, and therefore efficient for on-line calculation. As is observed in Tables 6.9 and 6.10, the model which shows the lowest sum of square prediction errors (loss function) is model II-b; however, model II-a, and the linear and the exponential models also have promise due to the fewer parameters. Model I requires six or even more parameters to predict a two-stage CCF drying process well, as compared to the other models.

The unsteady-state differential equation CCF dryer model and the continuous-flow dryer control algorithm are combined to form the simulation model for the control system of a two-stage CCF dryer. The results are discussed in the next section.

6.2.2) Concurrentflow Dryer Control

The input moisture content of grain entering a dryer may change slowly or suddenly. These changes are usually modeled as a ramp or step change, respectively.

Typically, different loads of grain are periodically delivered to the dryer during a working day. Within a load the grain moisture content is relatively constant, but it may change significantly between two loads. Grains from different fields usually have different moisture contents. Therefore, a way of modeling the inlet moisture content is as a sequence of random step signals, with constant moisture values between two step signals. Another way, is to consider that the inlet moisture changes linearly between samples, given a series of ramp inputs.

Two ways of modeling the inlet moisture content are considered in the theoretical analysis of the automatic control system: (a) a series of randomly distributed step changes, and (b) a series of ramp inputs. Table 6.11 presents the inlet moisture content signal characteristics.

Table 6.11: Inlet moisture content sets used as input in the simulation of a two-stage CCF grain dryer.

SET NUMBER	Moisture Content (%w.b.)			
	Min	Avg	Max	STD
1	18.0	20.4	23.0	1.3
2	17.6	20.7	25.6	1.1
3	17.8	20.8	25.0	1.9

where: Set1 is a randomly distributed step change
Set2 and Set3 are a series of ramp changes.

Before different control strategies can be compared, performance measures must be established. In grain drying, the objective of the control system is to control the drying process of the grain entering a dryer to a set moisture content, regardless of the variation in the inlet moisture content or drying conditions. In this study, the control behavior of the control systems is compared by simulation with respect to the following performance measures:

- <u>control performance, Se</u> (the standard deviation of the outlet moisture content from the setpoint)

$$Se = \sqrt{\frac{1}{N+1} \sum_{k=0}^{N} [Y(k)-\hat{W}]^2} \qquad \text{........(6.1)}$$

where Se = the root-mean-squared control error

N = number of samples

$\hat{W}$ = setpoint

- <u>average outlet moisture content</u>, MOavg

These performance measures were chosen because they reflect the most important points in the evaluation of a control system for a grain dryer. The Se is the standard deviation of the outlet moisture content from the setpoint. In other words, Se expresses the amount of grain which will leave the dryer with a moisture content differing from the setpoint. In practice, a large number of wet spots left in the dried grain would be dangerous because spoilage may result. The average moisture content of the dried grain must be close to the setpoint because the market price depends on a specific moisture content.

6.2.2.1) <u>Randomly Distributed Step Input Signal</u>

The step change in the inlet moisture content was simulated without control and with the five controllers described in Chapter 4.

Before the automatic controller of the grain dryer is turned on, values of the inlet moisture content, outlet moisture content and grain flow rate, which are stored in a data file are used to estimate the parameters of the control model. The rpm of the discharge auger motor in this simulation study is constant and equal to 20 before the control is switched on.

Figure 6.28 shows the outlet moisture content variation when no control is applied to the dryer using the inlet moisture content from Set1. As can be seen, the output follows the inlet moisture content trend and results in an average of 18.5%.

Figures 6.29-6.33 show the simulated results obtained with the five controllers using the inlet moisture content variation from Set1 for a setpoint equal to 16% w.b.. It is assumed that in a two-stage CCF corn dryer, 1% of the grain moisture is removed during cooling, which will bring the final moisture content down to 15% w.b..

A simulation with the pole placement controller (PP) is illustrated in Figure 6.29. The accuracy in control is good and is achieved quickly after the start. The average outlet moisture content is only 0.1% of the setpoint of 16% w.b. while the control error Se is 1.2%.

Figure 6.30 shows the results when using the minimum variance controller (MV-feedback/feedforward). Compared with the PP-controller, this controller gives the same Se value and an average outlet moisture content (15.7%) 0.3% from the setpoint. Also, the controlled variable takes longer to approach to the setpoint.

The simulation results with the minimum variance feedback control (MV-feedback) are illustrated in Figure 6.31. This controller gives a larger Se value (1.8) as compared with the previous controllers. The average outlet moisture content is 0.4% from the setpoint. The results confirms that by measuring only the outlet moisture content it will result in inaccurate control when significant variations in inlet moisture content are experienced.

A control based only on the measurement of the inlet moisture content does not offer acceptable control, as is illustrated in Figure 6.32. This simulation represents the results obtained with the MV

-feedforward controller. The controller gives a large control error Se (1.8%) and a MOavg 0.8% from the setpoint. Without the corrective action of a feedback loop, the controller is not capable of maintaining the outlet moisture content close to the setpoint.

The simulation results with the model-based control is shown in Figure 6.33. The value of the average outlet moisture content is 14.8% with Se equal to 1.5%. The MB control system is a feedforward controller without feedback loop. The controller reacts only to a change in the inlet moisture content and does not account for the error between the output and the setpoint. The controller is slow and results in 1.2% offset.

Table 6.12 lists the performance measures and the relevant data for each controller.

The results shown in Table 6.12 indicate that the best controller for a two-stage CCF dryer is the pole placement (PP). The less suitable controllers are the MV-feedforward and the model based. An observation of the average rpm values shows that the control input signal is generally larger with the PP-controller than with the MV and MB controllers. This means that the maximum capacity of the dryer is used with the PP-controller, hence resulting in high energy efficiency.

The minimum variance controller with a feedforward (MV-feedforward/feedback) does not show much improvement in control quality as compared with the MV-feedback. A possible explanation is that in the MV-feedback/feedforward controller there are only four estimated parameters compared to six parameters in the MV-feedback controller. Therefore, good control becomes dependent on a good estimate of the disturbance model. For the MV-feedback, the variations in the inlet

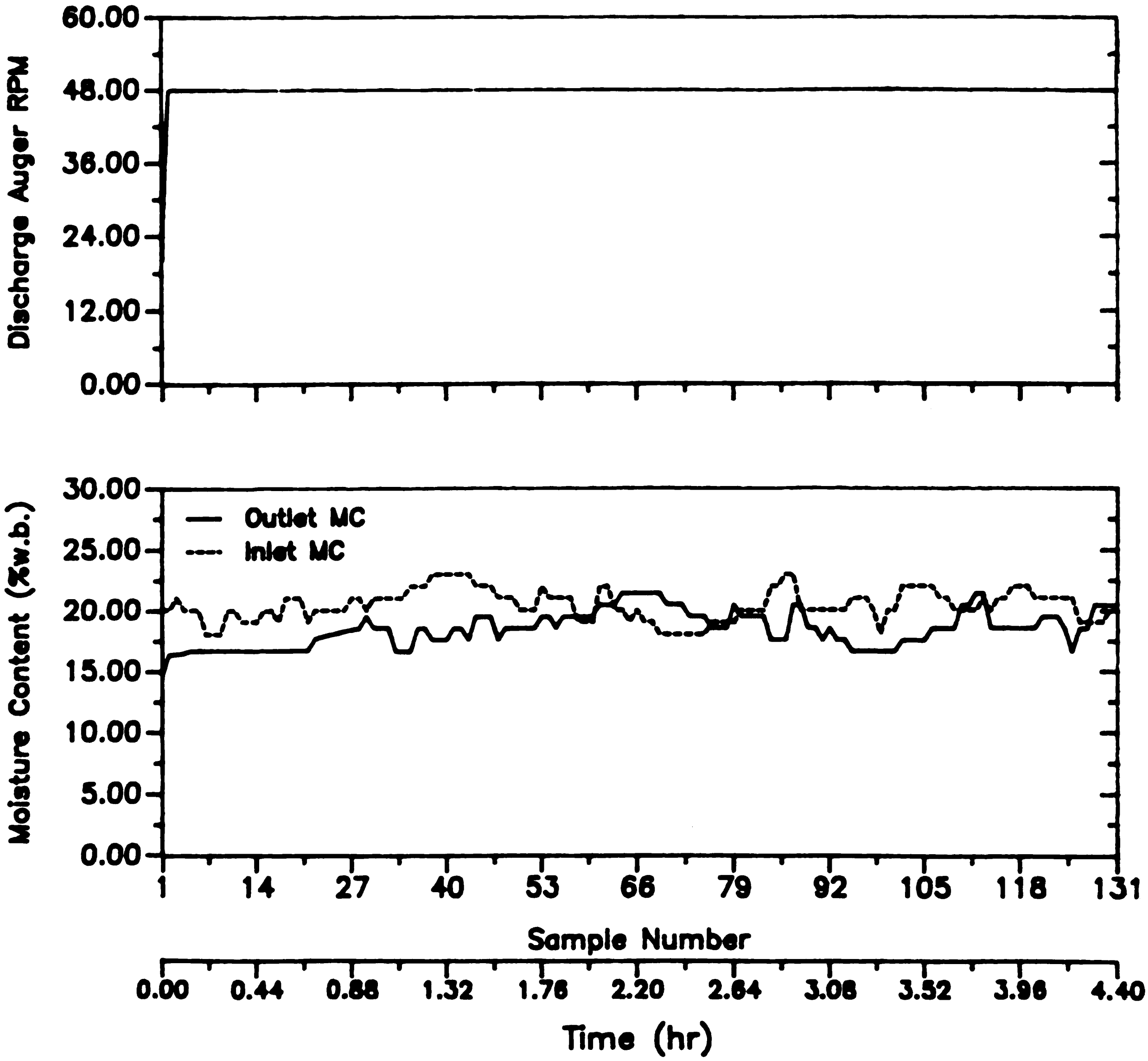

Figure 6.28: Simulation of the automatic control of a two-stage CCF dryer (no control).

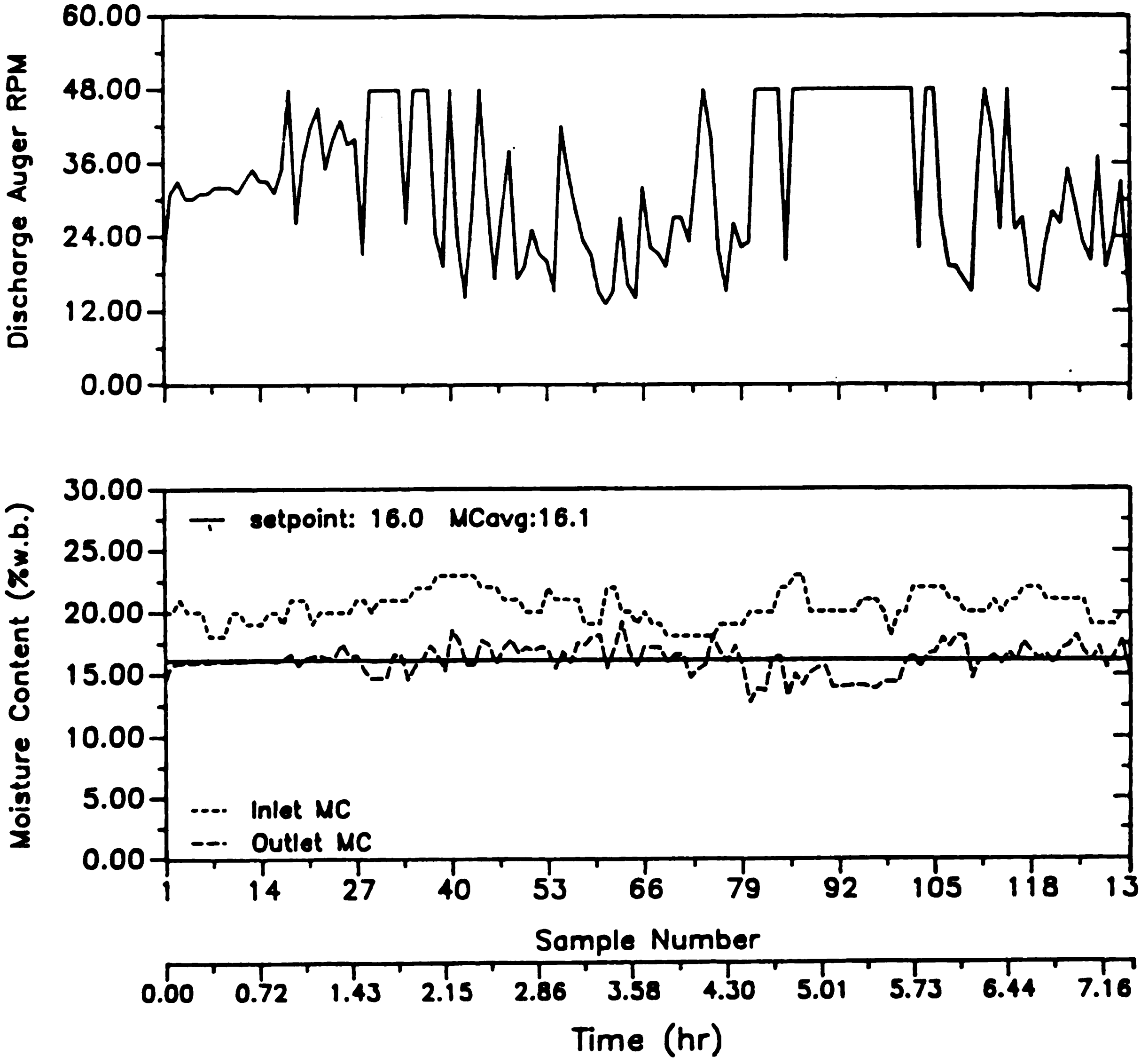

Figure 6.29: Simulation of the automatic control of a two-stage CCF dryer using the PP-controller (see Table 4.1 for dryer parameters).

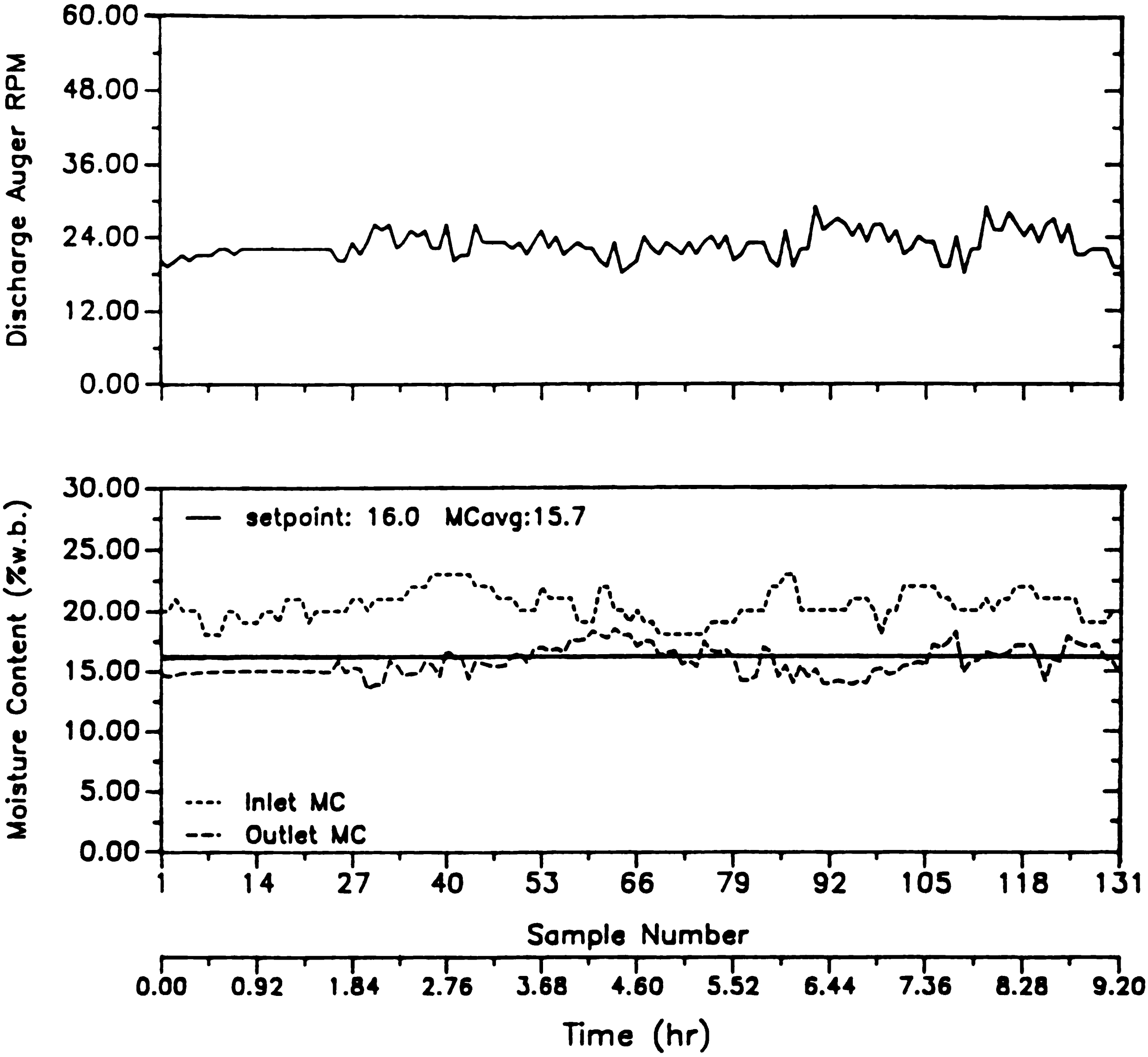

Figure 6.30: Simulation of the automatic control of a two-stage CCF dryer using the MV-feedback/feedforward controller (see Table 4.1 for dryer parameters).

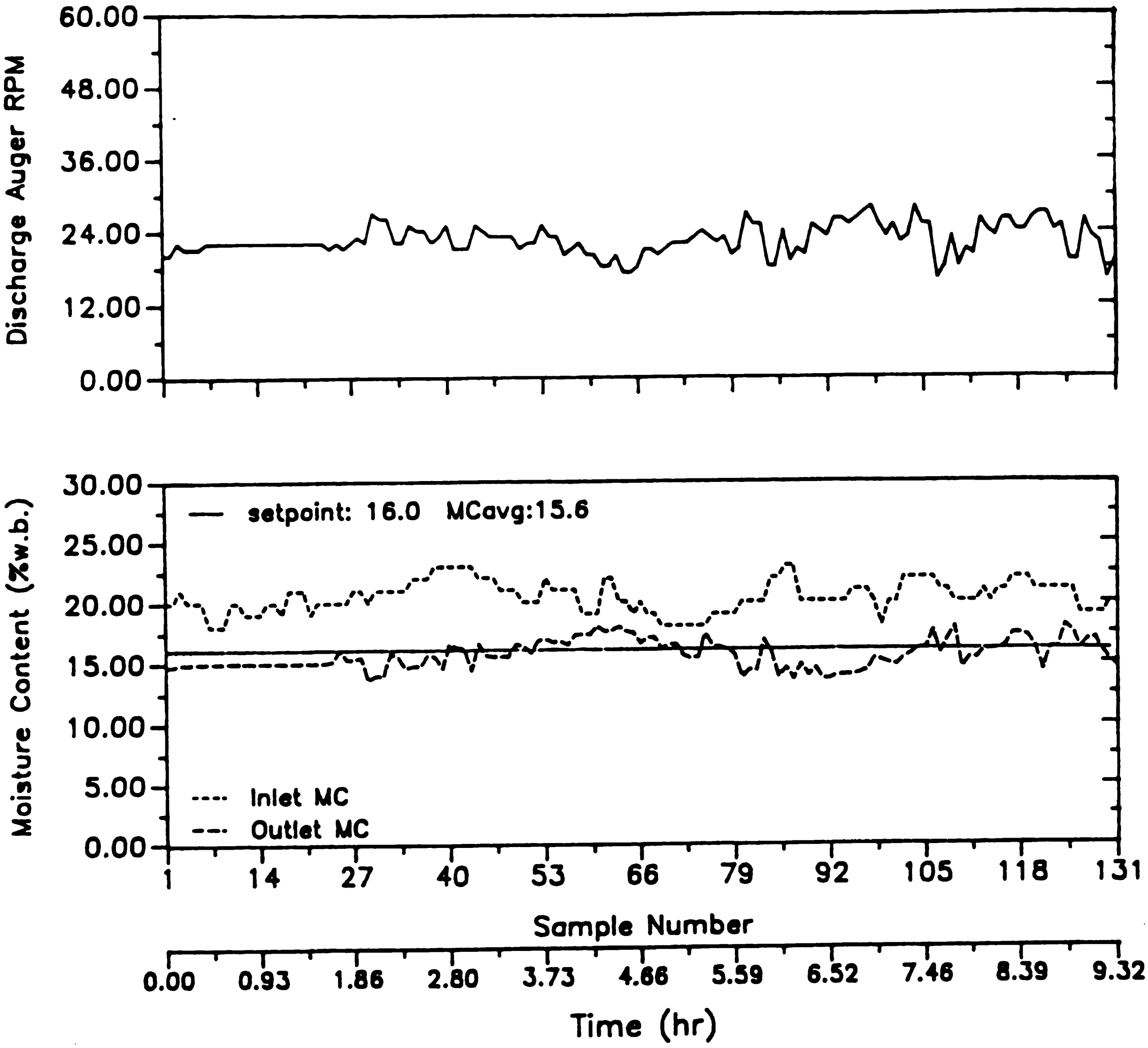

Figure 6.31: Simulation of the automatic control of a two-stage CCF dryer using the <u>MV-feedback controller</u> (see Table 4.1 for dryer parameters).

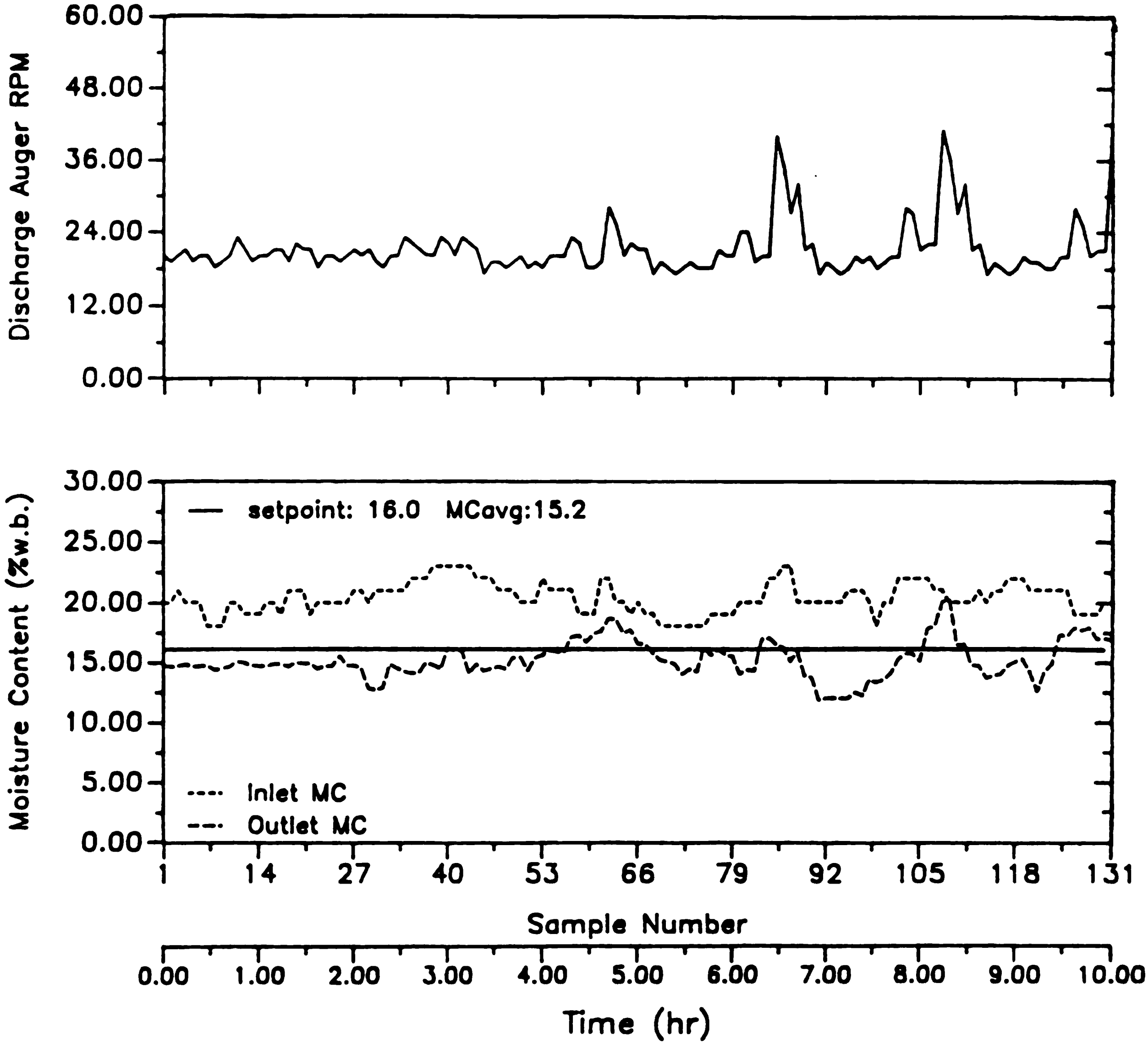

Figure 6.32: Simulation of the automatic control of a two-stage CCF dryer using MV-feedforward controller (see Table 4.1 for dryer parameters).

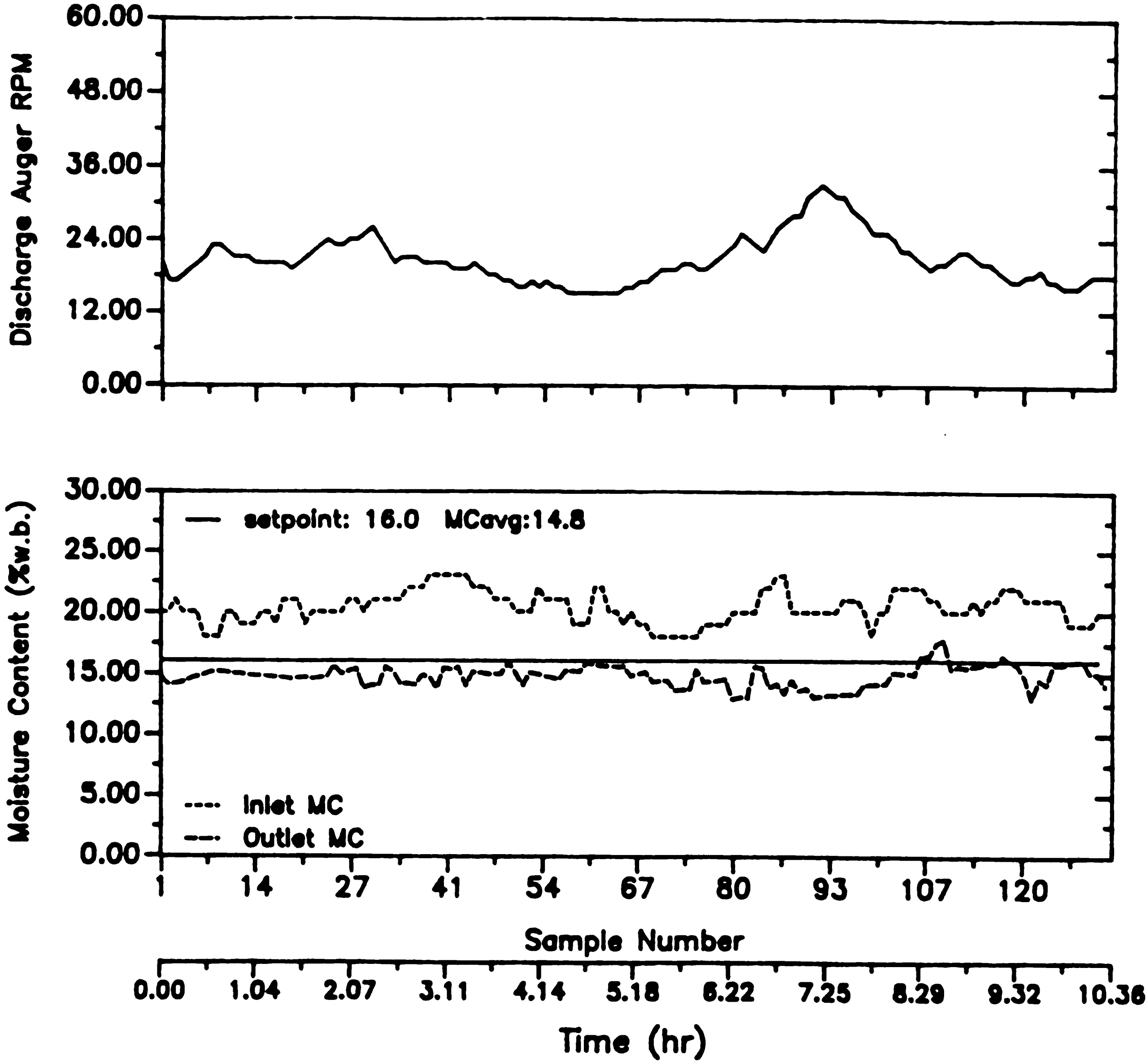

Figure 6.33: Simulation of the automatic control of a two-stage CCF dryer using MB-controller (see Table 4.1 for dryer parameters).

Table 6.12: Characteristic values of the different control performances with the inlet moisture content variation from Set1 and setpoint equal to 16% w.b. (N = 131).

PERFORMANCE MEASURES	CONTROLLER					NC
	PP[1]	MV[2]			MB	
		fdb	fdf	fdb+fdf		
Se(%)	1.2	1.2	1.8	1.2	1.5	--
MOavg(%)	16.1	15.6	15.2	15.7	14.8	18.5
MOmin(%)	12.7	13.5	11.8	13.5	12.8	15.0
MOmax(%)	19.2	18.0	20.3	18.5	17.8	21.0
MImin(%)	18.0	18.0	18.0	18.0	18.0	18.0
MIavg(%)	20.4	20.4	20.4	20.4	20.4	20.4
MImax(%)	23.0	23.0	23.0	23.0	23.0	23.0
MIstd(%)	1.3	1.3	1.3	1.3	1.3	1.3
RPMmin	13.0	16.0	17.0	18.0	15.0	--
RPMavg	32.6	22.4	21.2	22.6	20.6	--
RPMmax	48.0	28.0	42.0	29.0	33.0	--
RPMstd	11.8	2.5	4.6	2.2	4.0	--

[1] for β equal to 50
[2] for ρ equal to 0.01
where: fdb = feedback
fdf = feedforward
PP = pole placement controller
MV = minimum variance controller
MB = model-based controller
NC = no control (see Figure 6.28)
Se = see Eqn.(6.1)[standard deviation from the setpoint]
N = number of samples (the chosen value allows simulation for at least 7 hours drying time)

moisture content from Set1 can be well estimated by the noise polynomial [polynomial C in Eqn.(4.2)] when six parameters are used.

The value of the input weighting factor ρ used in the simulation tests was equal to 0.01 for the MV-controller. For the PP-controller, a value of 50 was chosen for β. These values give a good response for all controls investigated.

A second set of tests was simulated. The same inlet moisture content profile was used (see Set1 in Table 6.11). However, the setpoint was changed to 17% w.b. The objective was to analyze the reaction of the controllers to a step change in the reference value.

In Figure 6.34, the results, obtained with the pole placement controller (PP) are shown. The average outlet moisture content is 17.2%. This controller gives small Se (1.2) values and shows fast convergence to the setpoint.

Figure 6.35 shows the results of the MV-feedback/feedforward controller. The grain is overdried 0.7 points below the setpoint. Compared to the previous controller, this controller results in a larger Se (1.6%). The convergence of the controlled variable to the setpoint is slow, i.e., it takes about 3 hours or 40 samples for the outlet moisture content to approach the setpoint.

The MV-feedback control system simulation is shown in Figure 6.36. The results are similar to the MV-feedback/feedforward controller. It is observed that the quality of the control performance does not improve with the additional feedforward from the inlet moisture content in a minimum variance controller.

The simulation of the MV-feedforward control is shown in Figure 6.37. The average outlet moisture content is 15.3%, 1.7 points below the setpoint. The control error Se results in the largest (2.7%) with this controller.

The simulation result obtained with the MB-controller is presented in Figure 6.38. The average outlet moisture content is 16% with a control error of 1.4%. The discharge auger rpm changed from 16 to 48 rpm during the run; this change is due to the inlet moisture content variations occurring during the simulation.

Table 6.13 shows the results of the performance measures for the different control systems.

All the controlled cases studied are better than the uncontrolled case, except for the MV-feedforward which is the worst case.

The controller which achieves the average outlet moisture content closest to the setpoint and the lowest Se value is the pole placement controller.

The MV-feedback and the MV-feedback/feedforward controllers present very similar control behavior. The advantage of the latter is the few number of parameters required for estimation (as was discussed in section 4.1.1).

In conclusion, for a sequence of step changes in the input signal, the pole placement controller was superior to the MV and MB controllers for a two-stage CCF corn dryer; the PP-controller reacts fast to a change in the inlet/outlet moisture content and maintains good control over the entire drying period. The MV-feedback/feedforward controller gave good control performances when the working conditions are known. The model base controller as well as the MV-feedforward controller were not capable of maintaining the outlet moisture content

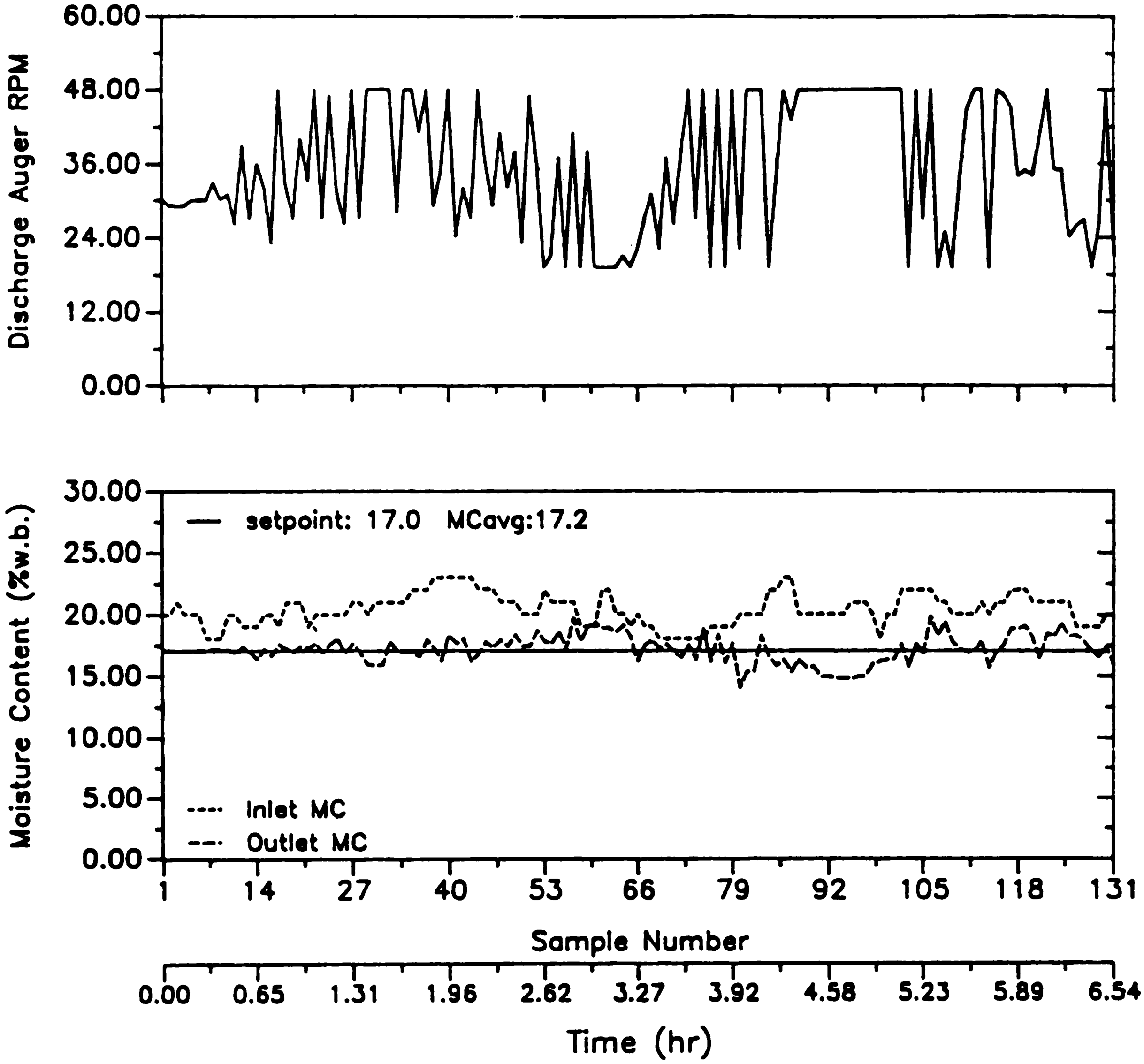

Figure 6.34: Simulation of the automatic control of a two-stage CCF dryer using <u>PP-controller</u> (see Table 4.1 for dryer parameters.)

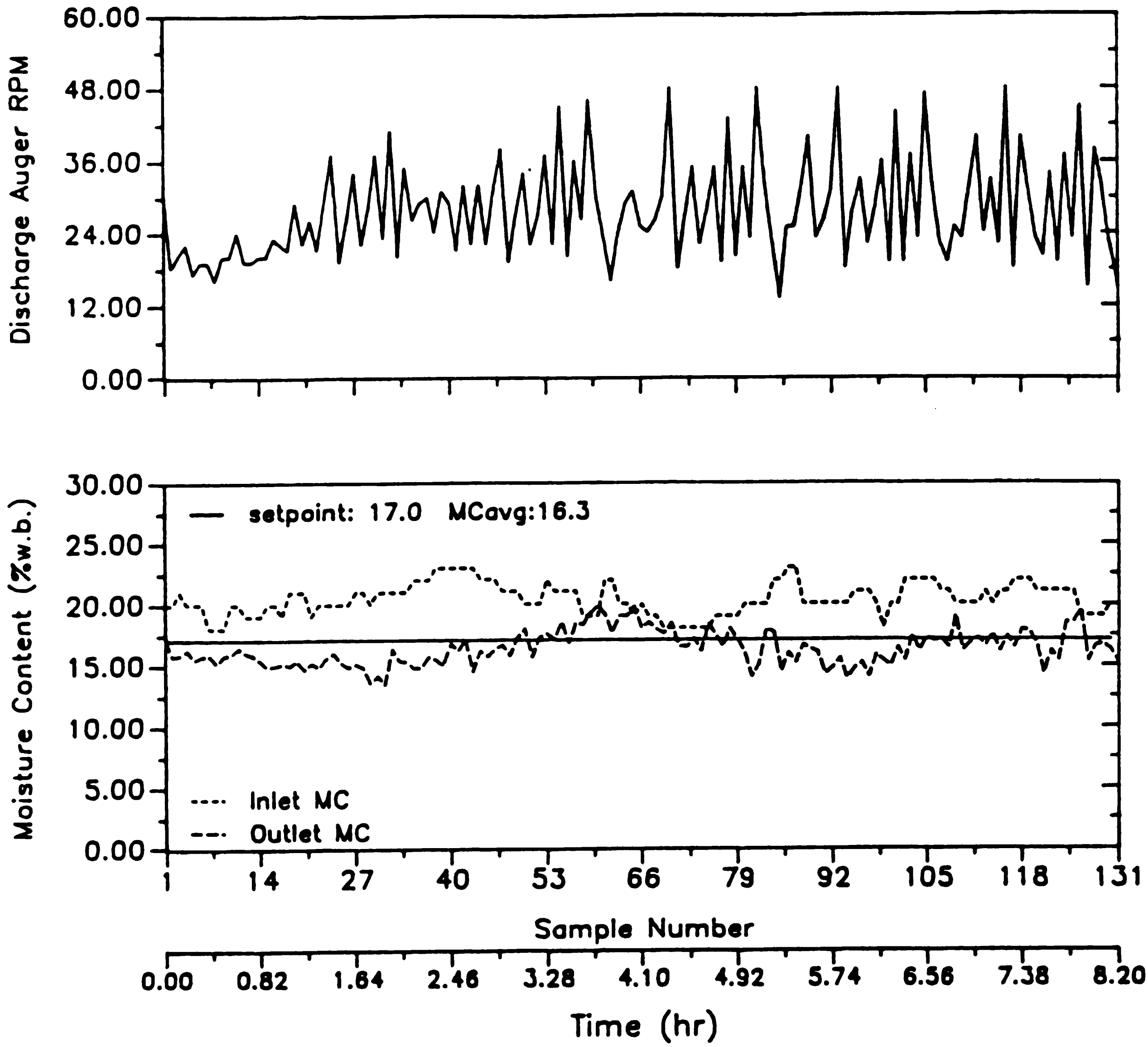

Figure 6.35: Simulation of the automatic control of a two-stage CCF dryer using <u>MV-feedback/feedforward</u> controller (see Table 4.1 for dryer parameters).

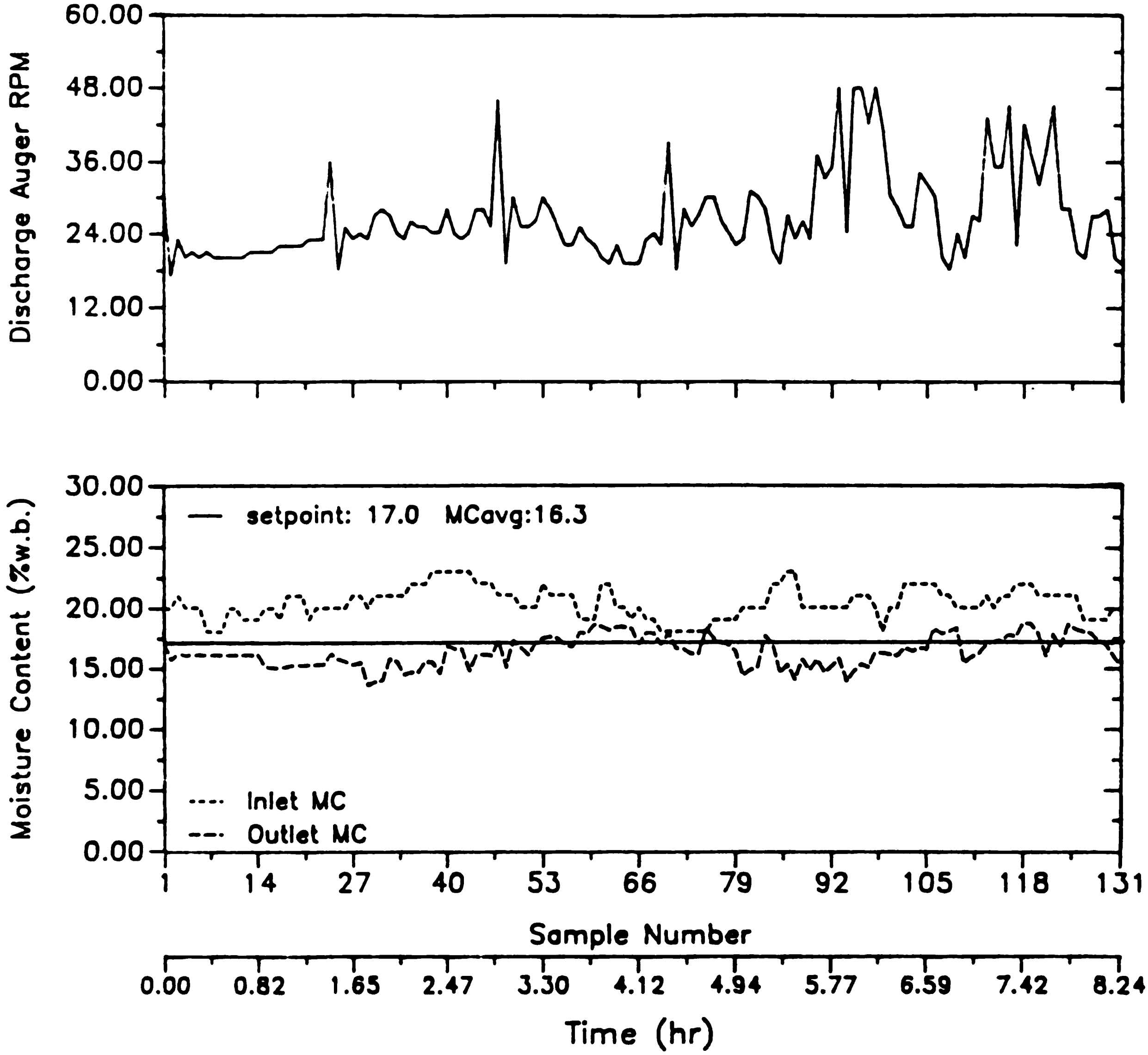

Figure 6.36: Simulation of the automatic control of a two-stage CCF dryer using the MV-feedback controller (see Table 4.1 for dryer parameters).

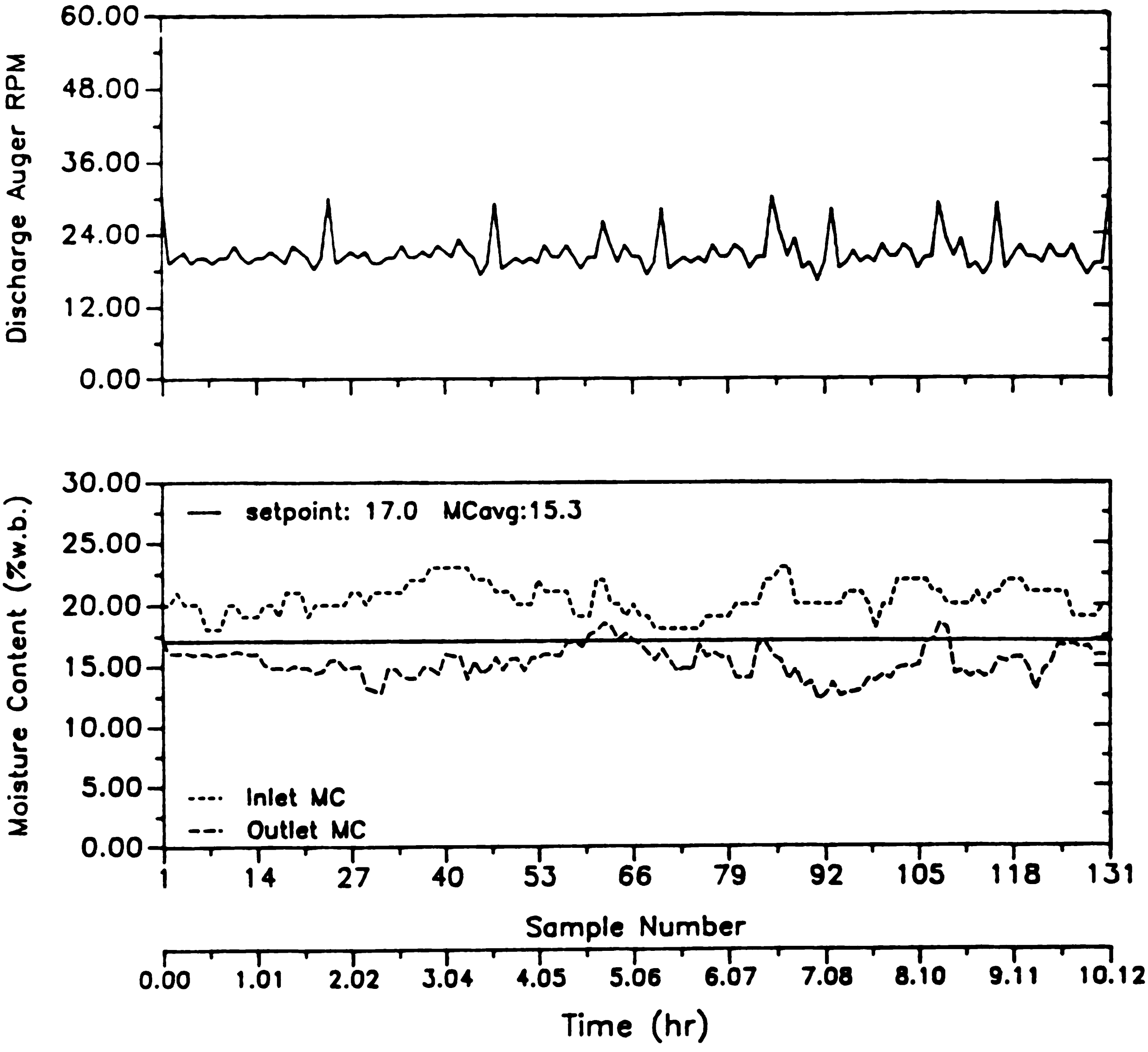

Figure 6.37: Simulation of the automatic control of a two-stage CCF dryer using MV-feedforward controller (see Table 4.1 for dryer parameters).

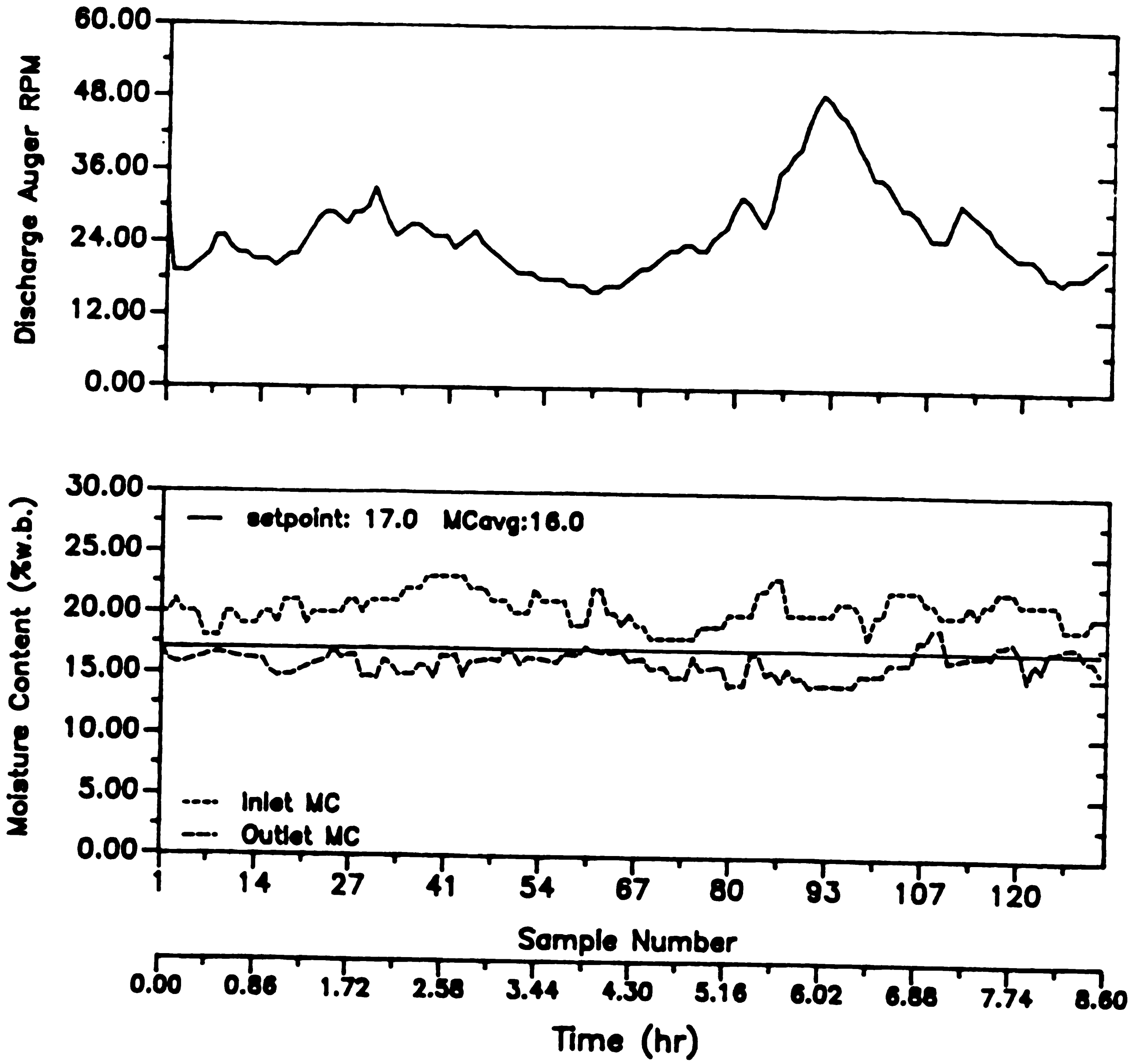

Figure 6.38: Simulation of the automatic control of a two-stage CCF dryer using MB-controller (see Table 4.1 for dryer parameters).

Table 6.13: Characteristic values of the different control performances with the inlet moisture content variation from Set1 and setpoint equal to 17% w.b. (N = 131).

PERFORMANCE MEASURES	CONTROLLER					NC
	PP[1]	MV			MB	
		fdb[2]	fdf[2]	fdb+fdf[3]		
Se(%w.b.)	1.2	1.4	2.7	1.6	1.4	--
MOavg(%)	17.2	16.3	15.3	16.3	16.0	18.5
MOmin(%)	14.0	13.5	12.1	13.4	14.1	15.0
MOmax(%)	19.9	18.8	18.5	19.9	19.0	21.0
MImin(%)	18.0	18.0	18.0	18.0	18.0	18.0
MIavg(%)	20.4	20.4	20.4	20.4	20.4	20.4
MImax(%)	23.0	23.0	23.0	23.0	23.0	23.0
MIstd(%)	1.3	1.3	1.3	1.3	1.3	1.3
RPMmin	19.0	17.0	16.0	13.0	16.0	--
RPMavg	35.4	26.6	20.6	27.5	25.7	--
RPMmax	48.0	48.0	31.0	48.0	48.0	--
RPMstd	10.8	7.3	7.3	8.3	7.2	--

[1] for β equal to 50.
[2] for ρ equal to 0.01
[3] for ρ equal to 0.05
where: fdb = feedback
fdf = feedforward
PP = pole placement controller
MV = minimum variance controller
MB = model-based controller
NC = no control (see Figure 6.28)
Se = see Eqn.(6.1)
N = number of samples (see Table 6.12)

close to the desired value. However, the results obtained with the MB-controller were better than with the MV-feedforward.

For the above reasons, the PP and the MV-feedback/feedforward controllers are preferred over the MV-feedforward, MV-feedback and MB controller, and are used in the following simulation study.

6.2.2.2) Ramp Input Signal

To simulate the dryer operation with more realistic inputs, two sets of data (Set2 and Set3 in Table 6.11) were used. They are based on variations in the inlet moisture content observed during a practical farm drying test. In Set2, the inlet moisture content varies widely during the first two hours and remains fairly constant over the last 4 hours. The grain inlet moisture content in Set3 fluctuates at random during the entire drying period.

These inputs were simulated without control, and with MV-feedforward/feedback and PP controllers. For simplicity, the MV-feedback /feedforward will be referred to as MV in this section. The results are shown in Figures 6.39 through 6.44. The details of the control performance are tabulated in Table 6.14.

Figures 6.39 to 6.41 present the simulation results using inlet moisture variation from Set2. The inlet moisture content has an average of 20.7%, a minimum of 17% and a maximum of 25.6%.

In Figure 6.39, the outlet moisture is shown when no control is applied to the dryer. The MOavg is 18.1% for a setpoint of 16%.

Figure 6.40 shows the results obtained with the PP-controller. The average outlet moisture content is only 0.1% from the setpoint and the control error is 1.9%. The large value of the control error is due to large fluctuation in the inlet moisture content during the first 40 samples. The discharge auger rpm is changed frequently in an effort to control the outlet moisture content as close to the setpoint as possible. As a result, part of the grain is overdried and part underdried. However, the result is better than for the uncontrolled case. The level of the control obtained is excellent taking into account the large and sudden variation in the inlet moisture content during the first two hours of drying.

The result obtained with the MV-feedback/feedforward controller is illustrated in Figure 6.41. Compared with the previous results (Figure 6.40), the MV-controller gives a smaller Se (1.5%) value and an average outlet moisture content 0.6% point below the setpoint of 16%. The 0.6% overdrying is a direct result of the large and rapid changes in the inlet moisture content. It is observed that with the MV-controller the variation of the outlet moisture content around the setpoint is reduced. However, in contrast with the PP-controller, the MV-controller tends to produce overdried grain. In Figure 6.41 it is noticed that at the end of the run and after the first 22 samples, the grain is overdried.

The simulation results using inlet moisture content variation from Set3 are shown in Figures 6.42 to 6.44. Table 6.14 list the results of the performance measures.

Figure 6.42 shows the results when no control is used. The grain is overdried, the average outlet moisture content is 18.1% for a setpoint of 16% w.b.

Figure 6.43 and 6.44 show the simulation results obtained with

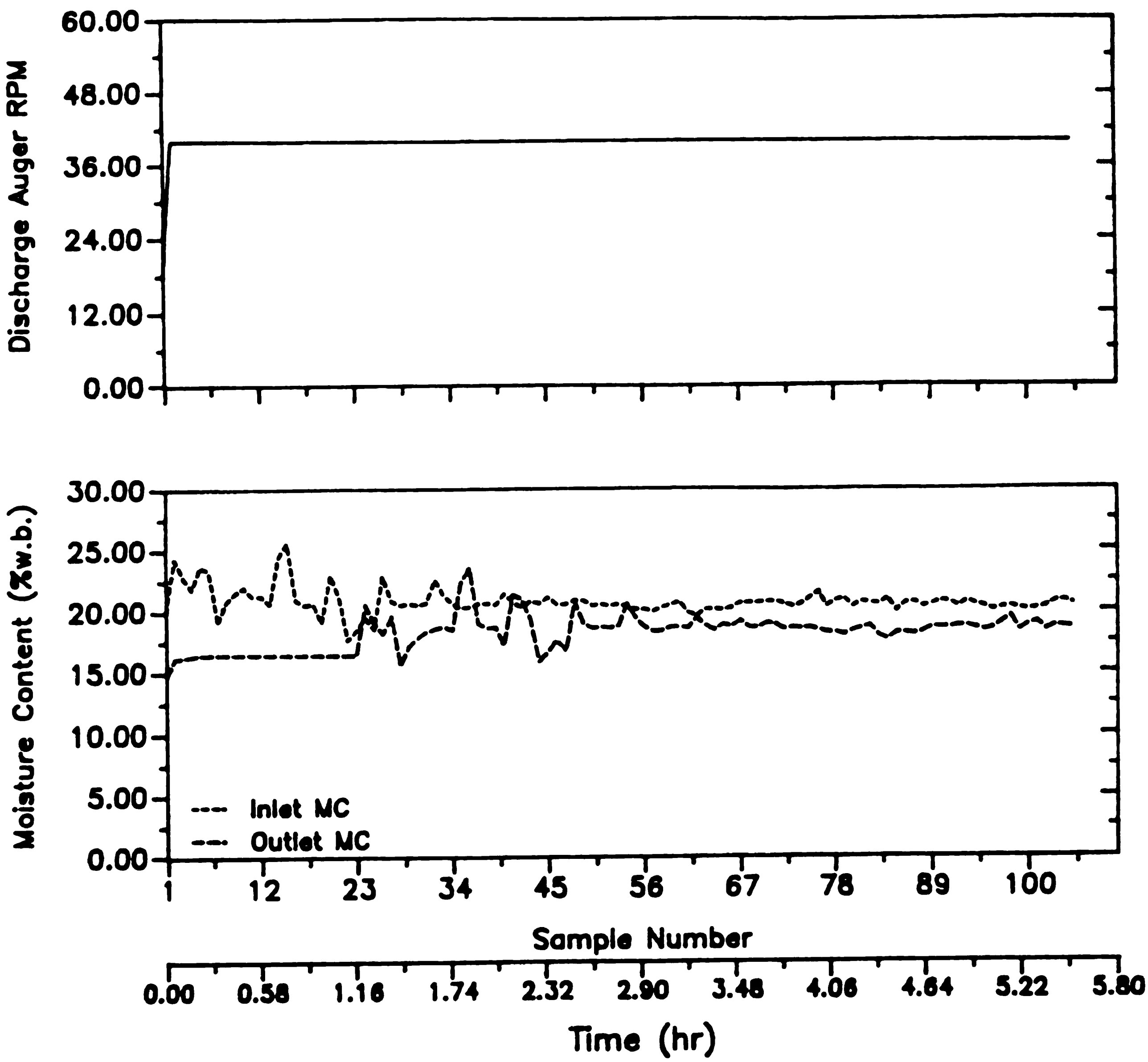

Figure 6.39: Simulation of the automatic control of a two-stage CCF dryer (no control, Set2) (see Table 4.1 for dryer parameters).

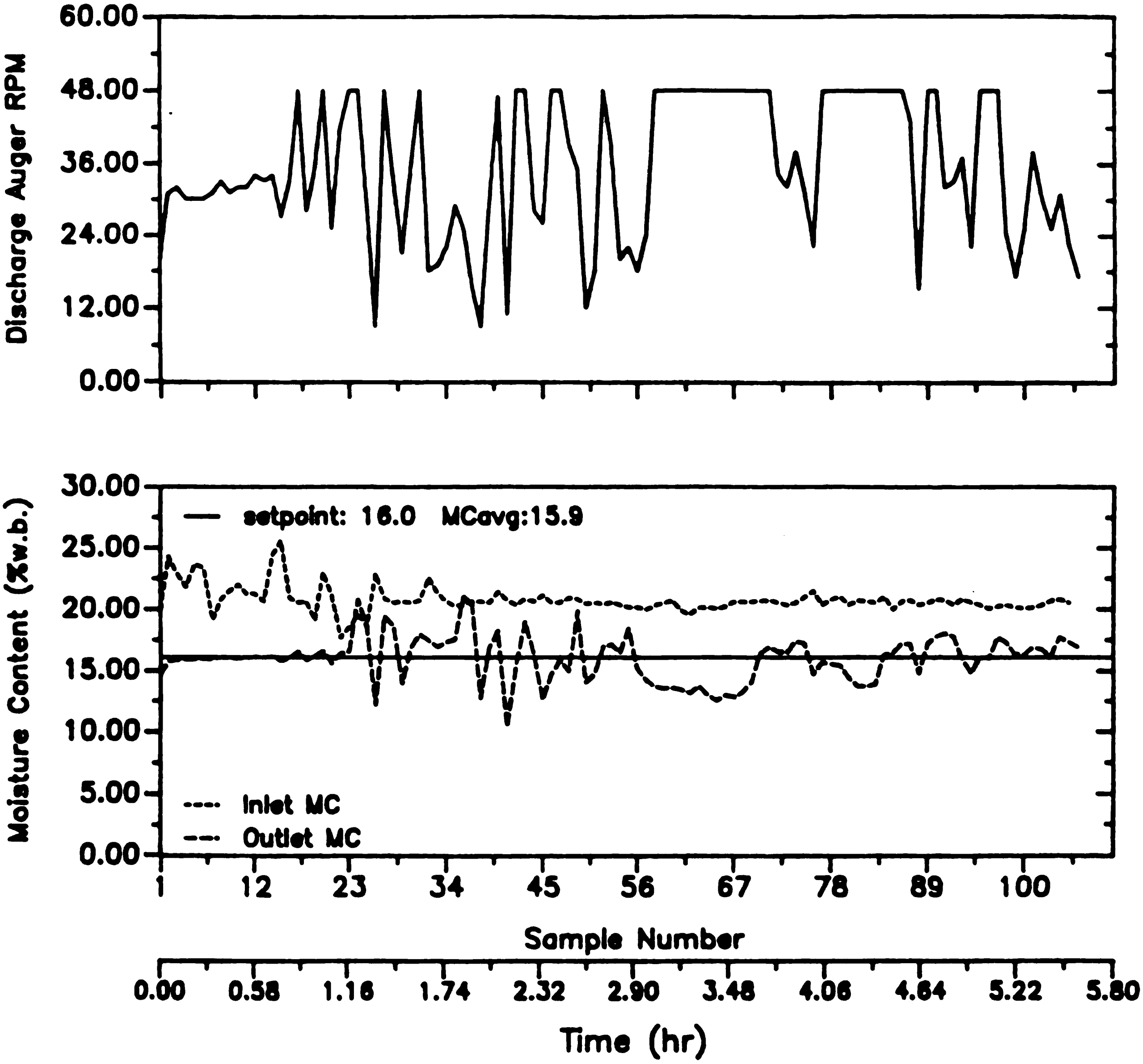

Figure 6.40: Simulation of the automatic control of a two-stage CCF dryer (Set2) using the PP-controller (see Table 4.1 for dryer parameters).

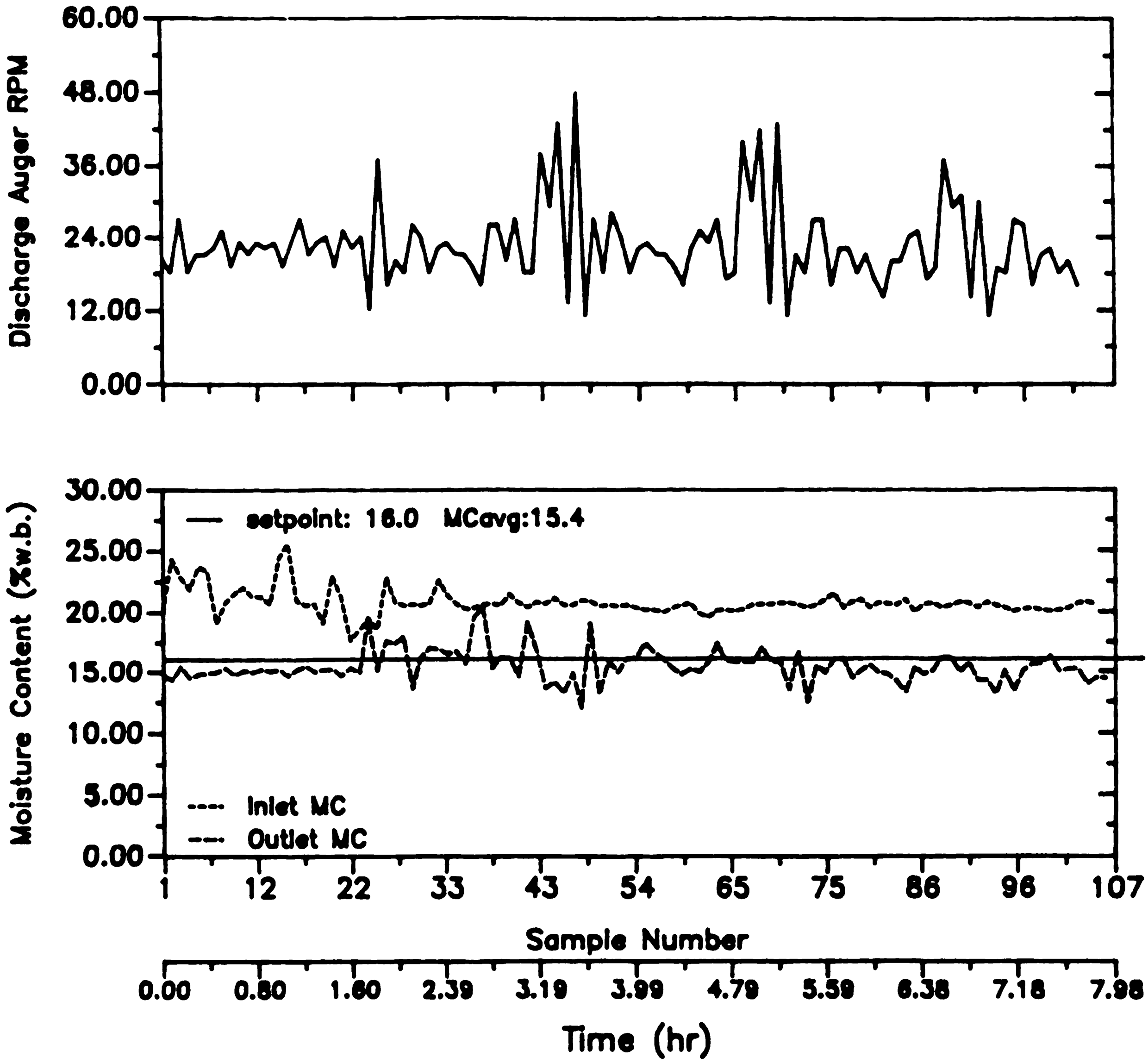

Figure 6.41: Simulation of the automatic control of a two-stage CCF dryer (Set2) using the MV-feedback/feedforward controller (see Table 4.1 for dryer parameters).

Table 6.14: Characteristic values of the different control performances with the inlet moisture content variation from Set2 and Set3 and, setpoint equal to 16% w.b..

PERFORMANCE MEASURES	CONTROLLER				NC	
	PP[1]		MV[2]			
	Set2	Set3	Set2	Set3	Set2	Set3
Se(%w.b.)	1.9	2.0	1.5	1.8	--	--
MOavg(%)	15.9	16.0	15.4	15.6	18.1	18.1
MOmin(%)	10.3	10.4	12.0	12.4	14.7	14.7
MOmax(%)	21.0	21.5	20.4	21.4	23.5	22.9
MImin(%)	17.6	17.8	17.6	17.8	17.6	17.8
MIavg(%)	20.7	20.8	20.7	20.8	20.7	20.8
MImax(%)	25.6	25.0	25.6	25.0	25.6	25.0
MIstd(%)	1.1	1.9	1.1	1.9	1.1	1.9
RPMmin	9.0	9.0	11.0	15.0	--	--
RPMavg	35.3	34.6	22.6	22.4	--	--
RPMmax	48.0	48.0	48.0	48.0	--	--
RPMstd	11.9	12.5	6.9	4.8	--	--

[1] for β equal to 50.
[2] feedback/feedforward with ρ equal to 0.05
where:

PP = pole placement controller
MV = minimum variance controller
NC = no control (see Figures 6.34 and 6.37)
Se = see Eqn.(6.1)
N = number of samples (see Table 6.12)
N = 106 for Set2
N = 130 for Set3

the PP-controller and the MV-controller, respectively. The inlet moisture content fluctuation made it impossible to maintain the outlet moisture content close to the setpoint. However, the controlled cases are better than the uncontrolled case.

The simulation run with the PP-controller (see Figure 6.43) resulted in an average outlet moisture content of 16%, exactly the desired value. The control error is 2%. The frequent change in the discharge auger rpm is because of the rapid change in the inlet moisture content. The controller performance can be considered excellent based on the average outlet moisture content achieved with the large variation in the inlet moisture content.

The MV-controller behaved as was expected (see Figure 6.44). The control error Se is 0.2% smaller than that of the PP-controller, and the average moisture content is 15.6%, 0.4% from the setpoint. Considering the large variation in the inlet moisture content, the controller performance is good. However, the MV-controller reacts slowly to changes in the inlet and the outlet grain moisture content compared to the PP-controller.

In conclusion, the pole placement control system can control a two-stage CCF corn dryer closer to the setpoint than the MV-feedback/ feedforward control. Further advantages with the PP-controller are that it contains few parameters (thus, they can be physically interpreted), and converges rapidly.

6.3) DISCUSSION

A series of six tests was conducted with the MV and PP

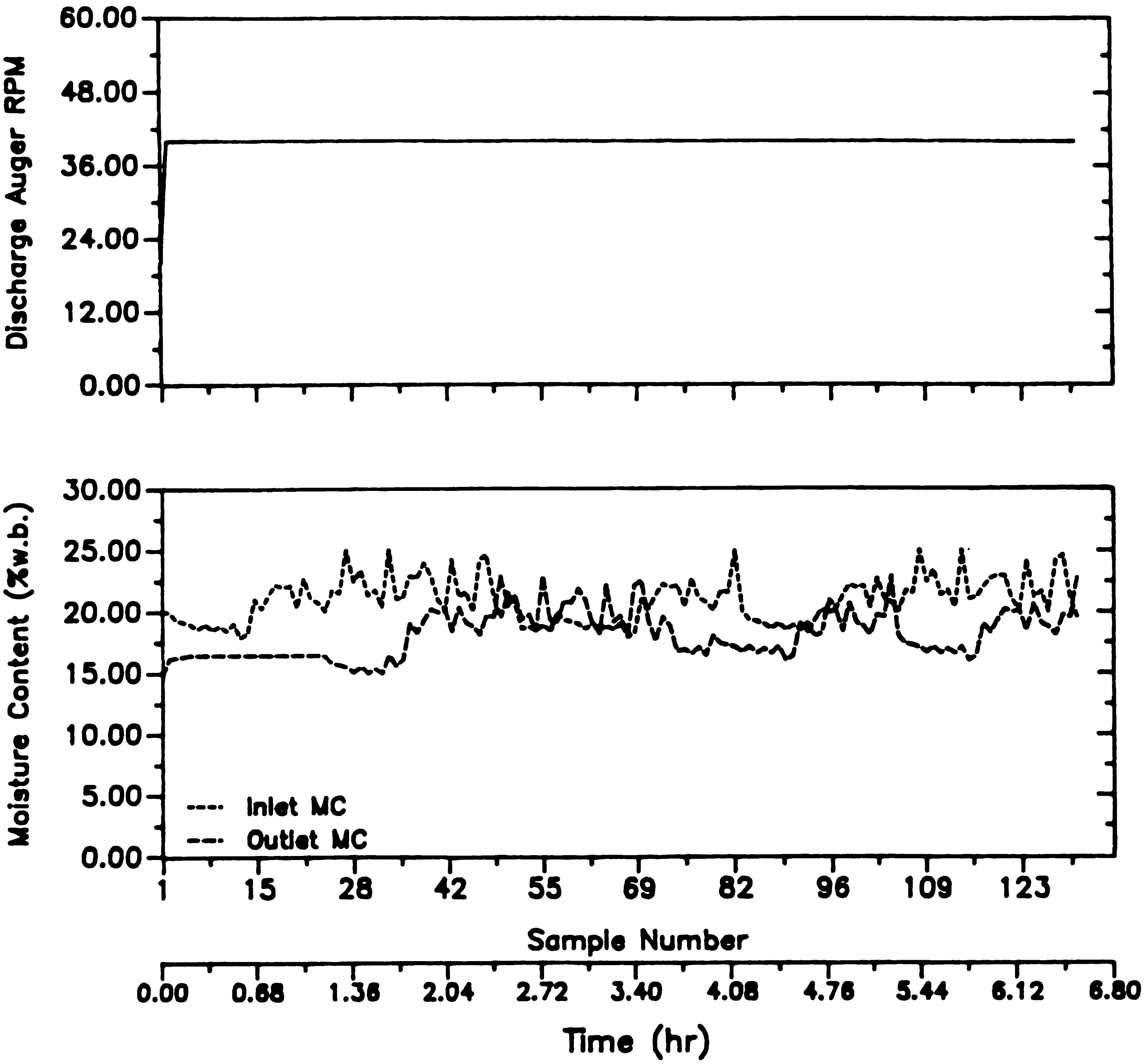

Figure 6.42: Simulation of the automatic control of a two-stage CCF dryer (no control, Set3) (see Table 4.1 for dryer parameters).

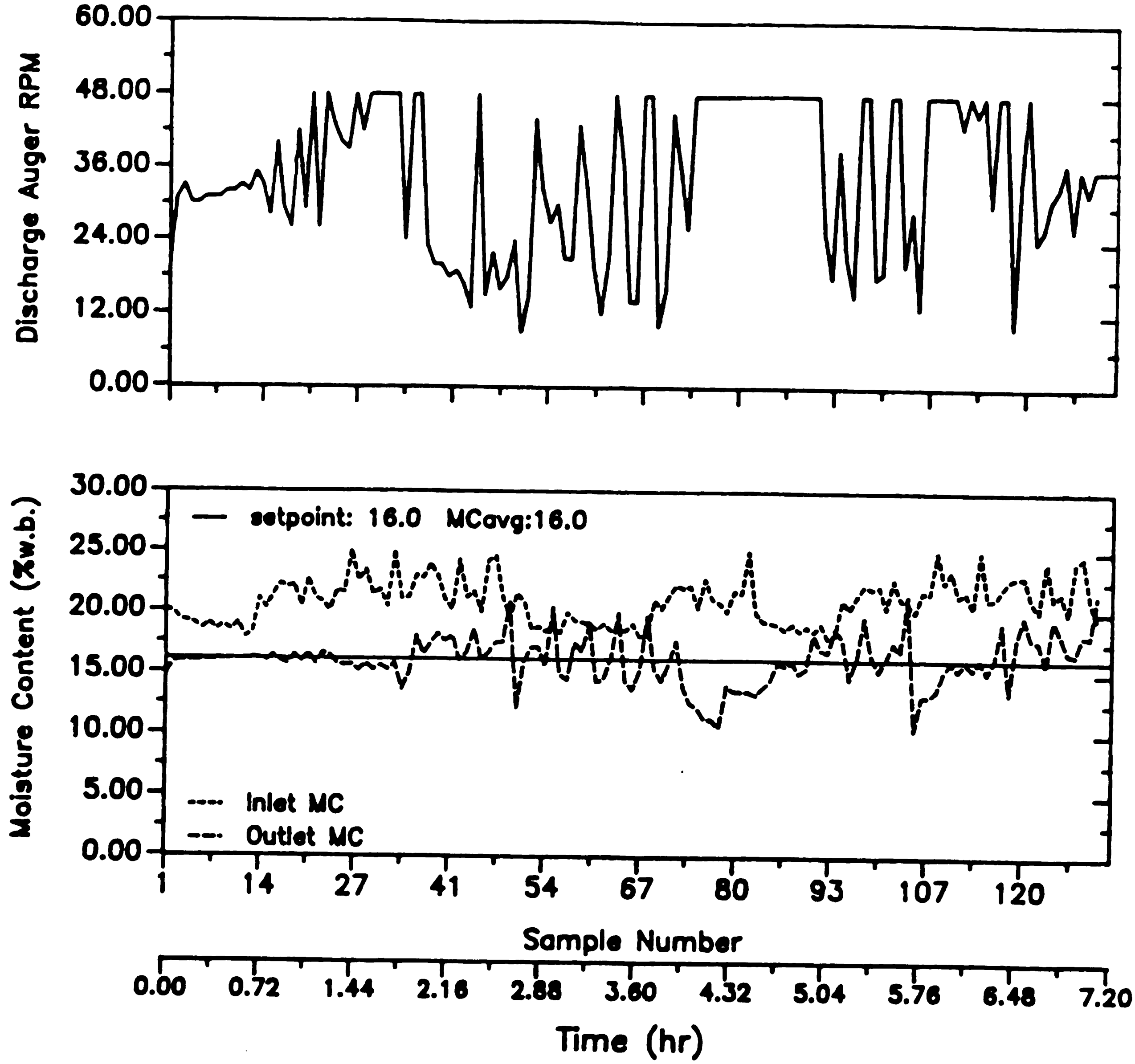

Figure 6.43: Simulation of the automatic control of a two-stage CCF dryer (Set3) using the PP-controller (see Table 4.1 for dryer parameters).

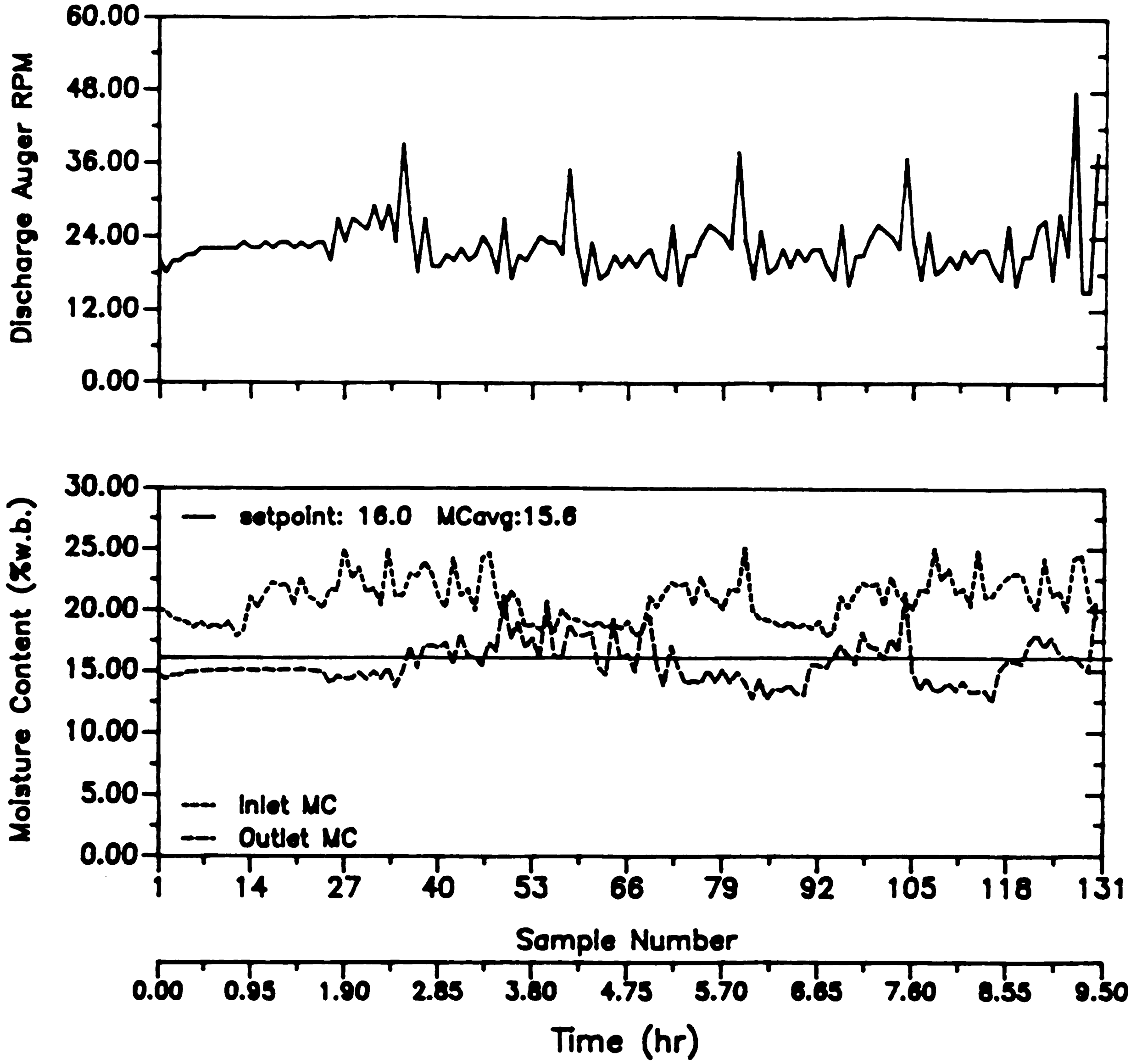

Figure 6.44: Simulation of the automatic control of a two-stage CCF dryer (Set3) using the MV-feedback/feedforward controller (see Table 4.1 for dryer parameters).

controllers on two commercial crossflow dryers over a period of two drying seasons. The controllers controlled the outlet moisture content well even for large inlet moisture content variations.

In order to develop an automatic controller for a multi-stage CCF corn dryer, a drying process model was required. Therefore, a differential equation concurrentflow-drying model was developed. The dryer model was used to simulate different control systems.

Different empirical models were evaluated in order to determine the best model for on-line control calculations. A simple but accurate linear model was developed for the automatic control of continuous-flow grain dryers.

Several control algorithms were analyzed. The pole placement control is stable and accurate; it can be used in any dryer and for any input/output signals.

6.3.1) Implementation

Implementation of the proposed control system is simple. It requires the same hardware and software as described in section 5.1.2 with the exception of the moisture meter. In order to use the fixed-distance sample strategy (see section 4.3.1) it is required to have a continuous moisture meter.

The software consists of a parameter estimation routine combined with the control algorithm. It requires less than 128k memory capability to run the control system. In addition to the control software, an expression relating rpm and GFR for the particular dryer is needed. If this information can not be found in the dryer specifications of the brochure, these values must be determined at the dryer site. The characteristic of the discharge mechanism must be known in order to give a well defined sample interval.

Before the dryer can be switched to automatic mode, the dryer has to run in manual mode for a period of time of about 2 hours in order to obtain acceptable starting values for the control parameters (i.e., recorded input/output values are used to estimate the dryer parameters until they converge to a constant value). However, this procedure is only necessary on the first day of the drying season. On the following days, the input and output variables collected previously are stored on a disk, and can be used to start the control program.

Personnel without excessive training can be instructed in the use of the control system in a few days.

6.3.2) Application to Other Dryer Types

The advantage of the adaptive control system described in this study is that it can be applied to different dryer and cereal types.

For a CCF rice dryer, the same models described in section 4.1.1 can be used. In that case, the manipulated variable is the drying air temperature instead of the grain flow rate. For a single-stage dryer, the control strategy is basically the same as used for the CCF corn dryer, i.e, the outlet and inlet moisture content are measured and the control input (inlet air temperature) is adjusted in order to maintain the output as close to the desired value as possible. For a multi-stage dryer, the strategy is more complex because the drying air temperature is different in each stage. One possibility is to set the inlet air temperature to a maximum value in the first stage and control only the last stage using the PP-controller. Another possibility is to control each stage separately using multi-variable systems design.

CHAPTER 7

CONCLUSIONS

1. Control algorithms have been developed for crossflow grain drying using generalized minimum variance and pole placement controllers.

2. A control system consisting of a microcomputer, a semi-continuous moisture meter, and control software has been implemented and successfully tested on two commercial crossflow grain dryers.

3. The average outlet moisture content in the commercial dryers was controlled to within ±0.3% of the setpoint during two drying seasons.

4. An unsteady state differential equation simulation model for multi-stage concurrentflow grain drying has been developed.

5. An adaptive control algorithm has been developed for a two-stage concurrentflow grain dryer.

6. Different linear models and an exponential model were considered in the design of the control system; the recursive prediction error method was used to estimate the parameters of the linear models.

7. The model II-b is the best model for predicting the dynamics of continuous-flow grain dryers based on the loss fuction values.

8. Simulation tests were performed to evaluate the controllers response to different inlet moisture content variations.

9. The pole placement was selected as the best controller based on simulation results, and is recommended for the automatic control of continuous-flow grain dryers.

10. The MV-feedback/feedforward controller gives a smaller control error than the PP-controller. However, it reacts slower to changes in working conditions, requires more parameters, and is more complex in than the PP-controller.

11. The MV-feedback controller shows similar performance as the MV-feedback/feedforward controller. The disadvantage of the former is that it requires more parameters to control the process adequately.

12. The MV-feedforward controller is considered the least desired system for continuous-flow grain dryers. The MB-controller gives better results than the MV-feedforward unit, but it is slow and requires a feedback loop to improve its performances.

13. The implementation of the proposed system is simple and requires little training. It can be adopted to different dryers and cereal types.

CHAPTER 8

SUGGESTIONS FOR FUTURE STUDY

1. To test the recommended controller on a commercial multi-stage concurrentflow corn grain dryer.

2. To develop different control strategies which would further decrease the variation in the manipulated variable; one possibility is to vary the inlet air temperature in addition to the grain flow rate.

3. To test the same control system on a concurrentflow rice dryer, i.e., to vary the inlet air temperature instead of the grain flow rate.

4. To investigate the possibility of reducing the CPU time of the control system simulation model using different numerical techniques.

9. REFERENCES

Åstrom, K.J and B. Wittenmark. 1984. Computer Controlled Systems: Theory and Design. Prentice-Hall. Englewood Cliffs, New Jersey.

Åstrom, K.J. 1970. Introduction to Stochastic Control Theory. Academic Press, New York, New York.

Åstrom, K.J. and B. Wittenmark. 1973. On self-tuning regulators. Automatica. 9,185-198.

Agness, J.B. and G.W. Isaacs. 1967. Grain drier control based on exhaust temperature sensing. Trans. ASAE. 10(1),110-113.

Anderson, J.C. 1985. Performance Evaluation of Commercial Crossflow and Concurrent-flow Grain Drying. M.S. Thesis. Michigan State University. East Lansing, Michigan.

Bakker-Arkema, F.W.; J.C. Anderson and A.Y. Eltigani. 1987. Facility operations drying-fuel cost control. For the presentation at the 58th Intern. Conf. of the Grain Elevator and Processing Society. Columbus, Ohio.

Bakker-Arkema, F.W.; J.C. Rodrigues, I.P. Schisler and C.M. Westelaken. 1982. A new commercial crossflow dryer with differential grain speed. Am. Soc. Agric. Engr. Paper No. 82-3007. St. Joseph, Michigan.

Bakker-Arkema, F.W.; L.E. Lerew, S.F. DeBoer and M.G. Roth. 1974. Grain drying simulation. Res. Report 224, Michigan State University, East Lansing, Michigan.

Bakker-Arkema, F.W.; L.E. Lerew, R.C. Brook and D.B. Brooker. 1978a. Energy and capacity evaluation of grain dryers. Am. Soc. Agric. Engr. Paper No.78-3523. St. Joseph, Michigan.

Bakker-Arkema, F.W.; R.C. Brook and L.E. Lerew. 1978. Cereal grain drying. In Advances in Cereal Science and Technology, Vol II. Am. Assoc. Cereal Chem. St. Paul, Minnesota.

Bakker-Arkema, F.W. 1984. Selected aspects of crop processing and storage: A review. J. Agric. Engng. Res. 30,1-22.

Bakker-Arkema, F.W. 1987. Class notes. Department of Agricultural Engineering, Michigan State University. East Lansing, Michigan.

Bakker-Arkema, F.W. 1988. Personal communication. Department of Agricultural Engineering, Michigan State University. East Lansing, Michigan.

Bakker-Arkema, F.W. 1988. Class notes. Department of Agricultural Engineering, Michigan State University. East Lansing, Michigan.

Bakker-Arkema, F.W.; C. Fontana, R.C. Brook and C.M. Westelaken. 1982. Concurrent flow rice drying. Am. Soc. Agric. Engr. Paper No. 82-3068. St. Joseph, Michigan.

Bakker-Arkema, F.W.; C. Fontana, S.J. Kalchik and C.M. Westelaken. 1984. Drying in commercial rice parboiling plants. Drying Techn. 2(3),423-433.

Bakker-Arkema, F.W. and C.W. Hall. 1965. Importance of boundary conditions in solving the diffusion equation for drying wafer. Trans. ASAE. 8(3),382-383.

Beck, J.V. and K.J. Arnold. 1977. Parameter Estimation in Engineering and Science. John Wiley and Sons. New York, New York.

Becker, H.A. and H.R. Sallans. 1960. Drying wheat in a spouted bed: On the continuous moisture diffusion controlled drying of solid particles in a well-mixed isothermal bed. Chem. Engr. Sci. 13(3),97-112.

Becker, H.A. and H.R. Sallans. 1960. Drying wheat in a spouted bed. Chem. Engr. Sci. 13(3),97-112.

Borsum, J.C. and F.W. Bakker-Arkema 1982. Microprocessor control of drying processes. Am. Soc. Agric. Engr. Paper No. 82-6006. St. Joseph, Michigan.

Boyce, D.S. 1966. Heat and mass transfer in ventilated grain. J. Agric. Engng. Res. 11(4),255-265.

Brook, R.C. 1977. Design of multistage grain dryers. Ph.D Dissertation. Michigan State University. East Lansing, Michigan.

Brook, R.C. and F.W. Bakker-Arkema. 1980. Concurrent flow drying of food grains. In Drying '80. Vol.1 Mc Graw-Hill International. Montreal, Canada.

Brooker, D.B.; F.W. Bakker-Arkema and C.W. Hall. 1981. Drying Cereal Grains. AVI Publishing. Westport, Connecticut.

Chu, S.T. and A. Hastrulid. 1968. General characteristics of variable diffusivity process and the dynamic equilibrium moisture content. Trans. ASAE. 11(15),709-710.

Claflin, J.K. and A.G. Fane. 1984. Fluid mechanics, heat and mass transfer and drying in spouted beds with draft tubes. In: Drying 1984. International Hemisphere Publishing Co. New York.

Clarke, D.W.; P.P. Kanjilal and C. Mohtadi. 1985. A generalized LQG approach to self-tuning control. Part I. Aspects and design. Int. J. Control. 41(6),1509-1523.

Clifford, W.H. 1972. Control of concurrent grain dryers. Am. Soc. Agric. Engr. St Joseph, Michigan.

CNEEMA. 1979. Official tests of Law SCE112S continuous grain dryer with heat economizer. Rep.No. 2688, Centre National d'Études et d'Experimentation de Machinisme Agicole. Antony, France.

Crank, J. 1957. The Mathematics of Diffusion. Claredon Press. Oxford.

Dalpasquale, V.A. and J.A.M. Pereira. 1985. Optimization of a cascade dryer for soybeans. Am. Soc. Agric. Engr. Paper No. 85-3514. St. Joseph, Michigan.

Eltigani, A.Y. 1987. Automatic control of commercial crossflow grain dryers. Ph.D. Dissertation. Michigan State University. East Lansing, Michigan.

Eltigani, A.Y.; J.C. Anderson, F.W. Bakker-Arkema and S. Shivvers. 1986. Automatic control of a commercial crossflow grain dryer. Am. Soc. Agric. Engr. Paper No. 86-6501. St. Joseph, Michigan.

Fábián, Z. and M. Samu. 1980. Automatic moisture control for grain driers. Grndl. Landtechnik. 30(5),174-178.

FAO. 1987. The 1986 Production Yearbook. FAO. Rome, Italy.

Fontana, C.; F.W. Bakker-Arkema and C.M. Westelaken. 1982. Concurrentflow vs. crossflow drying of long grain rice. Am. Soc. Agric. Engr. Paper No. 82-3569. St. Joseph, Michigan.

Forbes, J.F.; B.A. Jacobson, E. Rhodes and G.R. Sullivan. 1984. Model based control strategies for commercial grain drying systems. Can. J. Chem. Engr. 62,773-778.

Garcia, C.E. and M. Morari. 1982. Internal model control. 1. A unifying review and some results. Ind. Engr. Chem. Proc. Des. Dev. 21,308-314.

Gustafson, R.J. and R.V. Morey. 1981. Moisture and quality variations across the column of a crossflow grain dryer. Trans. ASAE. 24(6),1621-1625.

Hall, G.E. and R.J. Anderson. 1980. Batch internal recycling dryer (BIRD). Am. Soc. Agric. Engr. Paper No. 80-3515. St. Joseph, Michigan.

Hawk, A.L.; R.T. Noyes, C.M. Westelaken, G.H. Foster and F.W. Bakker-Arkema. 1978. The present status of commercial grain dryers. Am. Soc. Agric. Engr. Paper No. 78-3008. St. Joseph, Michigan.

Henderson, J.M. and S.M. Henderson. 1968. A computational procedure for deep bed drying analyses. J. Agric. Engng. Res. 13(2),87-95.

Henderson, S.M. 1974. Progress is developing the thin-layer drying equation. Trans. ASAE. 17(6),1167-1168,1172.

Holman, J.P. 1984. Heat Transfer. McGraw-Hill Book Co. New York.

Holtman, J.B. and G.L. Zachariah. 1969a. Continuous crossflow modelling for optimal control. Trans. ASAE. 12(5),430-432.

Holtman, J.B.; Zachariah, G.L. 1969b. Computer control for grain driers. Trans. ASAE 12(5) 433-437.

Hukill, W.V. 1954. Storage of Cereal Grain and their Products. Chapter IX. Am. Assoc. of Cereal Chem. St. Paul, Minnesota.

Husain, H.; S.C. Chen, J.T. Clayton and L.F. Whitney. 1972. Mathematical simulation of mass and heat transfer in high moist foods. Trans. ASAE. 15,732-736.

Huwizhen, L; R.V. Morey. 1984. Thin-layer drying of yellow-dent corn. Trans. ASAE. 27(3),581-585.

Igram, G.W. 1976. Deep bed drier simulation with intra-particle moisture diffusion. J. Agric. Engng. Res. 21,263-272.

Isermann R. and K.H. Lachmann. 1982. On the development and implementation of parameter-adaptive controllers. IFAC Software for Computer Control. 25-49. Madrid, Spain.

Isermann, R. 1981. Digital Control Systems. Springer-Verlag, New York.

Jaaksoo, U.J.; E.M. Talvis and J.M. Ummer. 1982. Microprocessor-based grain dryer control. IFAC Software for Computer Control. 3,473-477. Madrid, Spain.

Katic, Z. 1974. Trocknung von Maiskornern mit groszer Feuchtigkeit im Trommeltrockner. Muehle Mischufuttertechn. 111,651-654.

Kearns, D.L. ed. 1974. Fluidization and fluid-particles systems. AIChE Symp. Ser. 141.

Keey, R.B. 1972. Drying Principles and Practice. Pergamon Press, New York.

Kucera, V. 1979. Discrete Linear Control. Wiley. New York, New York.

Laws, N. and J.L. Parry. 1983. Mathematical modelling of heat and mass transfer in agricultural grain drying. Proc. R. Soc. Lond. A. 385,169-187.

Lerew, L.E.; F.W. Bakker-Arkema and R.C. Brook. 1972. Simulation of a commercial crossflow dryer: the Hart-Carter model. Am. Soc. Agric. Engr. Paper No. 72-829. St. Joseph, Michigan.

Lewis, W.K. 1921. The rates of drying solid materials. The J. Ind. and Engr. Chem. 13(5),427-432.

Ljung, L. and T. Soderstrom. 1983. Theory and Practice of Recursive Identification. The MIT Press. Cambridge, Massachusetts.

Luikov, A.V. 1966. Heat and Mass Transfer in Capillary-Porous Bodies. New York: Pergamon.

Mann, W. 1982. Digital control of a rotary dryer in the sugar industry. 6th IFAC/IFIP Conf. on Digital Computer Applications to Process Control. 73-90. Düsseldorf, F.R. Germany.

Marchant, J.A. 1984. Control of high temperature continuous flow grain driers. Agric. Engr. 40(4),145-149.

Meiering, A.G and H.J. Hoefkes. 1977. Dryer performance and energy use in corn drying. Can. Agric. Engr. 22(2),163-170.

Misra, M.K. and D.B. Brooker. 1980. Thin-layer drying and rewetting equation for shelled yellow corn. Trans. ASAE. 23(5),1254-1260.

Modén, P.E. and T.G. Nybrant. 1980. Adaptive control of rotary drum driers. 6th IFAC/IFIP Conf. on Digital Computer Applications to Process Control. 355-361. Düsseldorf, F.R. Germany.

Moreira, R.G. 1983. Dehydration of Almonds. M.S. Thesis. Michigan State University. East Lansing, Michigan.

Morey, R.V.; H.A. Cloud, R.J. Gustafson and D.W. Petersen. 1979. Evaluation of the feasibility of solar energy grain drying. Trans. ASAE. 22(3),409-417.

Nellist, M.E. 1974. The drying of reygrass seeds in deep bed. Ph.D. Dissertation. University of Newcastle-upon-Tyne, England.

Nellist, M.E. 1982. Developments in continuous flow grain dryers. Agric. Engr. 37(3),74-80.

Nellist, M.E. 1987. Modelling the performance of a crossflow grain drier. J. Agric. Engng. Res. 37(1),43-45.

Nellist, M.E. and O'Callaghan. 1971. The measurement of drying rates in thin-layers of reygrass seed. J. Agric. Engng. Res. 16(3),192-212.

Neter J. and W. Wasserman. 1974. Applied Linear Stochastic Models-Regression, Analysis of Variance, and Experimental Design. Richard D. Irwin, Inc. Homewood, Illinois.

Nonhebel, G. and A.A.H. Moss. 1971. Drying Solids in the Chemical Industry. CRC. Cleveland, Ohio.

Nybrant, T.G. 1986. Modelling and control of grain dryers. UPTEC 8625 R. Teknikum, Institute of Technology. Uppsala University, Uppsala, Sweden.

Nybrant, T.G. and P.J.S. Régner. 1985. Adaptive control of continuous grain dryers. Am. Soc. Agric. Engr. Paper No. 85-3011. St. Joseph, Michigan.

O'Callaghan, J.R.; D.J. Menzies and P.H. Bailey. 1971. Digital simulation of agricultural drier performance. J. Agric. Engng. Res. 16(3),223-244.

Olesen, H.T. 1978. Automatic control arrangement for continuous drying plant. British Patent 1502710. British Patent Office. London, UK.

Pabis, J. 1971. Effect of temperature and moisture content of wheat grain on the moisture flux of a fluidized bed dryer. In: Drying of Agricultural Products, ed. by J. Haman, S. Pabis and W. Zarember. Panstwowe Wydawnictwo Nawkowe. Warsaw, Pol.

Pabis, J. 1974. Application of moisture flux into calculation of the fluidization drying process. In: Drying of Agricultural Products, ed. by J. Haman, S. Pabis and W. Zarember. Panstwowe Wydawnictwo Nawkowe. Warsaw, Pol.

Pabis, S. and S.M. Henderson. 1961. Grain drying theory: A critical analysis of the drying curve of shelled maize. J. Agric. Engng. Res. 6,272-277.

Page, C. 1949. Factors influencing the maximum rates of drying shelled corn in layers. M.S. Thesis. Purdue University. Lafayette, Indiana.

Palmer, J. 1984. Selecting profitable automatic control systems. Am. Soc. Agric. Engr. Paper No. 84-1635. St. Joseph, Michigan.

Parry, J.L. 1985. Mathematical modeling and computer simulation of heat and mass transfer in agricultural grain drying: A review. J. Agric. Engng. Res. 32(1),1-29.

Passos, M.L.; A.S. Mujumdar and V.G.S. Raghavan. 1987. Spouted beds for drying: Principles and design considerations. In Advances in Drying, Vol 4. Mc Graw-Hill International. Montreal, Canada.

Pawlowiski, S. 1975. Newe Approximationsbeziehung und Nomogramm zur Ermittlung der Ausdehnung von homogenen Flieszbetten. Verfahrenstechnik. 9,74-77.

Pierse, R.O. and T.L. Thompson. 1981. Energy use and performance related to crossflow dryer design. Trans. ASAE. 24(1),216-220.

Rodrigues, J.C. 1981. Energy efficiency and grain quality characteristics of crossflow and concurrent flow dryers. Ph.D. Dissertation. Michigan State University, East Lansing, MI.

Rowe, R.J. and W.W. Gunkel. 1972. Simulation temperature and moisture content of alfalfa during thin-layer drying. Trans. ASAE 15(5),805-810.

Saeman, W.C. and T.R. Mitchell. 1954. Analysis of rotary dryer and cooler performance. Chem. Eng. Progr. 50(60),467-473.

Saradis, G.N.; J.M. Mendel and Z.Z. Nikolie. 1977. Report on definitions of self-organizing control processes and learning systems. IEEE Control Systems Society Newsletter.

Sharaf-Eldem, J.I.; J.L. Blaisdell and M.Y. Hamdy. 1980. A model for ear corn drying. Trans. ASAE. 23(5),1261-1265,1271.

Sharples, K.; P.G. Glekin and R. Warne. 1964. Computer simulation of rotary dryers. Trans. Inst. Chem. Engrs. 42(5),257-284.

Sherwood, T.K. 1936. Air drying of solids. Trans. Am. Inst. Chem. Engr. 32,150-168.

Steffe, J.F. 1979. Moisture diffusion and tempering in the drying of rough rice. Ph.D. Dissertation. University of California, Davis.

Steffe, J.F. and R.P. Singh. 1980. Liquid diffusivity of rough rice components. Trans. ASAE. 23(3),775-781,782.

Syarief, A.M.; R.V. Morey and R.J. Gustafson. 1981. Thin-layer drying rates for sunflower seeds. Am. Soc. Agric. Engr. Paper No. 81-3546. St. Joseph, Michigan.

Thompson, T.L. 1967. Predicted performances and optimal designs of convection grain dryers. Ph.D. Dissertation. Purdue University. Lafayette, Indiana.

Thompson, T.L.; R.M. Peart and G.H. Foster. 1968. Mathematical simulation of corn drying: A new model. Trans. ASAE. 11(4),582-586.

Thorpe, G.R. and A.N. Stokes. 1987. A stochastic approach to the drying of solids in a multi-stage fluidized bed. Drying Techn. 5(2),259-272.

Thorton, C.L. and G.J. Bierman. 1980. UDU' covariance factorization for Kalman filtering. In: Control and Dynamics System, Vol.16. Academic Press. New York.

Treybal, R.E. 1980. Mass Transfer Operation. Mc Graw-Hill. New York, New York.

Tuffs, P.S. and D.W. Clarke. 1985a. Self-tuning control of offset: A unified approach. IEE Proc. 132(3),100-110.

Vanecek, V.; M. Markvart and R. Drbehlav. 1966. Fluidized Bed Drying. Leonard Hill. Lodon, England.

White, G.M.; I.J. Ross and P.W. Westerman. 1973. Drying rate and quality of white shelled corn as influenced by dew-point temperature. Trans. ASAE. 16(1),118- 120.

Whitfield, R.D. 1986. An unsteady-state simulation to study the control of concurrent and counter-flow grain driers. J. Agric. Engng. Res. 33,171-178.

Young, J.H and T.B. Whitaker. 1971. Numerical analysis of vapor diffusion in a porous composite sphere with concentric shells. Trans. ASAE. 14(2),1051-1057.

Zachariah, G.L. and G.W. Isaacs. 1966. Simulating a moisture control system for continuous-flow driers. Trans. ASAE. 9(4),297-302.

Zuritz, C.A. and R.P. Singh. 1982. Simulation of a rough rice drying in a spouted bed. In: Drying 1982. International Hemisphere Publishing Co. New York.

10. APPENDICES

APPENDIX A: DERIVATION OF THE GMV CONTROLLER

GENERALIZED MINIMUM VARIANCE CONTROLLER-(GMV):

Derivation of the generalized minimum variance controller as described in Iserman (1980).

It is assumed that the process to be controlled is described by:

$$y(z) = \frac{B(z^{-1})}{A(z^{-1})} z^{-\tau} u(z) + \lambda \frac{C(z^{-1})}{A(z^{-1})} \xi (z) \qquad \text{.........(a.1)}$$

where: $A(z^{-1}) = 1 + a_1 z^{-1} + \ldots + a_m z^{-m}$

$B(z^{-1}) = b_1 z^{-1} + \ldots + b_m z^{-m}$

$C(z^{-1}) = 1 + c_1 z^{-1} + \ldots + c_m z^{-m}$

m = model order

τ = delay = 0.

Here $\xi(k)$ is a statistically independent signal

$$E\{\xi(k)\xi(k+\sigma)\} = \begin{cases} 1 & \text{for } \sigma = 0 \\ 0 & \text{for } \sigma \neq 0 \end{cases}$$

$$E\{\xi(k)\} = \bar{\xi} = 0 \qquad \text{.........(a.2)}$$

It is assumed that $w(k)$ (the reference value) is equal to 0, i.e. $e_w(k) = -y(k)$. The problem is to design a controller which minimizes the criterion:

$$I(k+1) = E\{y^2(k+1) + \rho u^2(k)\}. \qquad \text{.........(a.3)}$$

The controller must generate an input $u(k)$ such that the errors induced by the noise process $[\xi(k)]$ are minimized according to Eqn.(a.3). In the performance function I, $y(k+1)$ is taken insteady of $y(k)$, as $u(k)$ can only influence the controlled variable at time $(k+1)$ because of the assumption $b_0=0$. Therefore, $y(k+1)$ must be predicted on the basis of known signal values $y(k)$, $y(k-1)$, ... and $u(k)$, $u(k-1)$, ... Using Eqn.(a.1), a <u>prediction</u> of $y(k+1)$ is:

$$z\, y(z) = \frac{B(z^{-1})}{A(z^{-1})} z\, u(z) + \lambda \frac{C(z^{-1})}{a(z^{-1})} z\, \xi(z) \qquad \text{........(a.4)}$$

and

$$A(z^{-1}) z\, y(z) = B(z^{-1}) z\, u(z) + C(z^{-1}) z\, \xi(z) \qquad \text{.........(a.5)}$$

or

$$(1+a_1 z^{-1}+\ldots+a_m z^{-m}) z\, y(z) = (b_1 z^{-1}+\ldots+b_m z^{-m}) z\, u(z)$$
$$+ \lambda(1+c_1 z^{-1}+\ldots+c_m z^{-m}) z\, \xi(z). \qquad \text{.........(a.6)}$$

After multiplying and transforming back to the time domain, we obtain:

$$y(k+1) + a_1 y(k) +\ldots+ a_m y(k-m+1) = b_1 u(k) +\ldots+ b_m (k-m+1)$$
$$+ \lambda[\xi(k+1) + c_1 \xi(k) +\ldots+ c_m (k-m+1)] \qquad \text{.........(a.7)}$$

Therefore, the performance criterion of Eqn.(a.3) becomes:

$$I(k+1) = E\{[-a_1y(k)-\ldots-a_my(k-m+1) + b_1u(k)+\ldots+b_mu(k-m+1)$$
$$+ \lambda(c_1\xi(k)+\ldots+c_m(k-m+1)) + \lambda\xi(k+1)]^2 + \rho u^2(k)\}$$
$$\ldots\ldots\ldots(a.8)$$

At time instant k, all signal values are known with the exception of u(k) and ξ(k+1). Therefore, the expectation of ξ(k+1) only must be taken. In addition, ξ(k+1) is independent of all other signal values:

$$I(k+1) = \{-a_1y(k)-\ldots-a_my(k-m+1) + b_2(k-1)+\ldots+b_m(k-m+1)$$
$$+ \lambda[c_1\xi(k)+\ldots+c_m\xi(k-m+1)]^2$$
$$+ \lambda^2E\{\xi^2(k+1)\}$$
$$+ 2\lambda\{-a_1y(k)-\ldots+b_m(k-m+1)$$
$$+ \lambda[c_1\xi(k)+\ldots+c_m(k-m+1)]\}E\{\xi(k+1)\}$$
$$+ \rho u^2(k). \qquad \ldots\ldots\ldots(a.9)$$

Therefore, the condition for optimal u(k) becomes:

$$\frac{\partial I(k+1)}{\partial u(k)} = 2\{-a_1y(k)-\ldots-a_my(k-m+1)$$
$$+ b_1u(k)+b_2u(k-1)+\ldots+b_m(u-k+1)$$
$$+ \lambda[c_1\xi(k)+\ldots+c_m\xi(k-m+1)]\}b_1$$
$$+ 2\rho u(k) = 0 \qquad \ldots\ldots\ldots(a.10)$$

In this equation, the term in braces before b_1 can be replaced using Eqn.(a.7), giving:

$$[zy(z) - \lambda z\xi(z)]b_1 + \rho u(z) = 0 \qquad \text{....... (a.11)}$$

Applying Eqn.(a.4):

$$\lambda\xi(z) = \frac{A(z^{-1})}{C(z^{-1})}\, zy(z) - \frac{B(z^{-1})}{C(z^{-1})}\, zu(z) \qquad \text{........(a.12)}$$

then:

$$G_{mv}(z) = \frac{u(z)}{y(z(} = \frac{[C(z^{-1}) - A(z^{-1})]z}{zB(z^{-1}) + \frac{\rho}{b_1} C(z^{-1})} \qquad \text{........(a.13)}$$

APPENDIX B: DESCRIPTION OF THE PROCEDURE TO DETERMINE THE RELATIONSHIP BETWEEN RPM AND RESIDENCE TIME FOR CONTINUOUS-FLOW GRAIN DRYERS.

Table B.1 presents the experimental data obtained with the Meyer-Morton 850 crossflow dryer.

Table B.1: Experimental data for the Meyer-Morton 850 crossflow dryer.

RPM	SCR VOLTAGE	GFR (LB/HR)	RESIDENCE TIME (HR)
330	1.40	13,900	3.55
430	1.65	17,240	2.86
530	1.90	20,560	2.40
620	2.15	24,460	2.02
720	2.40	28,360	1.74
820	2.64	34,080	1.45

It is assumed that the relationship between the RPM and GRF can be described by a linear equation of this type:

$$GFR\ (ft^3/hr) = C_1 * (RPM) + C_2 \qquad ....(b.1)$$

The value of the constants C_1 and C_2 can be determined by a linear curve fitting method or by plotting GFR vs RPM in a linear paper and find the slope of the curve. For this particular case, C_1 was found to be equal 0.897 and $C_2 = 0$.

To determine the relationship between the residence time (T_r) and the RPM, the following procedure was used:

(1) recall that:

$$T_r = \ell/\text{rpm} \qquad \text{........(b.2)}$$

where T_r is in hour.

(2) $C_1 = 0.897$ (ft^3/rpm-hr)

(3) the volume of grain in the dryer is equal to:

$$\text{Volume} = \text{GFR}(ft^3/hr) * \text{residence time (hr)} \qquad \text{........(b.3)}$$

(4) then:

$$\text{Volume} = C_1 * \text{RPM} * T_r \qquad \text{........(b.4)}$$

(5) thus, from Eqn.(b.4) it is obtained:

$$T_r = \frac{\text{Volume}/C_1}{\text{RPM}} \qquad \text{........(b.5)}$$

(6) for the Meyer-Morton, the dryer holding capacity is 880 bushel, and the volume of grain is then: 880 bu * 1.25 (ft^3) = 1100 ft^3. Therefore, the residence time for a given RPM for the Meyer-Morton dryer can be determined by the following equation:

$$T_r = \frac{1,226.31}{RPM} \qquad \text{........(b.6)}$$

(7) The volume of grain to be discharged during a sample interval is equal to the total volume divided by the number of dryer layers. By considering that the dryer is divided in 10 layers, the sample time is then:

$$t_r = \frac{122.63}{RPM} \qquad \text{........(b.7)}$$

where t_r is in hours.

The values of the constants in Eqn.(5.6) can be determined by a linear curve-fitting method; here they were found to be equal to:

$$\text{Voltage} = 0.565 + 0.002543 * (\text{RPM}) \qquad \text{........(b.8)}$$

The same procedure is used to determine the residence time as a function of rpm for the Zimmerman dryer and the two-stage CCF drye.

MICHIGAN STATE UNIV. LIBRARIES
31293005756881